



Margarida Leonor Florindo Espadinha

Licenciatura em Química Aplicada

Enantiopure bicyclic lactams: synthesis and biological evaluation

Dissertação para obtenção do Grau de Mestre em Química
Bioorgânica

Orientador: Prof. Doutora Maria M. M. Santos, FF-UL

Elemento de Ligação: Prof. Doutora Paula Sérgio Branco, FCT-UNL

Presidente: Prof. Doutora Paula Sérgio Branco, FCT-UNL

Arguente: Prof. Doutor Vasco Bonifácio, IST-CQFM

Vogal: Prof. Doutora Maria M. M. Santos, FF-UL



FACULDADE DE
CIÊNCIAS E TECNOLOGIA
UNIVERSIDADE NOVA DE LISBOA

Outubro 2015

LOMBADA



Enantiopure bicyclic lactams: synthesis and biological evaluation

2015



Margarida Leonor Florindo Espadinha

Licenciatura em Química Aplicada

Enantiopure bicyclic lactams: synthesis and biological evaluation

Dissertação para obtenção do Grau de Mestre em Química
Bioorgânica

Orientador: Prof. Doutora Maria M. M. Santos, FF-UL

Elemento de Ligação: Prof. Doutora Paula Sérgio Branco, FCT

Presidente: Prof. Doutora Paula Sérgio Branco, FCT-UNL

Arguente: Doutor Vasco Bonifácio, IST-CQFM

Vogal: Prof. Doutora Maria M. M. Santos, FF-UL



Outubro 2015

Enantiopure bicyclic lactams: synthesis and biological evaluation

Margarida Leonor Florindo Espadinha, *Copyright*

A Faculdade de Ciências e Tecnologia e a Universidade Nova de Lisboa têm o direito, perpétuo e sem limites geográficos, de arquivar e publicar esta dissertação através de exemplares impressos reproduzidos em papel ou de forma digital, ou por outro qualquer meio conhecido ou que venha a ser inventado e de divulgar através de repositórios científicos e de admitir a sua cópia e distribuição com objectivos educacionais ou de investigação, não comerciais, desde que seja dado crédito ao autor e editor.

Acknowledgements

I would like to thank Professor Dr. Maria M. M. Santos for all the support, supervision and transmitted knowledge during the last year.

I would also like to thank Jorge Dourado for the synthesis of (*S*)-phenylalaninol-derived bicyclic lactams mentioned in this master thesis.

A big thanks to Dr. Lúcia Gonçalves and Dr. Raquel Frade for the biological assays in cell lines.

I would like to thank Professor Dr. Cristobal de los Rios for the NMDA receptor antagonist assays performed in *Universidad Autonoma de Madrid*, in Spain.

Dr. Elies Molins is gratefully acknowledged for performing the X-ray analysis.

I would also like to thank Professor Dr. Rosário Bronze for the elementary analysis performed.

I would like to thank everyone in lab 106-108, at *Research Institute for Medicines (iMed.Ulisboa)*, for their support and help during my work performed in *Faculdade de Farmácia* of *Universidade de Lisboa*.

I would also like to FCT (Fundação para a Ciência e a Tecnologia) by support through the research project PTDC/QUI-QUI/111664/2009, and in part by iMed.Ulisboa (UID/DTP/04138/2013).

Also, a special thanks to my family, mainly to my parents for financially sustaining me and for their support.

Finally, I would like to thank Ricardo who has been by my side in all important moments in the last years.

Part of the results of this work was included in the following scientific communication:

Poster

M. Espadinha, C. de los Rios, M. M. M. Santos, " Hit-to-lead optimization of Phenylalaninol-derived oxazolopyrrolidone lactams and evaluation as NMDA receptor antagonists", in the "7th iMed.Ulisboa Post Graduate Students Meeting", Faculdade de Farmácia, Lisbon, Portugal, 15-16 of July of **2015**.

Article in international journal

M. Pérez, M. Espadinha, M. M. M. Santos, "Indolo[2,3-*a*]quinolizidines and derivatives: Bioactivity and asymmetric Synthesis", *Curr. Pharm. Design* (thematic issue "Challenging organic syntheses and pharmacological applications of natural products and their derivatives") vol.21, **2015** (accepted).

Abstract

N-Methyl-*D*-Aspartate (NMDA) receptors are fundamental for the normal function of the central nervous system and have an important role in memory and learning. An overactivation of these receptors results into an influx of excess of calcium cation (Ca^{2+}) leading to neuronal loss associated with major degenerative disorders including Parkinson's and Alzheimer's diseases. Since the 80s, a big interest emerged of both academia and industry to develop drugs targeting the NMDA subtype of glutamate receptors with potential application for the treatment of some degenerative disorders. The main successes were amantadine (**39**) and memantine (**40**), two compounds which belong to adamantanes's family, approved by FDA and used currently in the clinic.

Another important area of therapeutic interest is cancer, which is considered the first and second causes of deaths on developed and developing countries, respectively. Statistical studies estimate that in 2030 the number of deaths caused by this disease will be 13.2 million. For this reason, it is essential the discovery of new methodologies and therapeutic agents for the treatment of cancer.

The main goal of this thesis is the enantioselective synthesis of small molecules, more precisely phenylalaninol- and tryptophanol-derived bicyclic lactams, with potential application as NMDA receptor antagonists and antitumor agents, respectively. From the library of phenylalaninol derivatives, two new were promising NMDA receptor antagonists were identified. In particular, compounds **1c** and **1d** revealed to be more active than the hit compound, **1a**, with IC_{50} values of 39 μM and 36 μM , respectively. Derivatives of another amino alcohol, (1*S*, 2*R*)-(-)-*cis*-1-amino-2-indanol, were also synthesized and a new antagonist, compound **6b**, was identified with IC_{50} value of 51 μM . A hit-to-lead process of these three compounds was performed and the determination of respective IC_{50} values is in progress.

For the series of tryptophanol derivatives, a hit compound (**4c**) was identified which revealed an IC_{50} value of 60 μM in MCF-7 cell lines (breast adenocarcinoma). A structural derivatization was performed, leading to five more active compounds (**8b-f**) with IC_{50} values between 6.7 and 9.0 μM , for the same cancer cell line. Furthermore, these five compounds were also evaluated in other cancer cell lines, and revealed to be selective for MCF-7 cell line, as well as non-toxic for normal cells (HEK 293).

Keywords: enantioselective synthesis, NMDA receptor, antagonists, cytotoxicity, anti-tumor agents.

Resumo

O receptor *N*-metil-*D*-aspartato (NMDA) é fundamental para a função normal do sistema nervoso central e responsável pela memória e aprendizagem. A activação excessiva destes receptores resulta num fluxo superior de iões cálcio (Ca^{2+}) que conduz a perda neuronal associada a grandes desordens degenerativas, incluindo as doenças de Parkinson e Alzheimer. Desde os anos 80, surgiu um grande interesse académico e da indústria sobre o potencial terapêutico de antagonistas dos receptores NMDA, mas precisamente os receptores de glutamato, com aplicação no tratamento de algumas doenças degenerativas. Os principais sucessos foram a amantadina e a memantina, dois compostos que pertencem à família dos adamantanos, e, atualmente, são aprovados pela FDA e estão comercialmente disponíveis como agentes terapêuticos.

Outra área de interesse é o cancro, que é considerada a primeira e a segunda causas de morte nos países desenvolvidos e nos países em desenvolvimento, respectivamente. Estudos estatísticos estimam que em 2030 o número de mortes causadas por esta doença seja 13,2 milhões. Por esta razão, é necessária a descoberta de novos métodos e agentes terapêuticos para o tratamento de cancro.

O principal objetivo desta tese é a síntese enantioselectiva de pequenas moléculas, mais precisamente oxazolpirrolidonas derivadas dos amino álcoois fenilalaninol e triptofanol, com aplicação como antagonistas dos receptores NMDA e agentes antitumorais, respectivamente. Nos derivados do fenilalaninol foram identificados dois novos compostos promissores: **1c** e **1d** revelaram ser mais activos que o composto de referência, **1a**, com valores de IC_{50} de 39.0 e 36.0 μM , respectivamente. Foram também sintetizados derivados de um outro amino-álcool, (1*S*, 2*R*) - (-) - cis-1-amino-2-indanol, e foi identificado um novo composto antagonista (**6b**) com IC_{50} = 51.0 μM . Foi realizado um processo de optimização destes três compostos e a determinação dos respectivos valores de IC_{50} está a decorrer.

No caso dos derivados do amino álcool triptofanol foi identificado o composto **4c**, que revelou um valor IC_{50} = 60.0 μM em linhas celulares MCF-7, que correspondem a um adenocarcinoma de mama. Posteriormente, foram realizadas derivatizações estruturais e cinco compostos (**8b-f**) demonstraram um aumento interessante de actividade com valores de IC_{50} entre 6.7 e 9.0 μM , para a mesma linha celular de cancro. Além disso, estes compostos foram avaliados em outras cinco linhas celulares de cancro, revelando-se selectivos para a linha celular cancerígena MCF-7 e não tóxicos para as células não tumorais (células HEK 293).

Index

Acknowledgements	I
Abstract	III
Resumo	V
Index of figures	IX
Index of schemes	XI
Index of tables	XIII
Index of graphs	XV
Abbreviations	XVII
Chapter I – Introduction	1
I.1 - Enantioselective synthesis	2
I.1.1 - Synthesis from the chiral pool	3
I.1.2 - Resolution of racemates	4
I.1.2.1 - Kinetic resolution	4
I.1.2.2 - Direct preferential crystallization	5
I.1.2.3 - Chromatography	6
I.1.3 - Asymmetric synthesis	6
I.1.3.1 - Chiral auxiliaries and chiral reagents	7
I.1.3.2 - Chiral catalysts and biotransformation	8
I.2 - Importance of enantioselective synthesis	8
I.3 - Synthesis of chiral non-racemic bicyclic lactams	9
I.4 - Neurodegenerative diseases	10
I.4.1 - Role of <i>N</i>-Methyl-<i>D</i>-Aspartate receptor in neurodegeneration	10
I.4.2 - Function and structure of NMDA receptor channel	11
I.4.3 - NMDA receptor antagonists	13
I.4.3.1 - Competitive antagonists acting at the glycine site	14
I.4.3.2 - Competitive antagonists acting at the glutamate site	16
I.4.3.3 - Non-competitive antagonists acting at ion channel	17
I.4.3.4 - Non-competitive antagonists acting at GluN2B subunit	19
I.4.3.5 - Oxazolopyrrolidones as NMDA receptor antagonists	19
I.5 - The worldwide problem of cancer	21
I.5.1 - Indole compounds as antitumor agents	21
Chapter II – Results and Discussion	25
II.1 - Synthesis of phenylalaninol and tryptophanol-derived bicyclic lactams	26
II.2 - Biological evaluation of phenylalaninol-derived bicyclic lactams	33

II.2.1 - Hit-to-lead optimization	36
II.3 - Biological evaluation of tryptophanol-derived bicyclic lactams	42
II.3.1 - Hit-to-lead optimization process	43
Chapter III – Conclusion and Future Work	51
Chapter IV – Experimental Procedure	53
IV.1 - General methods	54
IV.2 - General procedure for cyclocondensation reactions	54
IV.2.1 - (<i>S</i>) and (<i>R</i>)-phenylalaninol-derived bicyclic lactams	54
IV.2.2 - (<i>S</i>) and (<i>R</i>)-tryptophanol-derived bicyclic lactams	61
IV.2.3 - (<i>S</i>)-tyrosinol-derived oxazolopyrrolidone lactams	68
IV.2.4 - Indanol-derived oxazolopyrrolidone lactams	69
IV.3 - General procedure for Suzuki Coupling reactions	72
IV.3.1 - (<i>S</i>)-phenylalaninol-derived oxazolopiperidone lactams	72
IV.3.2 - (<i>R</i>)-tryptophanol-derived oxazolopiperidone lactams	73
IV.4 - General procedure for Indole Protection reactions	77
IV.4.1 - Method 1 for indole protection of (<i>R</i>)-tryptophanol-derived oxazolopyrrolidone lactams	77
IV.4.2 - Method 2 for indole protection of (<i>R</i>)-tryptophanol-derived oxazolopyrrolidone lactams	80
IV.5 - Cytotoxicity assay in human cell lines	82
Chapter V – References	83
Chapter VI – Annex	91
VI.1 - Measurement of cytosolic Ca ²⁺ concentrations increases induced by NMDA receptor.	91

Index of figures

Figure 1 – Common molecules (1 - 8) used in chiral pool synthesis	3
Figure 2 – Ionotropic glutamate receptors, NMDAR, KAR and AMPAR, and their antagonists (16 - 18).....	10
Figure 3 – The excitatory neurotransmitter glutamate (19) and glycine (20)	11
Figure 4 – Operation of a NMDA receptor: activation by glutamate (19) and glycine (20) allows the influx of Ca ²⁺ into the neuron	12
Figure 5 – Representation of GluN1-GluN2 NMDA receptor and their structure (subunits and domains).....	13
Figure 6 – Chemical structures of co-agonist glycine (20) and the first reported antagonists for glycine site, (<i>R</i>)-HA-966 (21), L-687,414 (22) and kynurenic acid (23).....	14
Figure 7 – Derivatives of kynurenic acid (23): 5,7-dichlorokynurenic acid (5,7-DCKA) (24), L-683,344 (25), L-689,560 (26), GV150526A (27) and GV196771A (28).....	15
Figure 8 – Chemical structures of quinoxalinedione derivatives DNQX (29) and ACEA-1021 (30); pyridazinoquinolinetriones derivative (31)	15
Figure 9 – GLYX-13 (32), a polypeptide compound that acts in glycine site	16
Figure 10 – Structure of compounds inspired in glutamate (19): D-AP5 (33), CGP 37849 (34) and CGS 19755 (35)	16
Figure 11 – Structure of cyclic compounds that act in GluN2 subunit	17
Figure 12 – Schematic representations of NMDA receptor channel blockers	18
Figure 13 – Chemical structures of non-competitive antagonists of GluN2B: ifenprodil (46), Ro 25-6981 (47) and compounds 48 and 49 , patented by <i>Cold Spring Harbor Laboratory</i>	19
Figure 14 – Oxazolidine derivatives (50 and 51) patented in 2009. Oxazolopirrolidone (1a) antagonist of NMDA receptor reported by our group	20
Figure 15 – Some of biological activities responsible of indole moiety	22
Figure 16 – Chemical structure of tubulin inhibitors: BPR0L075 (52) and derivative (53), D-24851 (54)	23
Figure 17 – Antitumor agents: panobinostat (55) and aplysinopsin analog (56)	23
Figure 18 – Chemical structures of <i>L</i> -tryptophan (57) and DNMT1 inhibitors (RG108 (58) and their analogs 59 and 60)	24
Figure 19 – <i>L</i> -tryptophan derivatives 61 and 62 reported with inhibitory bioactivities against β-D-galactosidase and β-D-glucosidase	24
Figure 20 – Chemical structure of compound 3b and respective crystallographic representation	32
Figure 21 – ¹ H-NMR spectra of compound 3b between 3.0 and 4.7 ppm	32
Figure 22 – ¹ H-NMR spectra of compound 6e between 3.00 and 6.20 ppm	38

Figure 23 – Chemical structure of compound 6e and respective crystallographic representation	39
Figure 24 – Several perspectives of compound 6e	39
Figure 25 – Chemical structure of hit compound 4c , a (<i>R</i>)-tryptophanol-derived oxazolopyrrolidone lactam	43
Figure 26 – Compounds 9a , 9c and 9f , corresponding to protections of nitrogen atom of the indole protections	44
Figure 27 – Chemical structures of compounds 8a-c	46
Figure 28 – Compound 4i , (<i>R</i>)-tryptophanol-derived oxazoloisindolinone	46
Figure 29 – Compounds presented in second screening of 4c optimization	47

Index of schemes

Scheme 1 – Chiral pool synthesis, asymmetric synthesis and resolution: distinct methods to get enantiomerically pure compounds	2
Scheme 2 – Asymmetric synthesis of (+)-deplancheine (14) by a Pictet-Spengler cyclization from a (<i>S</i>)-tryptophanol-derived lactam	4
Scheme 3 – Illustration of kinetic and dynamic kinetic resolution with the use of a biocatalyst	5
Scheme 4 – Representation of the direct preferential crystallization process	6
Scheme 5 – Use of a chiral auxiliary in the synthesis of enantiopure piperidines	7
Scheme 6 - Synthesis of non-racemic bicyclic lactam derived from (<i>R</i>)-phenylglycinol (15)	9
Scheme 7 – Illustration of retrosynthetic analysis of oxazolopyrrolidone	26
Scheme 8 – Reaction mechanism for the synthesis of compound 1a	27
Scheme 9 – Spatial arrangement of diastereomers (<i>3S</i> , <i>7aR</i>) and (<i>3S</i> , <i>7aS</i>).	28
Scheme 10 – Representation of resonance hybrid of imine.....	31

Index of tables

Table 1 – Reaction yields for (<i>S</i>)-phenylalaninol-derived bicyclic lactams	29
Table 2 – Reaction yields for (<i>R</i>)-phenylalaninol-derived bicyclic lactams	29
Table 3 – Reaction yields for (<i>S</i>)-tryptophanol-derived oxazolopyrrolidone lactams	30
Table 4 – Reaction yields for (<i>R</i>)-tryptophanol-derived oxazolopyrrolidone lactams	30
Table 5 – Chemical shift (δ) of C-7a in (<i>S</i>)-phenylalaninol and (<i>S</i>)-tryptophanol derivatives ..	33
Table 6 – IC ₅₀ values determined for compounds 1a , 1c , 1d and memantine (40).....	35
Table 7 – (<i>S</i>)-tyrosinol derivatives synthesized and respective reaction yields	36
Table 8 – (1 <i>S</i> , 2 <i>R</i>)-(-)- <i>cis</i> -1-Amino-2-indanol derivatives synthesized and respective reaction yields	37
Table 9 – Others derivatives of (1 <i>S</i> , 2 <i>R</i>)-(-)- <i>cis</i> -1-Amino-2-indanol and (<i>S</i>)-tyrosinol	38
Table 10 – IC ₅₀ value obtained for compound 6b	40
Table 11 – Screening of (<i>S</i>)- and (<i>R</i>)-tryptophanol-derived bicyclic lactams 3b – f and 4a – h	42
Table 12 – IC ₅₀ values of selected compounds of (<i>S</i>) and (<i>R</i>)-tryptophanol library	43
Table 13 – IC ₅₀ values of optimized compounds	46
Table 14 – Yields of reactions of optimization	48
Table 15 – IC ₅₀ values of optimized compounds.....	49
Table 16 – IC ₅₀ values of the most promising compounds in several cell lines	50

Index of graphs

Graph 1 – Screening of (<i>S</i>)-phenylalaninol-derived bicyclic lactams 1a – i	34
Graph 2 – Screening of (<i>R</i>)-phenylalaninol-derived bicyclic lactams 2a – i	34
Graph 3 – Results of inhibition of Ca ²⁺ increase by 6a and 6b compounds ((1 <i>S</i> , 2 <i>R</i>)-(-)- <i>cis</i> -1-Amino-2-indanol derivatives)	40
Graph 4 – Results of inhibition of Ca ²⁺ increase of compounds 5a - b and 6c - e	41
Graph 5 – Screening of optimized compounds at 50µM, in MCF-7 cell lines	44
Graph 6 – Screening of optimized compounds at 20µM, in MCF-7 cell lines	45
Graph 7 – Screening of last optimized compounds at 20µM, in MCF-7 cell lines	48

List of Abbreviations

AcOEt	ethyl Acetate
AMPA	α -amino-3-hydroxy-5-methyl-4-isoxazolepropionic acid
AMPAR	α -amino-3-hydroxy-5-methyl-4-isoxazolepropionic acid receptor
ATD	amino-terminal domain
Bn	benzyl
Boc	<i>tert</i> -butyloxycarbonyl
c	concentration
¹³C-NMR	carbon nuclear magnetic resonance
CDCl₃	deuterated chloroform
CNS	central nervous system
CH₂Cl₂	dichloromethane
CTD	carboxy-terminal domain
CV	cell viability
d	doublet
dd	double doublet
dt	double triplet
DMF	dimethylformamide
DMSO	dimethylsulfoxide
DNMT	DNA methyltransferases
Dopa	3,4-dihydroxyphenylalanine
equiv.	equivalent
Et	ethyl
FC	flash chromatography
g	gram
h	hour
¹H-NMR	proton nuclear magnetic resonance
HPLC	high pressure liquid chromatography
Hz	hertz
IAPs	inhibitors apoptosis proteins
IC₅₀	half maximal inhibitory concentration
iGluRs	ionotropic glutamate receptors

IUPAC	International Union of Pure and Applied Chemistry
<i>J</i>	coupling constant
KA	kainic acid
KAR	kainic acid receptor
LBD	ligand binding domain
LiAlH₄	lithium aluminum borohydride
m	multiplet
MDM2	mouse double minute 2 homolog
MDMX	mouse double minute 4 homolog
MeOD	deuterated methanol
mGluR	metabotropic glutamate receptor
min	minute
mL	milliLiter
mmol	millimole
mp	melting point
MTT	3-(4,5-dimethyl-2-thiazolyl)-2,5-diphenyl-2H-tetrazolium
NaCl	sodium chloride
NaH	sodium hydride
NaHCO₃	sodium bicarbonate
nM	nanoMolar
NMDA	<i>N</i> -Methyl- <i>D</i> -Aspartate
NMDAR	<i>N</i> -Methyl- <i>D</i> -Aspartate receptor
NMR	nuclear magnetic resonance
NO	nitric oxide
NOESY	nuclear overhauser effect spectroscopy
Pd(PPh₃)₂Cl₂	bis(triphenylphosphine)palladium(II) dichloride
ppm	parts per million
p53	tumor protein p53
q	quartet
RNA	ribonucleic acid
ROS	reactive oxygen species
rt	room temperature
s	singlet

T	temperature
t	triplet
TD	trans-membrane domain
TEA	triethylamine
THF	tetrahydrofuran
TLC	thin layer chromatography
Ts	tosyl
δ	chemical shift
μM	microMolar

Chapter I – Introduction

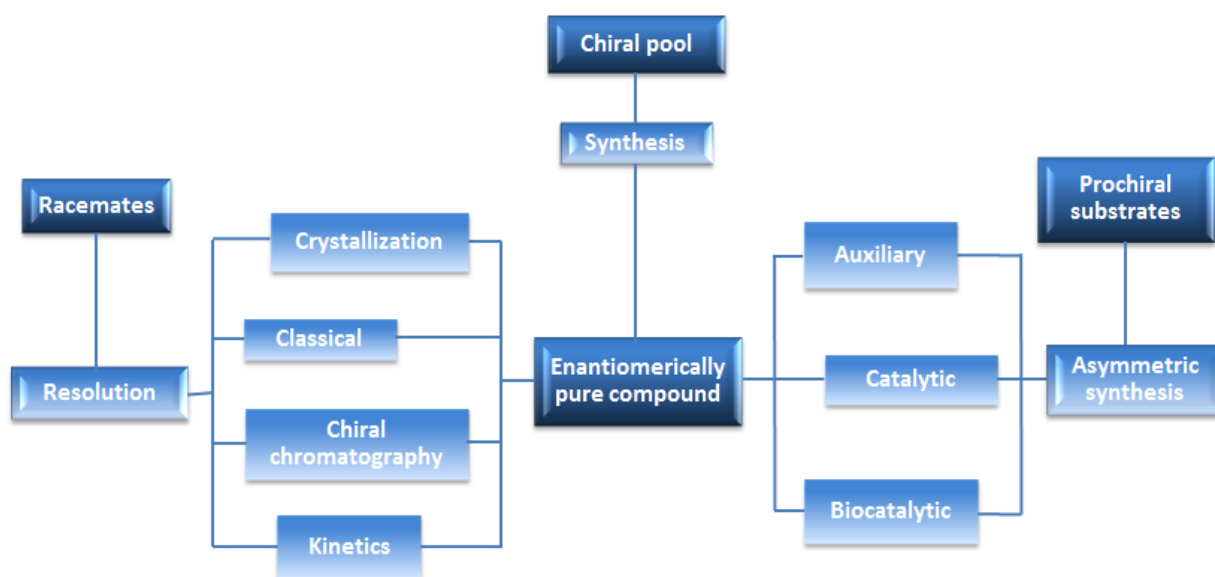
I.1 – Enantioselective synthesis

An enantiomer is defined by IUPAC as a pair of molecular entities which are mirror images of each other and non-superposable. This is possible if the molecule has one or more chiral centers and this feature is responsible for the ability of the enantiomers to rotate the plan-polarized light (+/-) by equal amounts but in opposite directions [1].

Currently, there are distinct methodologies to access enantiomerically pure compounds. These methodologies can be divided into three main categories:

- Use of chiral starting material, chiral-pool, such as amino acids/ alcohols, alkaloids and carbohydrates;
- Resolution of a racemic mixture;
- Use of chiral agents in order to introduce a chiral center in a prochiral molecule. This approach is called asymmetric synthesis.

On scheme 1 are shown these three methodologies of synthesis/resolution to obtain a single-enantiomer [2].



Scheme 1 – Chiral pool synthesis, asymmetric synthesis and resolution: distinct methods to get enantiomerically pure compounds [2].

I.1.1 – Synthesis from the chiral pool

The chiral pool method is based on the use of optical active raw material that is available from a natural source. The strategy is to use these molecules as precursors in the synthesis of more complex molecules, by manipulating the chiral starting material to obtain the target molecule [2]. For many decades the chiral pool method was the only process of synthesis known to obtain a chiral molecule. Nowadays it is still an attractive and economic way of enantioselective synthesis [3]. Carbohydrates, amino acids, alkaloids and terpenes are very important members of the chiral pool (figure 1) [2].

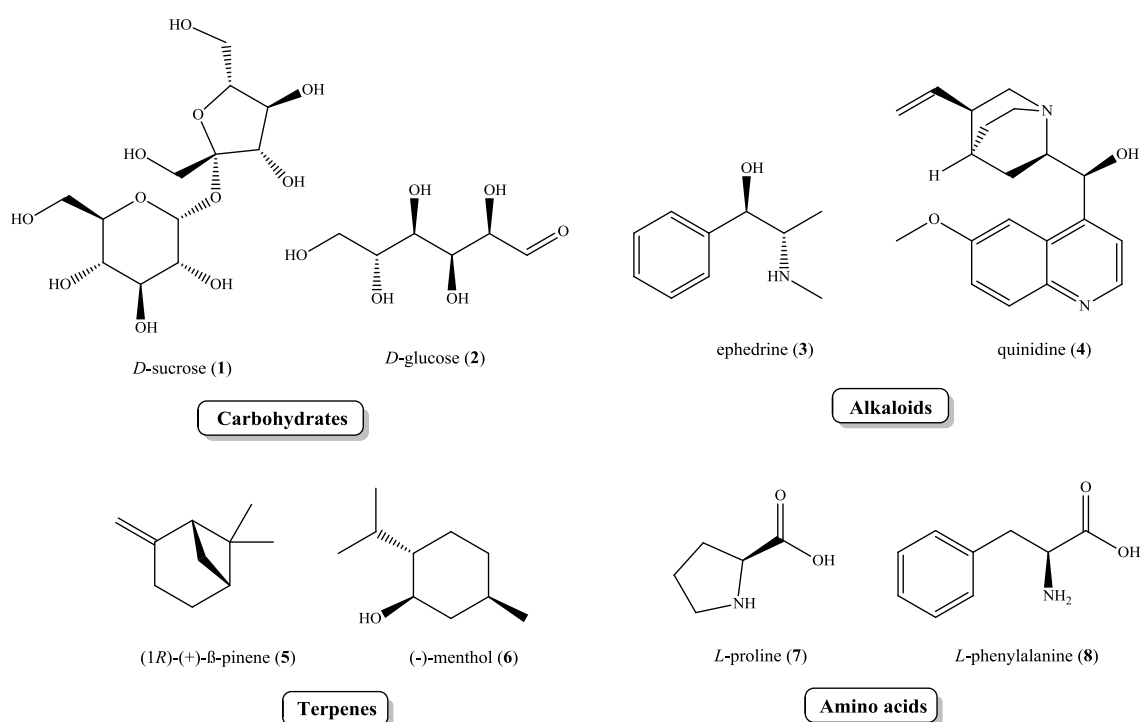
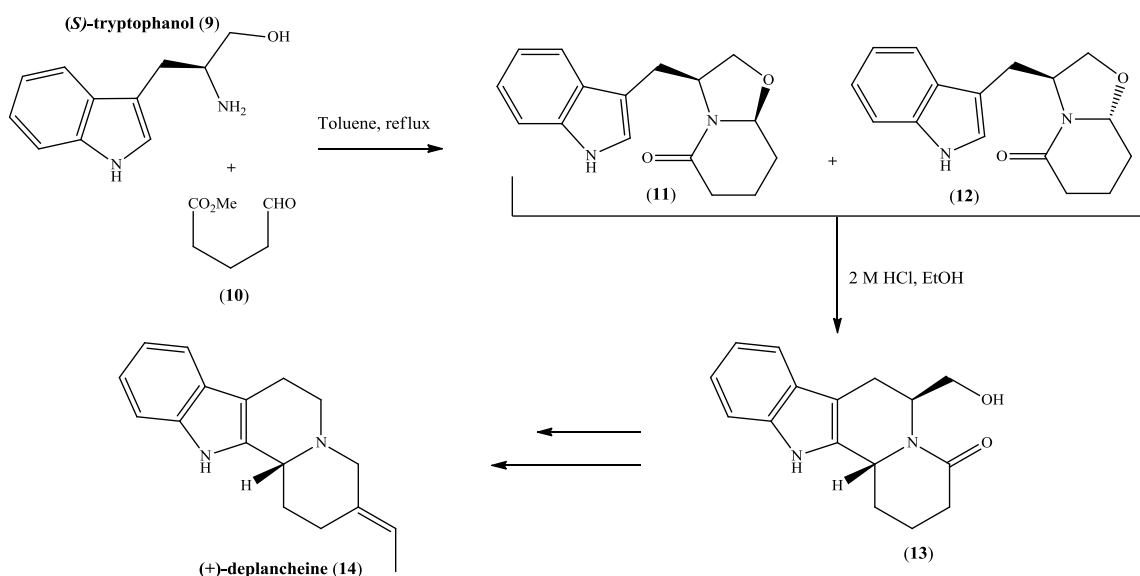


Figure 1 – Common molecules (1 - 8) used in chiral pool synthesis.

The synthesis of some natural products as (+)-deplancheine (**14**), an alkaloid with an unusual corynantheine-type structure that was isolated from the plant *Alstonia deplanchei* is an example of this synthesis. The synthesis was proposed by Steven M. Allin, in 2005, and starts with the amino alcohol (*S*)-tryptophanol (**9**) to give a (*S*)-tryptophanol-derived lactams **11** and **12**. A Pictet-Spengler cyclization of lactam and successive reactions leads on the synthesis of (+)-deplancheine (**14**) (scheme 2) [4].



Scheme 2 – Asymmetric synthesis of (+)-deplancheine (**14**) by a Pictet-Spengler cyclization from a (*S*)-tryptophanol-derived lactam [4].

In the 90s, the chiral pool synthesis was the most used method to synthesize chiral compounds with potential therapeutic use, representing 80% of the asymmetric synthesis methods. Currently, just 25% of the commercial drugs are synthesized from the chiral pool [2].

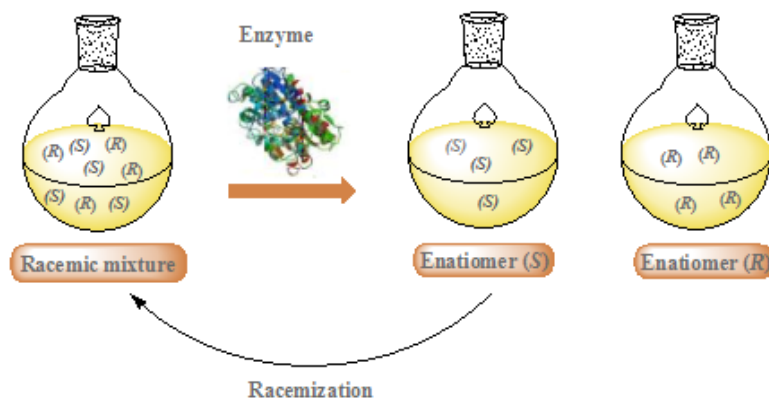
I.1.2 - Resolution of racemates

The resolution is characterized by the separation of a racemate into its components and can be divided into three categories: kinetic resolution, direct preferential crystallization and chromatography [2].

I.1.2.1 - Kinetic resolution

A kinetic resolution is based on the difference of reactivity between enantiomers in the presence of a chiral agent, i.e., chiral catalyst or reagent. The most reactive species is readily transformed into the product, while the slow reactive species results in unreacted substrate (scheme 3). The chiral catalyst can be a biocatalyst (enzyme or microorganism) or a chemocatalyst (chiral acid/base or chiral metal complex). Kinetic resolution is not a very efficient method because the maximum theoretical yield is 50%. Dynamic kinetic resolution is based on the rapid racemization of the unreacted enantiomer before its transformation into a product (scheme 3). This process is more efficient because it is possible to isolate the product up to 100% yield (there is total

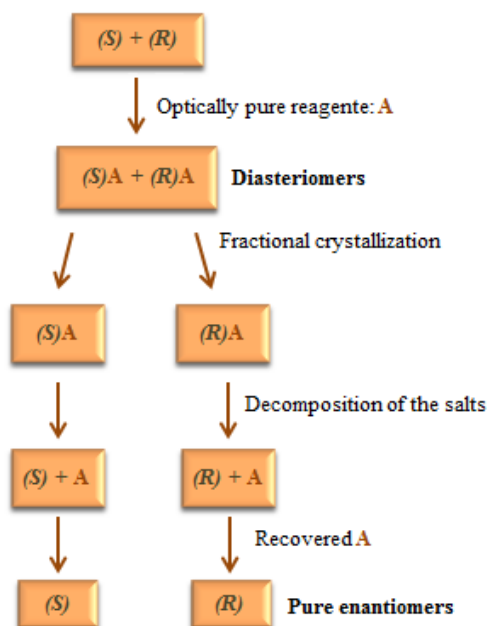
consumption of the racemic mixture). The racemization of the unreacted substrate can be accomplished by using a catalyst [2, 5].



Scheme 3 – Illustration of kinetic and dynamic kinetic resolution with the use of a biocatalyst [2, 5].

I.1.2.2 - Direct preferential crystallization

Crystallization is the process of formation of crystals of the desired product by precipitating from a solution. This method has been explored for the separation and resolution of enantiomers from a racemic mixture [2]. Crystallization of diastereomeric derivatives is frequently used and is considered a “classical resolution”. The main goal of this process is to interact a mixture of enantiomers with an enantiopure compound. This will result in two diastereomers which have different physical properties that can be separated by normal fractional crystallization. The resolving reagent (enantiopure compound) should react easily, in good yield and must be separated from substrate, in the last step of the process substrate. After separation, decomposition of the salts is easily performed by a change in pH (scheme 4) [5].



Scheme 4 – Representation of the direct preferential crystallization process.

I.1.2.3 - Chromatography

Resolution by preparative chiral chromatography has the same principles as standard chromatography methodology [2]. This technique is an important tool for the separation of enantiomers [5]. There are two types of chromatography, more precisely HPLC (High Pressure Liquid Chromatography) to separate a mixture of enantiomers: direct and indirect methods. The direct method is characterized by the use of a chiral selector and the enantiomers are separated by the formation of noncovalent diastereomeric pairs of molecules.

In the indirect method it is used a classical reverse-phase column and requires derivatization of the racemate with a chiral reagent to form a mixture of diastereomers. These diastereomers have different physical properties and can be separated easily [2].

I.1.3 - Asymmetric synthesis

Asymmetric synthesis is a reaction or a sequence of reactions where the configuration of one or more new stereocenters is selectively formed. There are two approaches to perform an asymmetric reaction:

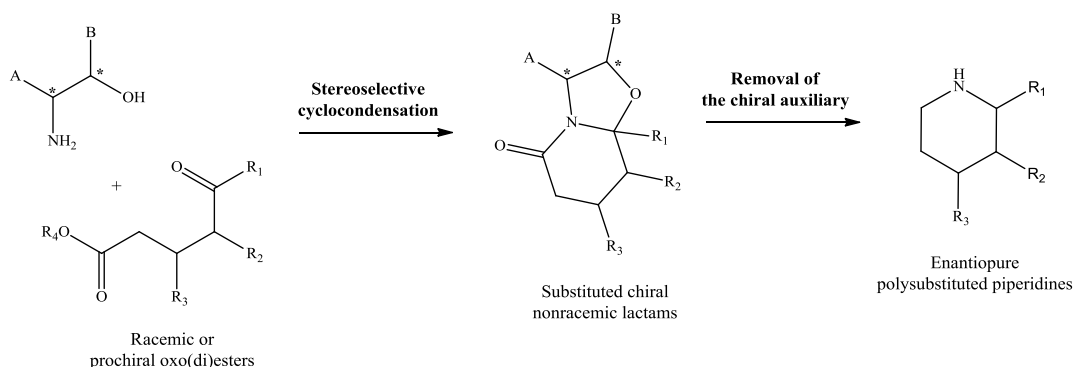
- The starting material is an achiral molecule that is enantioselective converted into a chiral molecule;

- The starting material is a chiral molecule that is diastereoselectively converted into a new chiral molecule.

Despite the impressive progress in recent years in asymmetric syntheses, the most used method of production to obtain a single enantiomer in industrial synthesis is the resolution of racemic mixtures. However, asymmetric synthesis is a powerful tool in pharmaceutical area due to the important role of chirality in biological activity [2].

I.1.3.1 – Chiral auxiliaries and chiral reagents

Without chiral auxiliaries, a prochiral molecule reacts with an achiral reagent leading to a racemate mixture because the transition states of two enantiomers have the same energy. When a chiral auxiliary is incorporated in a prochiral molecule, one diastereomer will have more energy than the other – stereoselective reaction. This case of asymmetric synthesis is a limited approach because is necessary of attachment and removal steps (scheme 5) [5, 6].



Scheme 5 – Use of a chiral auxiliary in the synthesis of enantiopure piperidines.

Asymmetric synthesis by chiral reagents is a convenient method for an efficient formation of stereogenic centers. The chiral reagent will be part of the final product's structure and it's responsible for the formation of new chiral centers.

I.1.3.2 – Chiral catalysts and biotransformation

Asymmetric catalysis is defined as a type of catalysis where a chiral catalyst allows the formation of a chiral compound. Each molecule of catalyst can induce chirality of thousands of chiral molecules [5].

Biocatalyst has an important role in asymmetric synthesis and not surprisingly, many microorganisms are used to synthesize optically active compounds. Nature is available to give many important enzymes such as esterases, amidases, aldolases and others, and for this reason, this type of catalysis is considered profitable, as well as a “green” methodology [2]. Associated with various methodologies of synthesis, biocatalysts can be a powerful tool for the synthesis of important molecules, such as alkaloids [7].

The methodology of enantioselective synthesis used to obtain most of the compounds synthesized in this thesis was based in chiral pool synthesis.

I.2 - Importance of enantioselective synthesis

In 1848, Louis Pasteur discovered for the first time that salts of tartaric acid exist in two isomeric forms. He proposed that these two forms were different compounds and that each compound could rotate the plane of polarized light in opposite directions. This important information was the first step for the discovery of more racemic mixtures and the beginning for enantioselective synthesis. However, just a century later the phenomenon of chirality was considered essential not only in the life of animals and plants but also in pharmaceutical and others important industries. This importance is easily understood since chirality is present in proteins, amino acids, nucleosides, hormones and other chiral compounds that are fundamental for the existence of life [8, 9].

With the advent of new techniques, investigations were facilitated into the biological roles played by enantiomers, as well as in the large-scale preparation of enantiopure compounds. Today, researchers and regulatory authorities know how important is the stereochemistry in the action of a drug and the contribution in the development of enantioselective synthesis is always a good investment [8, 10].

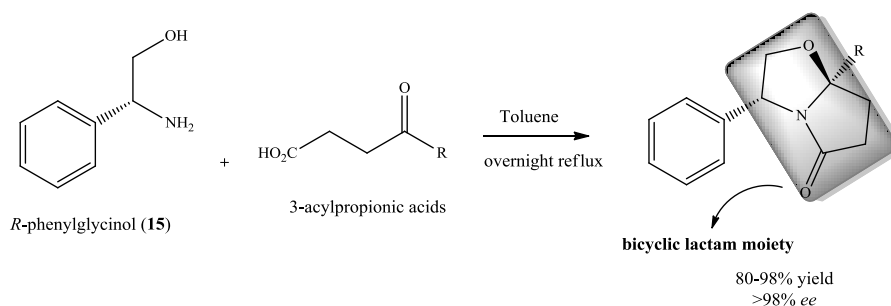
Approximately 56% of the drugs in the market are chiral products and 88% of the last ones are racemic mixtures. It is well known that enantiomers have different biological activities. Sometimes one enantiomer is more potent than other, others each enantiomer has a specific biological target. Dopa (3,4-dihydroxyphenylalanine), a known precursor of dopamine, was used in racemic form for the treatment of Parkinson disease. Later, it was discovered that the *D*-

isomer was responsible for the appearing of agranulocytosis. As a consequence, today only *L*-dopa is used in the clinic [9].

I.3 - Synthesis of chiral non-racemic bicyclic lactams

Bicyclic lactams are well studied and have been used as intermediates to produce new chiral compounds in high enantiomeric purity.

Meyers was the first to introduce the use of enantiopure amino alcohols and γ -ketoacids in the synthesis of non-racemic bicyclic lactams. This synthesis allows an asymmetric construction of quaternary carbon centers. The first reaction reported was with the use of (*R*)-phenylglycinol (**15**) and 3-acylpropionic acids (scheme 6) [11].



Scheme 6 – Synthesis of non-racemic bicyclic lactam derived from (*R*)-phenylglycinol (**15**) [10].

This approach is considered the most expedient since it involves just a one-step reaction with the formation of a new chiral center. Amino alcohols/acids are abundant in nature and are commercially available. They can also be obtained by reduction of the corresponding amino acid with lithium aluminum hydride or synthesized from the beginning [12-15].

After the first efficient methodology reported for synthesis of bicyclic lactams others publications emerged, including the use of this type of compounds as precursors for the synthesis of pyrrolidines, pyrrolidinones, piperidones, quinolizidines, indolizidines, azepines derivatives and others type of compounds [16-25].

In this thesis, chiral non-racemic bicyclic lactams were synthesized starting from different enantiopure amino alcohols amino alcohols, in order to be evaluated as NMDA receptor antagonists and as potential anti-tumor agents.

I.4 – Neurodegenerative diseases

Nervous system dysfunction is associated to neurodegenerative diseases and result from the gradual and progressive loss of neural cells.

Alzheimer, Parkinson and Huntington are three examples of diseases associated to neurodegeneration. These disorders result in accumulation of insoluble filamentous aggregates that take the form of amyloid. These aggregates are composed by proteins or peptides and each disease is characterized by a specific type of amyloidogenic protein [26, 27].

With the increase in life expectancy of world population, neurodegenerative diseases are currently one of the largest societal concerns. Nowadays there is a lack of care for this type of diseases and the most common treatments are drugs for chronic use. These treatments are not efficient and are just a way to delay the biochemical processes of neurodegenerative diseases. So, it is important the development of more effective therapies and to combat the economic costs associated with current therapies [26, 28].

I.4.1 – Role of *N*-Methyl-D-Aspartate receptor in neurodegeneration

N-Methyl-D-Aspartate receptors, also known as NMDA receptors, belong to the family of ionotropic glutamate receptors (iGluRs) and their agonist is *N*-methyl-D-aspartic acid (**16**). There are two other receptors that comprise the family of iGluRs: receptors of kainic acid (KAR) and receptors of α -amino-3-hydroxy-5-methyl-4-isoxazolepropionic acid (AMPA) (figure 2). All these receptors are related to the normal development of nervous system and are associated with a number of neurodegenerative diseases [29, 30].

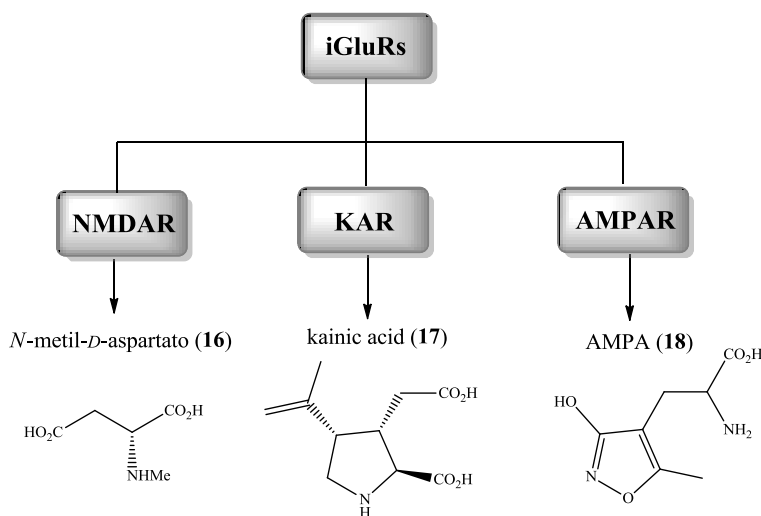


Figure 2 – Ionotropic glutamate receptors, NMDAR, KAR and AMPAR, and their antagonists **16** - **18**.

The amino acid glutamate (**19**) (figure 3) is the major excitatory neurotransmitter in central nervous system (CNS) and is responsible for 40% of synapses in CNS. The local of action of glutamate is on ionotropic and metabotropic glutamate receptors. These receptors are located at presynaptic terminal and postsynaptic membrane at synapses in the brain and spinal cord. Glutamate (**19**) plays an important role in neural activation [31].

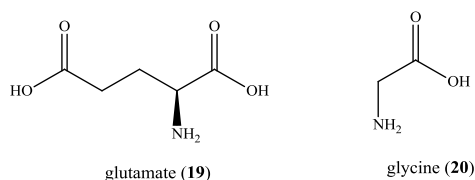


Figure 3 – The excitatory neurotransmitters glutamate (**19**) and glycine (**20**).

Ionotropic glutamate receptors are fundamental for the normal function of central nervous system and responsible for the memory and learning [32]. The NMDA receptors are neural ionotropic channels, ligand-gated and voltage dependent. Excessive activation of NMDA receptors leads to neuronal loss associated with major degenerative disorders including Parkinson's and Alzheimer's diseases [33].

The neurotransmitter glutamate (**19**) is released into the synaptic cleft during the normal synaptic transmission. In this moment, glutamate (**19**) is available to do the activation of NMDA receptors for a brief period of time. When excess of glutamate (**19**) exists derived from accumulation in synaptic cleft, this leads to cell death, a phenomenon also called as excitotoxicity. This over activation of NMDA receptors results into an influx of excess of calcium cation (Ca^{2+}). High levels of Ca^{2+} have serious consequences into normal functions of mitochondrial system and the production of reactive oxygen species (ROS), and nitric oxide (NO) radicals result in cell death by oxidative stress and excitotoxicity [33-35].

I.4.2 - Function and structure of NMDA receptor channel

Understanding the mechanism of action, structure and others features of this receptor is a good way for the discovery of new treatments for current diseases.

Activation of NMDA receptor is a complex process that occurs when their agonist and co-agonist, respectively glutamate (**19**) and glycine (**20**) (figure 3), bind to the correspondent pocket. Glycine (**20**) acts as a modulator and this amino acid is present in the extracellular fluids at constant levels. Besides glycine, other molecules can activate NMDA receptor as co-agonists (e.g. *D*-serine, *L*-serine, *D*-alanine and *L*-alanine) [38]. After activation, the ion channel of the

receptor is opened resulting in the exit of magnesium cation (Mg^{2+}) that is blocking the channel, leading to an influx of Ca^{2+} , as illustrated in figure 4. This is a natural process of NMDA receptor and is very important for postsynaptic depolarization [36-38].

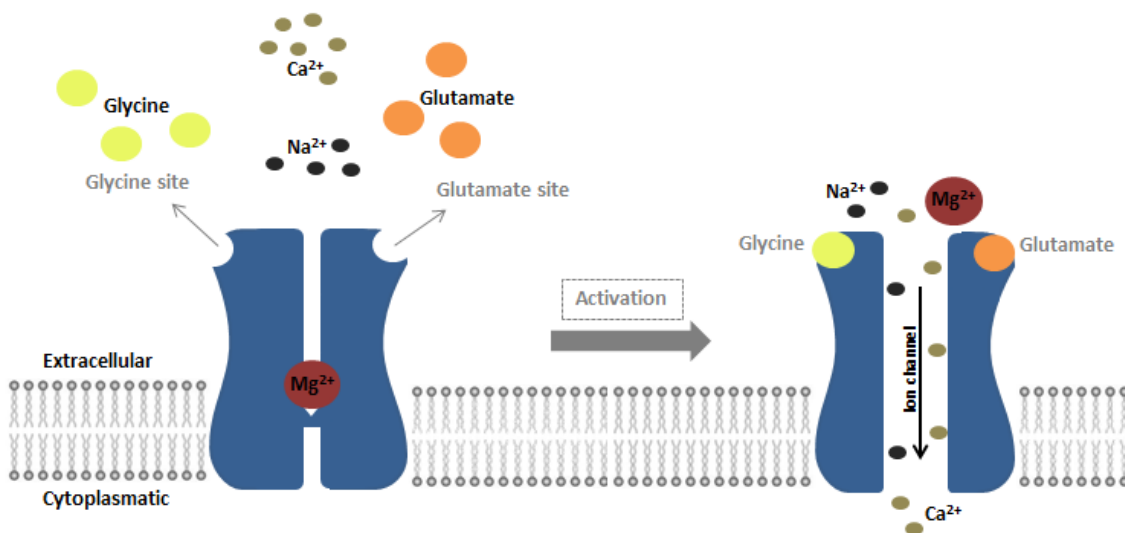


Figure 4 – Operation of a NMDA receptor: activation by glutamate (19) and glycine (20) allows the influx of Ca^{2+} into the neuron.

Functional NMDA receptors consist of three different subunits termed GluN1-3. GluN1 subunit is processed by RNA posttranscriptional that results into eight different splice variants called metabotropic glutamate receptors (mGluR1-8) [32, 36]. GluN2 subunit is encoded by four genes (GluN2A-D) and GluN3, less common, has two variants (GluN3A and GluN3B) [39]. All these subunits are similar, i.e. are homologous and their distribution in the receptor is well organized. Functional NMDA receptor heterotetramers are constituted by two or more homologous monomers [36]. NMDA receptor is characterized by two obligatory GluN1 subunits that can be combined with two others GluN2 and/or GluN3 subunits [39]. Most native NMDA receptors appear with two GluN1 and two GluN2 subunits [40]. The structure of the receptor can be classified in four distinct domains: amino-terminal domain (ATD), ligand binding domain (LBD), trans-membrane domain (TD) and carboxy-terminal domain (CTD) [30, 41]. All the domains are in connection and the attachment between LBD and TD domains is responsible for formation of the ion channel. The last domain (CTD) is a way of transmembranes helices communicate with intracellular medium [36].

A typically NMDA receptor needs the simultaneous presence of two different ligands for their activation, normally glutamate (19) and glycine (20) [36]. These bindings occur in the LBD domain which is also divided into two domains: S1 and S2. S1 domain is in contact with S2 and is a fairly rigid domain. By the other hand, bottom domain S2 is flexible and mobile, which is

essential for the binding of agonists and co-agonists. The S1 and S2 domains form the binding site for glutamate (**19**) in GluN2 and for glycine (**20**) in GluN1 (figure 5) [39, 43].

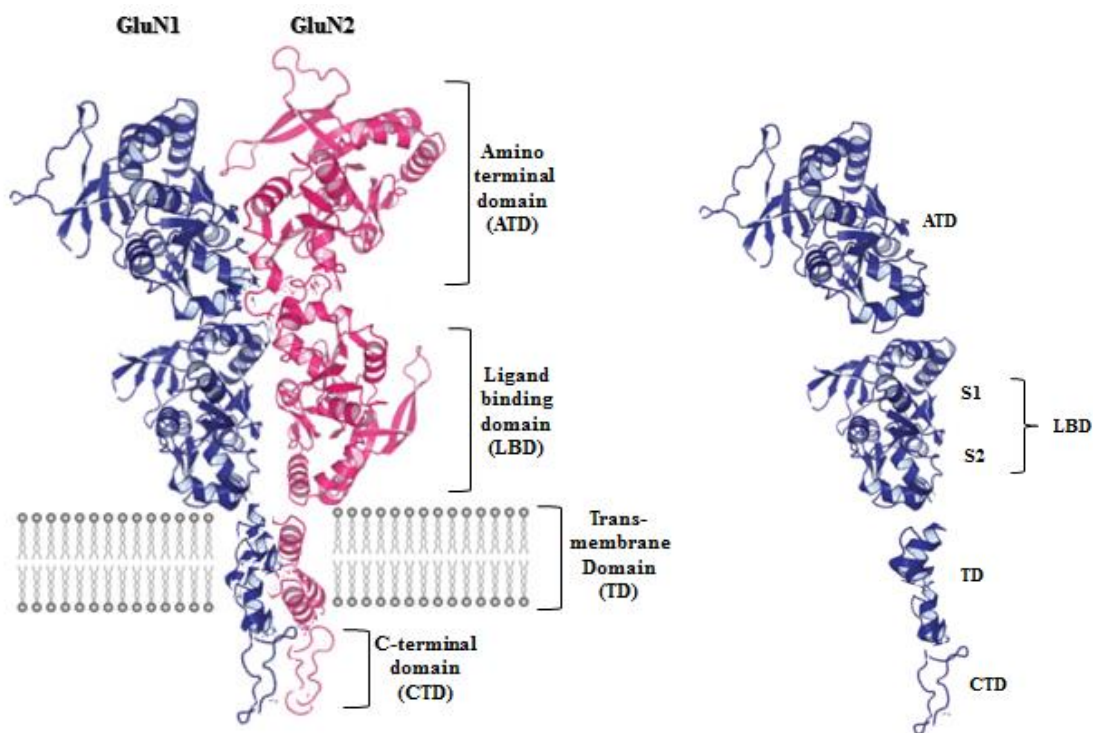


Figure 5 – Representation of GluN1-GluN2 NMDA receptor and their structure (subunits and domains).

The determination of all these features was not possible without the efforts of crystallography where the well resolution of a receptor structure is fundamental to understand the mechanism of action and to determine therapeutic targets [42].

I.4.3 - NMDA receptor antagonists

Since the 80s, emerged a big interest of both academia and industry about the therapeutic potential of drugs targeting the NMDA subtype of glutamate receptors [38]. The development of new drugs has been a slow process because in the first years there was little information about the structure of this receptor. Currently with two solved crystal structures of all domains (ATD, LBD, TD and CTD) it becomes easier to understand which modulators regulate the receptor and differentiate the NMDA receptor from the closely related AMPA receptor [38, 42, 43]. However, there is a thin line between the effective treatment and adverse CNS effects, which turns the study of new NMDA receptor antagonists in a very difficult task [38]. So, for clinical purposes it is important that neuroprotective agents block the overactivation of NMDA

receptor, while the normal neurotransmission is protected, to avoid adverse effects like drowse, hallucinations and coma [26, 44]. It is known that neuroprotective agents which completely block NMDA receptors also impair normal synaptic transmission, leading to numerous side effects [45].

NMDA receptor is a strong candidate for a therapeutic target because the many possible combinations of subunits are responsible for a diversity of functions. Moreover, this receptor has a big variety of binding sites for antagonists [29]. The antagonists can be classified according to the mode of action. There are competitive NMDA antagonists when the local of action is the binding sites of glutamate (**19**) and glycine (**20**), non-competitive antagonists as channel blockers and antagonists that act in others binding sites inducing changes in the receptor [46].

In the next sections, will be reported the several binding sites in the NMDA receptor.

I.4.3.1 – Competitive antagonists acting at the glycine site

Recent studies suggest that glycine site antagonists have better therapeutic profiles than other antagonists as channel blockers or glutamate site antagonists [46]. In fact, in the former cases NMDA receptor blockade led to psychotomimetic effects and learning impairment, while the use of competitive glycine site antagonists did not produce this type of side effects [47, 48].

When the amino acid glycine (**20**) binds to the GluN1 subunit promotes the open of ion channel. So, an antagonist that acts at the glycine site has to compete with high levels of this endogenous compound.

Between 1978 and 1993, the first antagonists of glycine (**20**) were identified: (*R*)-HA-966 (**21**), L-687,414 (**22**) and kynurenic acid (**23**) (figure 6) [49-51].

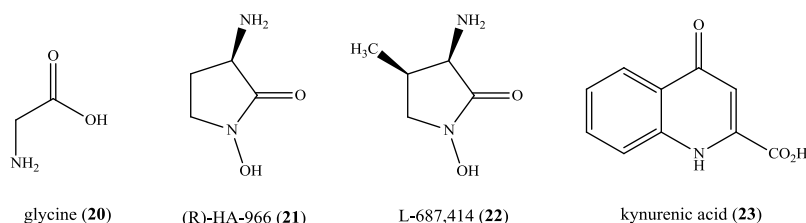


Figure 6 – Chemical structures of co-agonist glycine (**20**) and the first reported antagonists for glycine site, (*R*)-HA-966 (**21**), L-687,414 (**22**) and kynurenic acid (**23**).

Later, some derivatives of kynurenic acid (**23**) (compounds **24** - **26**) and indole-2-carboxylates (compounds **27** and **28**) lead to a series of potent antagonists of GluN1 subunit (figure 7). The compound L-689,560 (**26**) is one of the most potent antagonist discovered for the binding site of glycine with an IC_{50} value of 7.8nM ($[H^3]$ -glycine) [52-55].

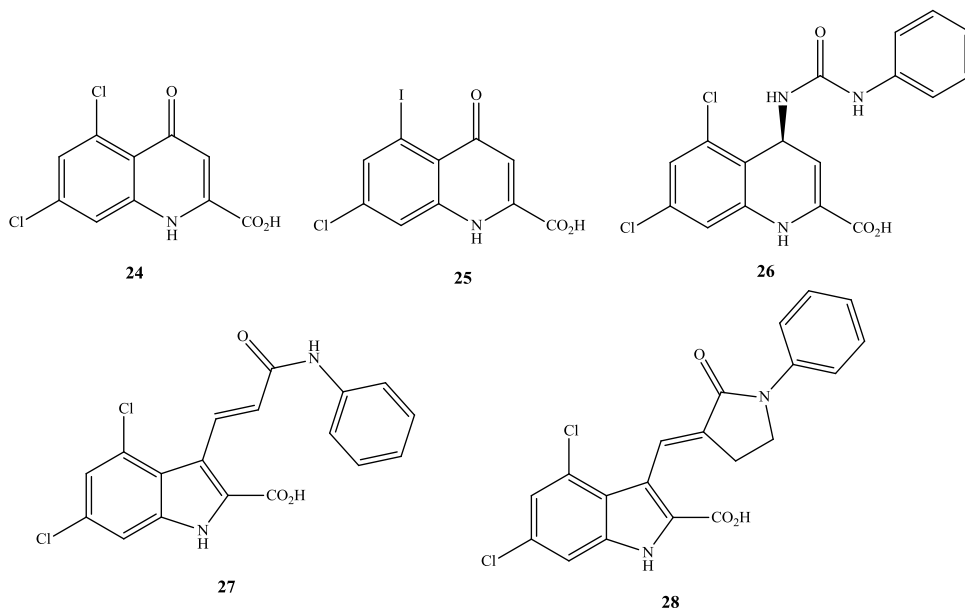


Figure 7 – Derivatives of kynurenic acid (**23**): 5,7-dichlorokynurenic acid (5,7-DCKA) (**24**), L-683,344 (**25**), L-689,560 (**26**), GV150526A (**27**) and GV196771A (**28**).

In 1997, derivatives of quinoxalinedione (compounds **29** - **31**) were reported as potent and selective glycine binding site antagonists but these compounds suffered from poor water solubility [56]. In 2007, a new family of pyridazinoquinolinetriones derivatives were reported, as example compound **31** with IC_{50} of 207nM for ($[H^3]$ -glycine). Beyond the good activities, these compounds did not revealed problems of solubility in water [57].

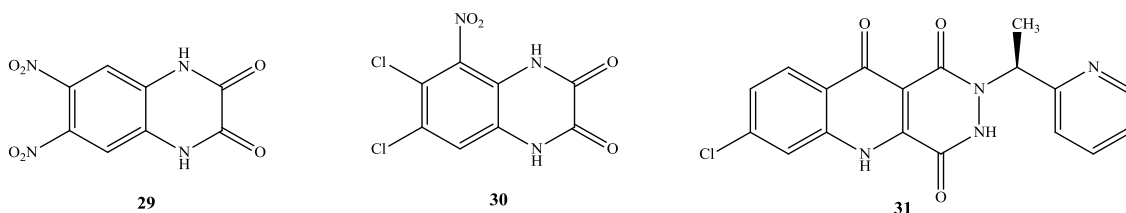


Figure 8 – Chemical structures of quinoxalinedione derivatives DNQX (**29**) and ACEA-1021 (**30**); pyridazinoquinolinetriones derivative (**31**).

More recently, in 2008, Merz Pharm. disclosed 156 quinolone derivatives that act as agonists of the glycine site. These compounds can also act against pain conditions and brain injury [58, 59]. In 2011, Northwestern University filed a patent of a new type of antagonists of GluN1 subunit based on polypeptides (e.g. GLYX-13 (**32**), figure 9) [29, 60].

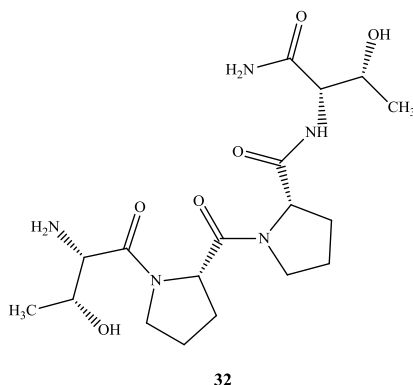


Figure 9 – GLYX-13 (**32**), a polypeptide compound that acts at the glycine site.

I.4.3.2 – Competitive antagonists acting at the glutamate site

The first antagonists of NMDA receptor discovered were antagonists of glutamate binding site (GluN2 subunit) and consisted in variations of glutamate structure [61]. In the 80s, several compounds were designed to mimic their endogenous ligand, glutamate (**19**). In figure 10 are presented some of these compounds that have in common carboxylic, phosphate and amine groups [62]. These three functional groups are important for an antagonist of GluN2 domain and are representative of three charge centers. More precisely, two negative charges correspond to carboxylic and phosphate groups and a positive charge is from primary or secondary amine [63]. Compound **33**, which has a K_i of $1.4\mu\text{M}$ for NMDA receptor, is constituted by an alkyl chain that promotes flexibility, by the other hand compound **35** has a more rigid structure ($\text{IC}_{50}=50\text{nM}$). Unfortunately these compounds revealed to have problems crossing the blood-brain barrier [64].

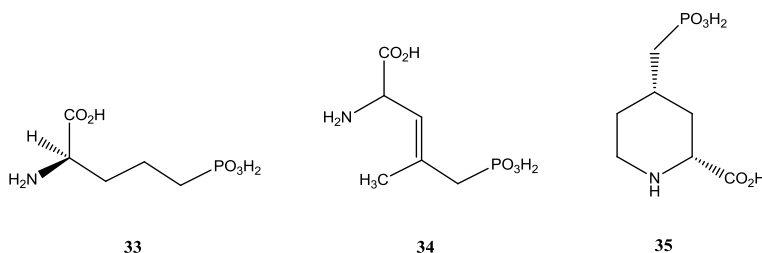


Figure 10 – Structure of compounds inspired in glutamate: D-AP5 (**33**), CGP 37849 (**34**) and CGS 19755 (**35**).

Other variety of ring structures and additional groups emerged that lead to more potent antagonists than compound D-AP5 (**33**). For example, compound NPC 17742 (**36**) which has in addition a cyclohexane ring, EAB 515 (**37**) with a biphenyl group, and ACPED (**38**) with a cyclobutane ring. These three compounds also showed high affinity to NMDA receptors. In case of EAB 515 (**37**) ($K_i=270\text{nM}$, [^3H]CGP-39653), enantiomer *R* was also tested but didn't show activity for the receptor, which is a proof that the stereochemistry of a molecule is crucial in these cases [65, 66]. Also, the presence of ionic charges is an important requirement to develop antagonists of the glutamate binding site.

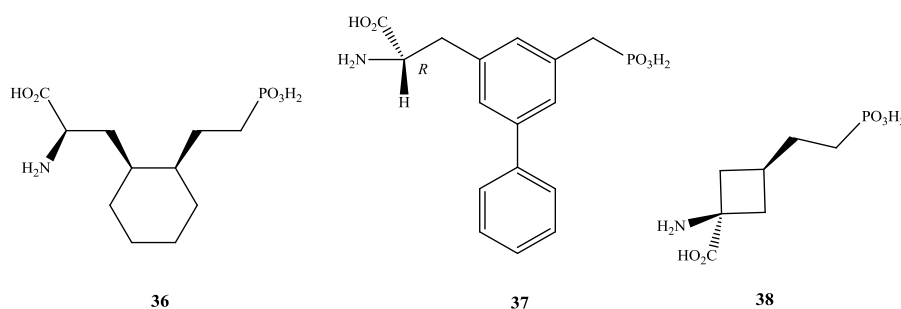


Figure 11 – Structure of cyclic compounds that act in GluN2 subunit.

I.4.3.3 – Non-competitive antagonists acting at ion channel

Channel blockers are non-competitive antagonists and the site of action is in transmembrane domain (TD). This class of compounds can only act when the ion channel is opened, i.e. after activation of the receptor by their two co-agonists: glutamate (**19**) and glycine (**20**) [61]. Normally, ion channel blockers are small molecules with low molecular weight and not very polar, in order to be able to cross blood-brain barrier [26].

Ketamine (**41**) and Phencyclidine (also called PCP, **43**), were two of the first compounds described as ion channel blockers. PCP (**43**) was discovered in 1926 and patented in the 50s by *Parke, Davis and Company* Pharmaceuticals. Unfortunately this compound was associated to negative symptoms such hallucinations, delusions, lack of logical thinking and lethargy [29, 67, 68]. Currently, ketamine (**41**) is used in veterinary as anesthetic agent [69]. MK-801 (**42**) was discovered in 1982 by *Merck Institute for Therapeutic Research* [70]. It has the same mechanism of action of PCP (**43**): interaction with ion channel ($K_i=37.2\text{ nM}$). It is also selective for NMDA receptor and did not revealed affinity for others iGluRs [71].

Dextromethorphan (**44**) belongs to the class of non-competitive compounds. Dextrorphan (**45**) is a dextromethorphan metabolite, with the same mechanism of action, but more potent. In 2010, it was approved by Food and Drug Administration (FDA) a mixture of dextromethorphan (**44**) and other compound for the treatment of pseudobulbar affect, a neurologic disorder [29]. Most of the compounds previously reported were in clinical trials but these newly developed agents do not support good therapeutic utility because of the side effects associated [39].

The most important channel blockers reported until today are the derivatives of adamantane. Memantine (1-amino-3,5-dimethyl-adamantane, compound **40**) was registered in Germany in 1978 by *Merz and Company* for a variety of CNS-indications. It was first synthesized in 1963 by researchers *Eli Lilly* in the discovery of new agents to lower elevated blood sugar levels. However only ten years later it was discovered that the mechanism of action is on the ion channel. Currently it is clinically used for the treatment of Alzheimer's disease, it is well tolerated by patients and has an IC_{50} value of 1.04 μM [39, 72, 73].

Amantadine (1-amino-adamantane, compound **39**) has a simplified structure and a different therapeutic profile from memantine (**40**). It's commercially used for the treatment of Parkinson's disease and has an IC_{50} value of 92 μM . The interaction of these two drugs with the NMDA receptor is made in the amine protonated form [73, 74].

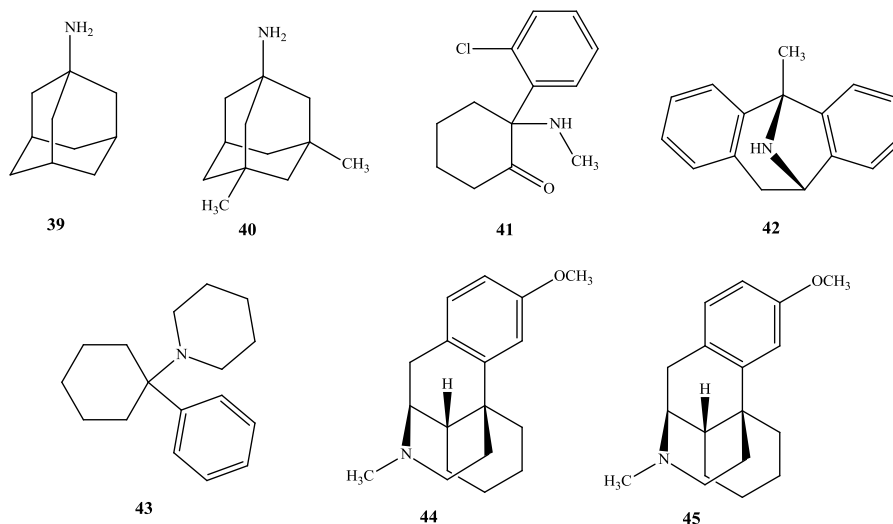


Figure 12 – Schematic representations of NMDA receptor channel blockers.

I.4.3.4 – Non-competitive antagonists acting at GluN2B subunit

The studies around new antagonists of GluN2B subunit have allowed new information about their role in clinical indications of several CNS diseases [48]. Ifenprodil (**46**) and Ro 25-6981 (**47**) were the first selective compounds reported for GluN2B subunit with IC_{50} values of 0.34 μ M and 0.009 μ M, respectively. Ro 25-6981 (**47**) is an analog of ifenprodil (**46**) and proved to be more potent in biological tests [75-77]. After this a series of phenylethanolamine-based compounds was patented by *Cold Spring Harbor Laboratory*. These compounds were discovered based on the X-ray structure of GluN1/GluN2B subunits bound to ifenprodil (**46**). Compounds **48** e **49** (figure 13) are representative examples and no more biological data was revealed about this class of compounds [29].

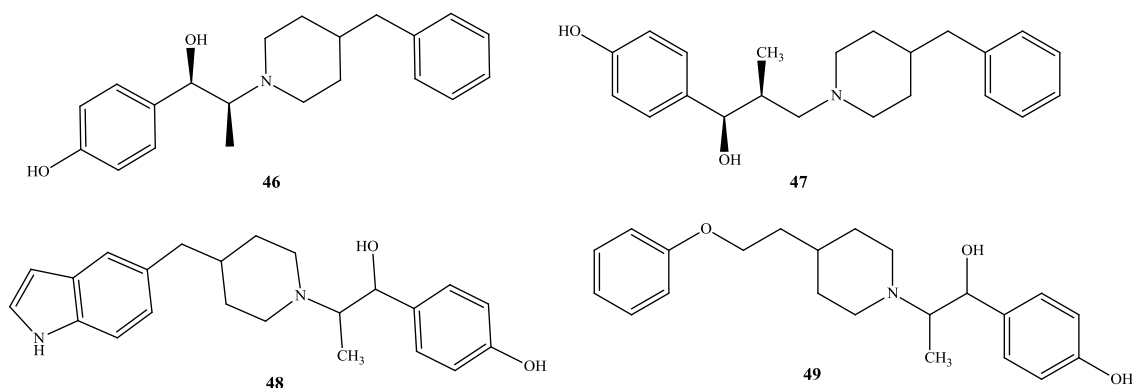


Figure 13 – Chemical structures of non-competitive antagonists of GluN2B: ifenprodil (**46**), Ro 25-6981 (**47**) and compounds **48** and **49**, patented by *Cold Spring Harbor Laboratory*.

I.4.3.5 – Oxazolopyrrolidones as NMDA receptor antagonists

In 2009, a new class of NMDA receptor antagonists was patented: oxazolidine derivatives. Two of these compounds (**50** and **51**) are presented in figure 14 and correspond to oxazolidines substituted with various lipophilic groups. The mechanism of action is until now unknown [78]. Based on these oxazolidine antagonists Santo's group decided to synthesize a small library of enantiopure oxazolopyrrolidones and evaluate as NMDA receptor antagonists. The results were promising with the discovery of a hit compound (**1a**) that revealed an IC_{50} of 62 μ M and to be 1.5 more active than amantadine (**39**) [79].

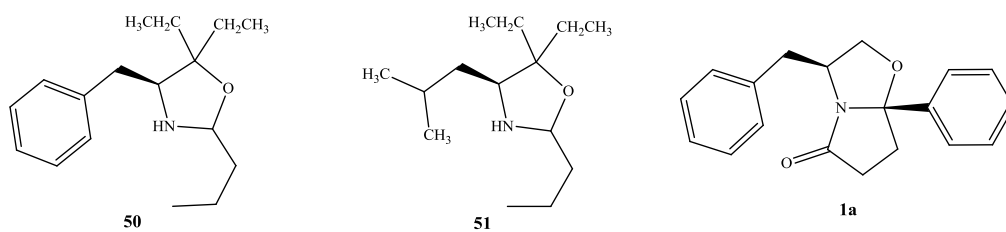


Figure 14 – Oxazolidine derivatives (**50** and **51**) patented in 2009. Oxazolopirrolidone (**1a**) antagonist of NMDA receptor reported by Santo's group.

Based on these results, one of the main goals of the present dissertation is a hit-to-lead optimization of compound **1a** as NMDA receptor antagonists.

I.5 – The worldwide problem of cancer

Cancer is considered the first and second causes of deaths in developed and in developing countries, respectively [80]. It is estimated that in 2008 cancer was the major cause of mortality contributing to 7.6 million deaths and in 2030 this number will increase to 13.2 million [81, 82]. The incidence of cancer is increasing in developed countries and this is related to economic development. With population aging and growth have been increasingly incorrect choices associated to cancer such smoking, bad eating habits, sedentary lifestyle and day-to-day stress, as well [80, 83] Highly refined foods, as example sugars, saturated fats and meat contribute to an increase of cancer incidence and are a result of mechanization and modernization of processes, very popular in North America and parts of Europe [83].

The type of cancer varies dramatically between geographic regions, i.e. some cancers are more common in people of developing countries (cervical and stomach), others in developed countries like breast and prostate cancers. Although, this distribution of type of cancers is not only responsible for the economic development of geographic regions. There are other factors involved such genetic differences between populations, variations in lifestyle, medicinal practices and environmental exposures [82-84]. So, it's important increase efforts to halt the spread and beat this dramatic disease.

I.5.1 – Indole compounds as antitumor agents

Cancer disease is characterized by a process where exists a loss of balance between cell division and cell death. At the same time there are some cells that should have died but did not receive the essential signals and the problem can arise on any step of the complex mechanism of apoptosis [85]. There are some mechanisms that can contribute to evasion of apoptosis and carcinogenesis: defects and mutations in p53 protein, reduced expression of caspases and increased expression of inhibitors apoptosis proteins (IAPs), for example [86].

Oncology is the therapeutic area that has more poor records for investigational drugs in clinical development, comparing with others areas such cardiology, for example. The continuous discovery of more antitumor agents has an important role to combat the relentless and lethal nature of this disease [87].

In the past decade a large number of efforts were made to synthesize different heterocyclic compounds and their derivatives with promising variety of biological activities. Heterocyclic chemistry is known to be one of the most valuable sources of novel compounds with biological

interest, in particular compounds that possess indole moiety [88, 89]. Half of the therapeutic agents have in their structure a heterocyclic ring and several of these compounds have a five-member nitrogen-containing ring [88]. Indole nucleus, a heterocyclic aromatic system, is very important for biomedical area because is introduced in proteins in the form of amino acid tryptophan, is present in skeletons of indole alkaloids and is also part of the structure of serotonin, a key neurotransmitter in CNS [88, 90]. As mentioned before, indole moiety are associated a lot biological activities that are illustrated in the figure 15, presented below [90, 91].

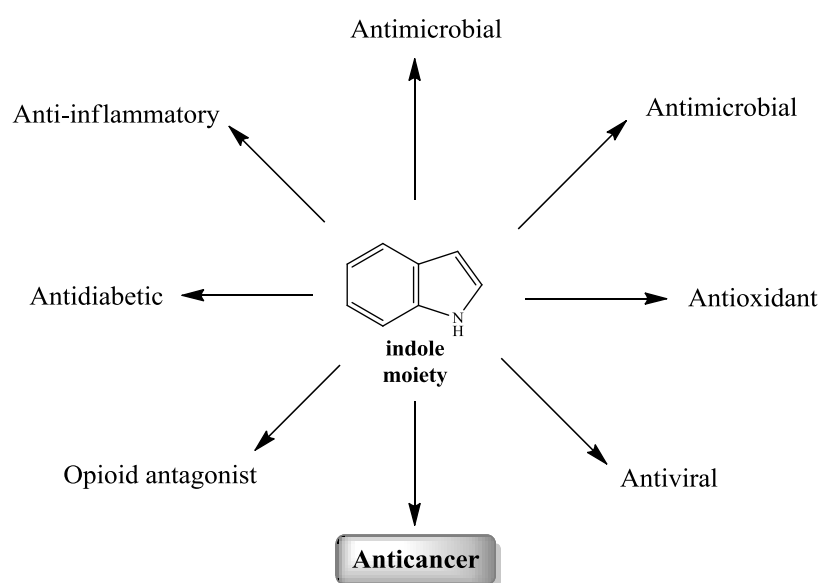


Figure 15 – Some of biological activities responsible of indole moiety.

Focusing only in anticancer properties of indole moiety, there are some reviews in the literature that report several compounds described as antitumor agents containing indole nucleus [88, 89, 91]. Tubulin polymerization inhibitors are a good example of compounds that have indole nucleus as core structure (figure 16) [89, 90].

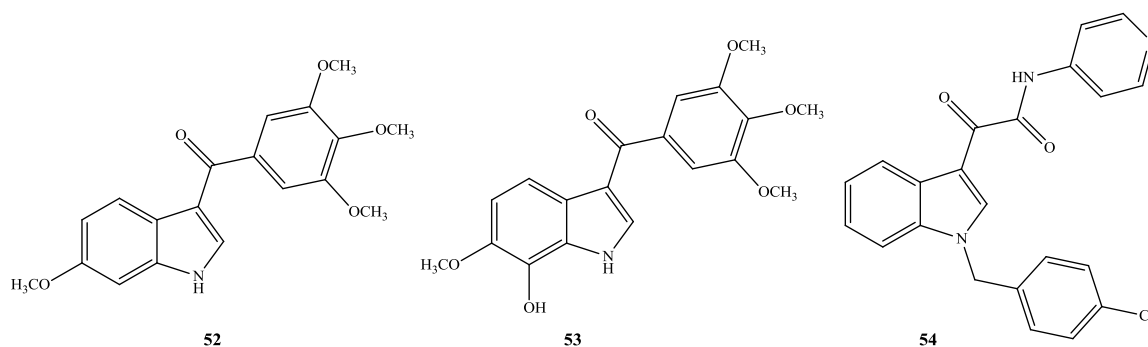


Figure 16 – Chemical structure of tubulin inhibitors: BPR0L075 (**52**) and derivative (**53**), D-24851 (**54**).

Other two examples of antitumor agents are present in figure 17. Panobinostat (**55**), a hydroxamic acid, was developed by *Novartis* for the treatment of several types of cancers. This compound was tested against Hodgkin's Lymphoma in Phase III clinical trials, against breast cancer and prostate cancer in Phase II clinical trials, and against chronic myelomonocytic leukemia in Phase I clinical trials [89]. Compound **56** is a tryptophan-derived that belongs to aplysinopsin, a class of marine natural compounds isolated from sponges, corals, sea anemone and nudibranch. This family of compounds has potential for the development of medicines because demonstrated toxicity against many cancer cells and also revealed anti-plasmodial and antimicrobial activities [89, 91, 92].

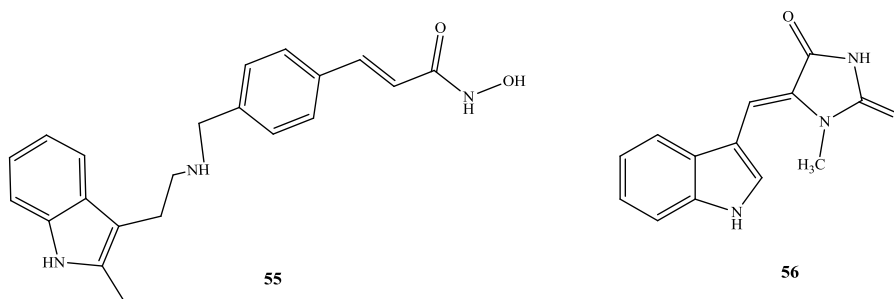


Figure 17 – Antitumor agents: panobinostat (**55**) and aplysinopsin analog (**56**).

DNA methyltransferases (DNMT) are a family of enzymes and promising drug targets in cancer. Analogs of *N*-phthaloyl-*L*-tryptophan (RG108, compound **58**, figure 18) were reported as inhibitors of DNMT1. RG108 (**58**), the first reported inhibitor, is a derivative of *L*-tryptophan (**57**) incorporated into a phthalamide structure with a DNMT1 IC_{50} of 390 μ M. The enantiomer (*R*) was also tested but revealed a decrease of activity, showing that stereochemistry in biological targets is an important consideration. Some modifications in base structure of RG108

(**58**) provided an increase of activity – analogs **59** (DNMT1 $IC_{50} = 20 \mu M$) and **60** (DNMT1 $IC_{50} = 40 \mu M$) [93].

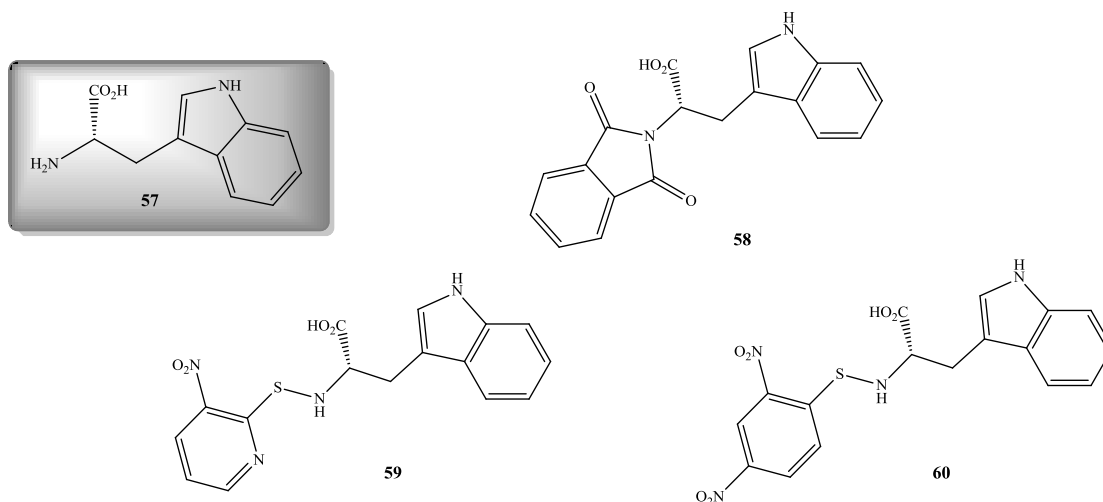


Figure 18 – Chemical structures of *L*-tryptophan (**57**) and DNMT1 inhibitors (RG108 (**58**) and their analogs **59** and **60**).

More recently, other derivatives of *L*-tryptophan (**57**) were reported, but in this case as inhibitors of β -D-galactosidase and β -D-glucosidase, enzymes that are involved in a range of metabolic disorders, such as cancer. Compounds **61** and **62** (figure 19) are the most potent compounds for this class of inhibitors: compound **61** with 37% of inhibition and compound **62** with 49% of inhibition, both at $100\mu M$, against β -D-galactosidase and β -D-glucosidase, respectively [94].

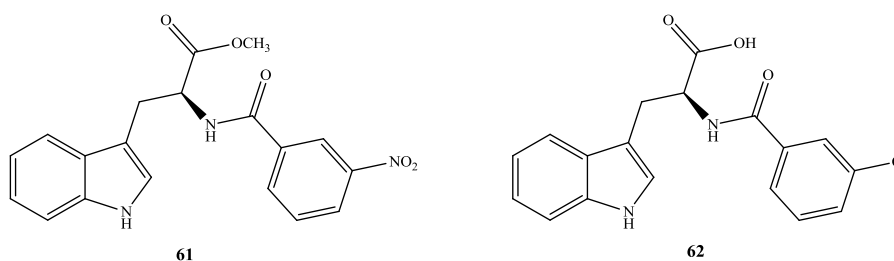


Figure 19 – *L*-tryptophan derivatives **61** and **62** reported with inhibitory bioactivities against β -D-galactosidase and β -D-glucosidase.

Our group is also interested in the study of tryptophanol derivatives with application as antitumor agents [95]. In this thesis it was also explored the synthesis of tryptophanol-derived bicyclic lactams and was performed their evaluation of activity in several cancer cell lines.

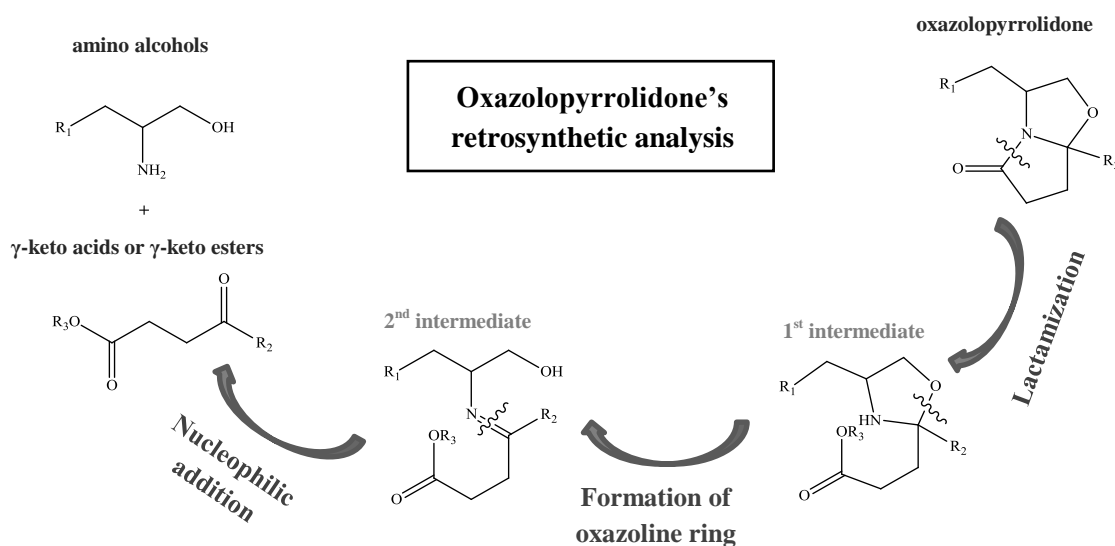
Chapter II – Results and Discussion

II.1 – Synthesis of phenylalaninol and tryptophanol- derived bicyclic lactams

Santos's group has two therapeutic areas of interest: cancer and neurodegenerative diseases. In this thesis both areas were addressed with the synthesis of compounds based on previously works. Compound **1a** revealed to be a NMDA receptor antagonist and were also described some (*S*)-tryptophanol-derived oxazolopiperidone lactams as antitumor agents [79, 95].

The first objective of this thesis was the construction of two different libraries: 1) (*S*) and (*R*)-phenylalaninol-derived bicyclic lactams. 2) (*S*)- and (*R*)-tryptophanol-derived bicyclic lactams. The first library was evaluated as NMDA receptor antagonists and the second library was evaluated as antitumor agents.

Proceeding to a retrosynthetic analysis of the oxazolopyrrolidone moiety is possible to conclude that it can be synthesized starting from amino alcohols and γ -keto acids or γ -keto esters, also known by oxoacids (scheme 7). It is shown the three heterocyclic disconnections which give rise to commercial available starting materials.

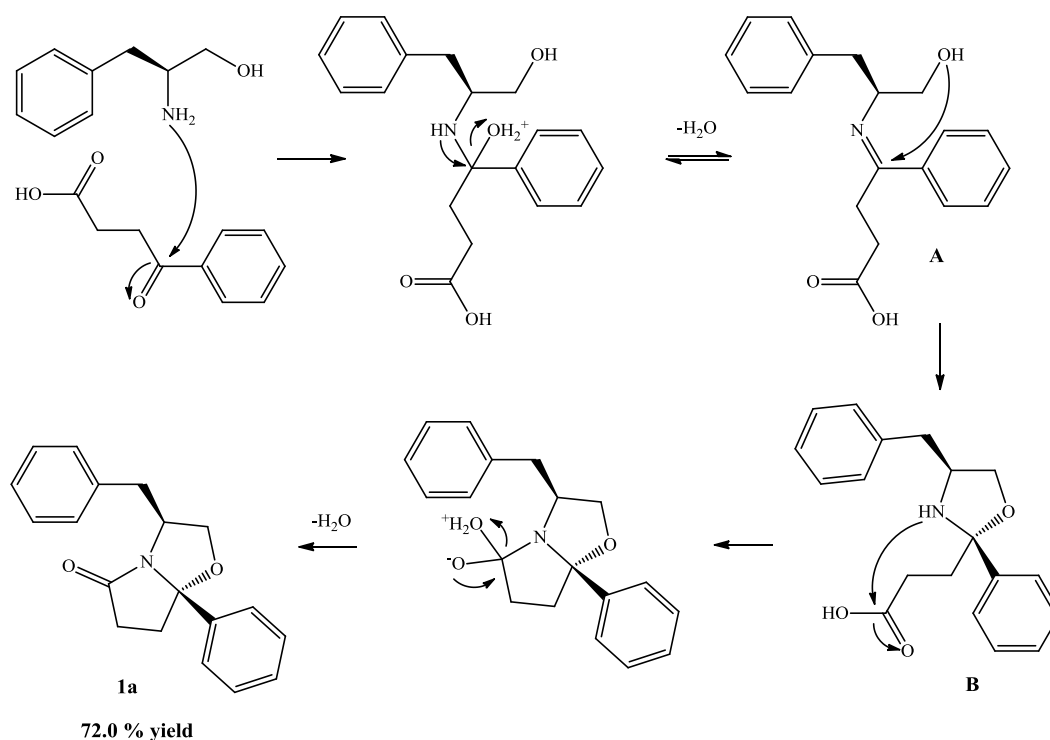


Scheme 7 – Illustration of retrosynthetic analysis of oxazolopyrrolidone.

This type of cyclocondensation reactions were performed as reported in literature [79]. Toluene was used as solvent and the reactions were finished between 16 and 24h (overnight) at reflux, under inert atmosphere and using a *Dean-Starck* apparatus. To have a successfully reaction with good yields it is essential the elimination of water inside the reaction medium in order to move

the chemical equilibrium for the formation of products. Also, it is important to use an excess of oxoacid to ensure good yields.

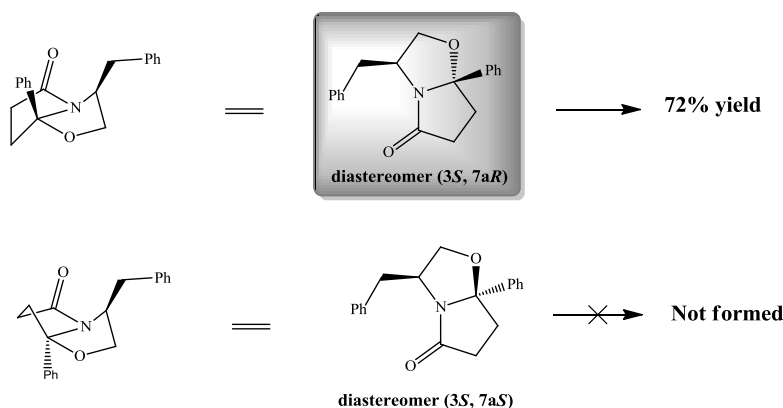
The mechanism of the reaction is shown below in scheme 8 using as example the synthesis of compound **1a** (the first NMDA receptor antagonist discovered by Santos's group). The reaction starts with the nucleophile attack of the free amine of (*S*)-phenylalaninol to the carbonyl group of γ -keto acid, resulting in dehydration forming the imine group (intermediate **A**). Then, the hydroxyl group attacks the imine, forming an oxazolidine ring (intermediate **B**). At last, the attack of the amine to carboxylic acid forms the pyrrolidone ring, with the exit of a molecule of water. For tryptophanol-derived oxazolopyrrolidone lactams the reaction mechanism proceeds in the same way. It is an interesting reaction because is possible the formation of two heterocyclic rings with a new chiral center.



Scheme 8 – Reaction mechanism for the synthesis of compound **1a**.

Is important to highlight that in these reactions was only observed the formation of one diastereomer: (*3S*, *7aR*) in case of *S* derivatives and (*3R*, *7aS*) for *R* derivatives. Analyzing example of scheme 9, this fact can be explained by steric hindrance between hydroxyl group and benzyl of (*S*)-phenylalaninol for the formation of diastereomer (*3S*, *7aS*). In diastereomer (*3S*, *7aR*) hydroxyl group attacks in opposite direction of benzyl group and, for this reason, have

lower steric hindrance (scheme 9). The other reason can also be related to spatial arrangement of two heterocyclic-fused rings: is more favorable in case of diastereomer (3*S*, 7*aR*) without repulsion between carbonyl group and the beak of the five-membered ring (scheme 14). So is possible to conclude that these cyclocondensation reactions are stereoselective i.e., only forms one of the two possible diastereomers. The control of stereoselectivity was made by ¹H-NMR.



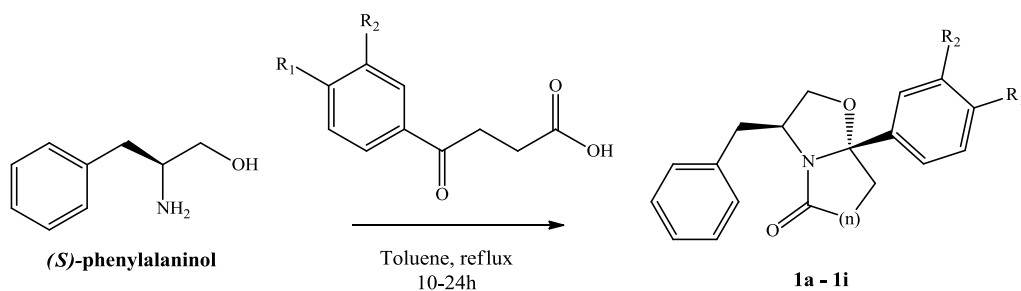
Scheme 9 – Spatial arrangement of diastereomers (3*S*, 7*aR*) and (3*S*, 7*aS*).

With the exception of (*R*)-tryptophanol, all enantiopure amino alcohols and oxoacids were purchased. A variety of oxoacids with different substituents in the phenyl group were selected in order to construct a chemical diverse library of compounds.

The yields of the reactions were moderate to excellent, according with several references in literature, and the respective results are summarized in tables 1-4 [4, 11, 16, 79]. Compounds **1a-i** and **2a-i** were obtained in yields between 69.0 and 99.8% and for compounds **3a-h** and **4a-h** the values of yields were between 53.0 and 95.1%.

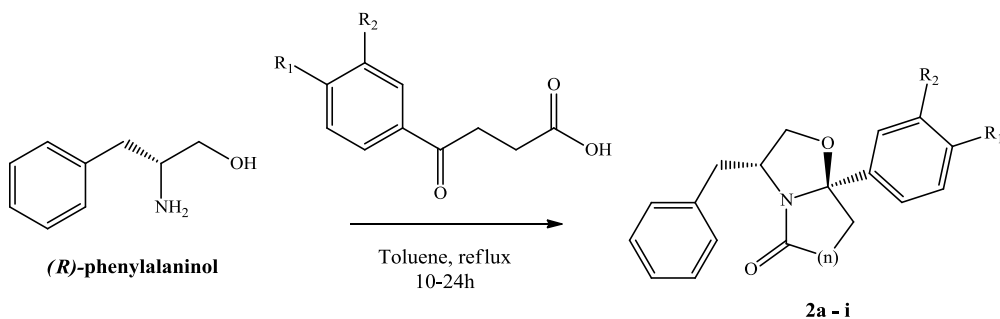
Compounds **1i** and **2i** are two examples of oxazolopiperidone lactams in phenylalaninol's library. These compounds have a role in this library: understand if exists a difference between pyrrolidone and piperidone rings in biological activity.

Table 1 – Reaction yields for (*S*)-phenylalaninol-derived bicyclic lactams.

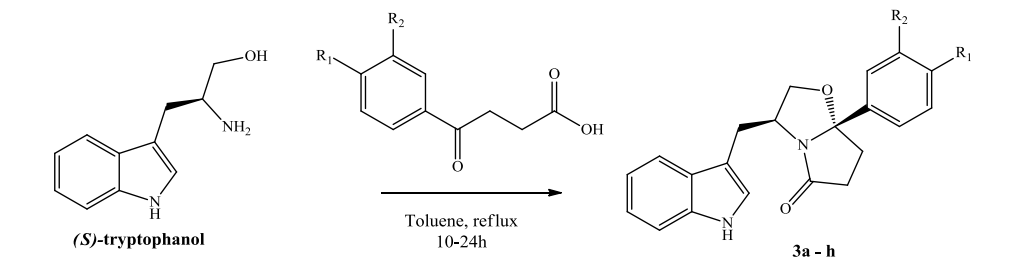


S-phenylalaninol derivatives					
Reference	R ¹	R ²	N	Yield (%)	
1a	H	H	1	72.0	
1b	F	H	1	91.2	
1c	Cl	H	1	94.9	
1d	Br	H	1	99.8	
1e	CH ₃	H	1	93.2	
1f	OCH ₃	H	1	79.8	
1g	SO ₂ CH ₃	H	1	88.0	
1h	OCH ₃	F	1	87.6	
1i	H	H	2	86.6	

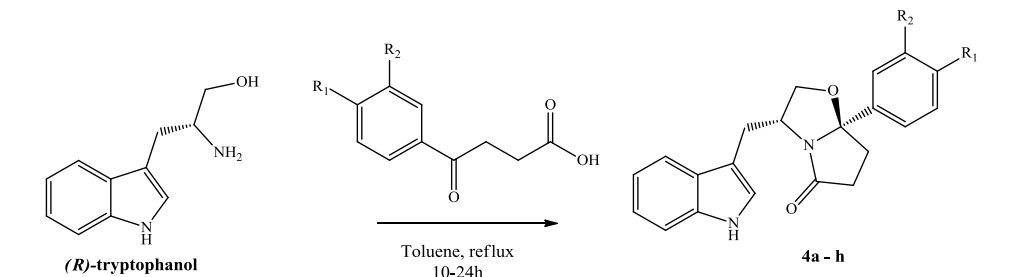
Table 2 – Reaction yields for (*R*)-phenylalaninol-derived bicyclic lactams.



R-phenylalaninol derivatives					
Reference	R ¹	R ²	N	Yield (%)	
2a	H	H	1	80.1	
2b	F	H	1	82.6	
2c	Cl	H	1	83.1	
2d	Br	H	1	75.8	
2e	CH ₃	H	1	74.6	
2f	OCH ₃	H	1	73.4	
2g	SO ₂ CH ₃	H	1	69.0	
2h	OCH ₃	F	1	81.5	
2i	H	H	2	86.3	

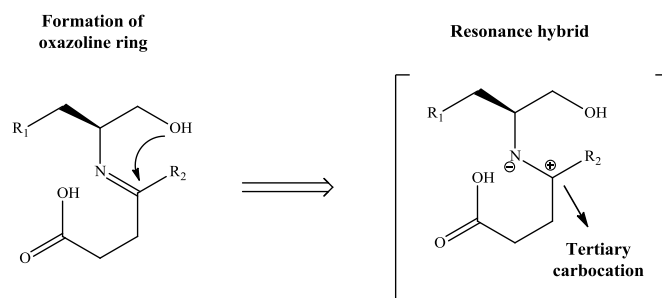
Table 3 – Reaction yields for (*S*)-tryptophan-derived oxazolopyrrolidone lactams.


<i>S</i> -tryptophan derivatives			
Reference	R ¹	R ²	Yield (%)
3a	H	H	71.8
3b	F	H	83.3
3c	Cl	H	81.9
3d	Br	H	72.3
3e	CH ₃	H	53.0
3f	OCH ₃	H	69.3
3g	SO ₂ CH ₃	H	60.5
3h	OCH ₃	F	67.4

Table 4 – Reaction yields for (*R*)-tryptophan-derived oxazolopyrrolidone lactams.


<i>R</i> -tryptophan derivatives			
Reference	R ¹	R ²	Yield (%)
4a	H	H	95.1
4b	F	H	69.7
4c	Cl	H	66.7
4d	Br	H	82.5
4e	CH ₃	H	85.5
4f	OCH ₃	H	55.6
4g	SO ₂ CH ₃	H	74.9
4h	OCH ₃	F	69.3

The reason for good yields is the stability of imine (intermediate **A**) which can be represented by the correspondent resonance hybrid (scheme 10).



Scheme 10 – Representation of resonance hybrid of imine.

The absolute configuration of compounds synthesized in these two initial libraries is known by other previously work done, with the same amino alcohols, by our group and others, as well [11, 79, 96]. It is possible to determine the absolute configuration of the new chiral center formed by a NMR experience: nuclear Overhauser effect spectroscopy (NOESY). This technique allows to observe the correlations between protons that are in the same side of the plane and so the *S* or *R* configuration of that specific chiral center. Other auxiliary and important technique is the optical rotation. It is related with the ability of a chiral molecule to rotate the plane of polarized light which is represented by a positive or negative value.

For phenylalaninol derivatives, compounds **1a** and **2a** were objects of comparison for the new molecules synthesized and these two compounds are totally described in paper of Santos *et al.*, published in 2013. The optical rotation of compound **1a**, (*S*)-phenylalaninol derivative, has a value of $+4.7^\circ$ ($c = 1.9$, CH_2Cl_2) and for compound **2a**, (*R*)-phenylalaninol derivative, the value is -3.0° ($c = 2.4$, CH_2Cl_2). So, theoretically all the bicyclic lactams synthesized although (*S*)-phenylalaninol have an opposite optical rotation comparing with (*R*)-phenylalaninol bicyclic lactams. The experimental measures are according to the expected for all phenylalaninol derivatives. For tryptophanol library was also measured the optical rotations and the results were consistent: opposite values between (*S*)-tryptophanol and (*R*)-tryptophanol derivatives.

The absolute configuration of the tryptophanol derivatives was confirmed by X-ray crystallography for compound **3b** (figure 20). According with crystallographic representation the phenyl group, with substituent fluorine in *para* position, is in same side of the plane than indole group.

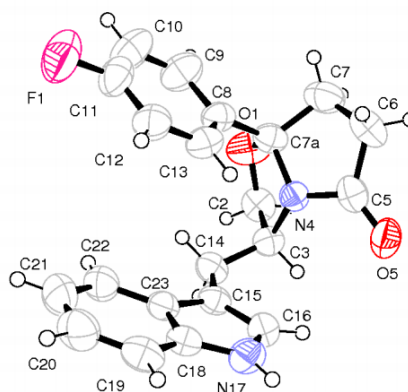
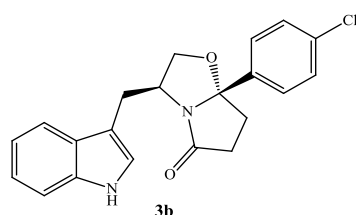


Figure 20 – Chemical structure of compound **3b** and respective crystallographic representation.

The synthesized compounds were characterized by NMR. In $^1\text{H-NMR}$ spectrum of tryptophanol all the alkyl protons appear between 3.70 and 2.0 ppm. For bicyclic lactams, the most important signals in $^1\text{H-NMR}$ spectra correspond to H-2, H-3 and CH_2Ar (figure 21). H-3 appears as a multiplet, normally between 4.35 and 4.70 ppm and is the most deshielding alkyl proton. H-2 are diastereotopic protons which means that they have different chemical environment and both signals are characterized by double doublets around 4.05 – 4.25 ppm and 3.50 – 4.05 ppm. Sometimes, H-2 protons are represented by a false triplet, a typical signal from a coalescence of double duplet. The protons of CH_2Ar appear at upfield, generally between 3.00 – 2.20 ppm. All these protons are shown in figure 21, in a selected zone of $^1\text{H-NMR}$ spectrum of compound **3b**.

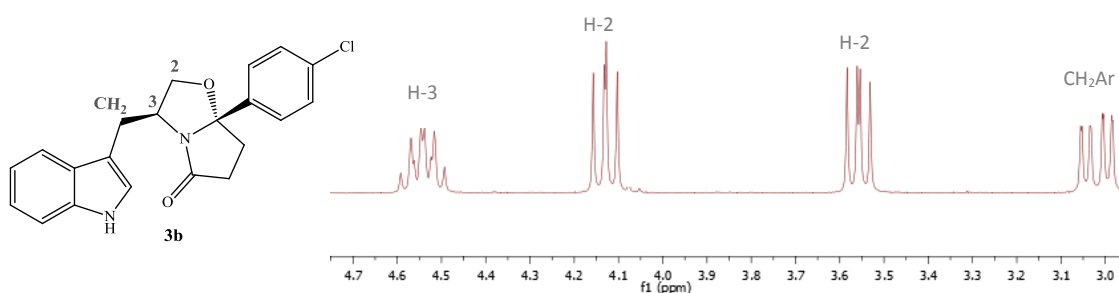


Figure 21 – $^1\text{H-NMR}$ spectra of compound **3b** between 3.0 and 4.7 ppm.

The $^{13}\text{C-NMR}$ spectra is also helpful, mainly to understand if the compound is the expected diastereomer. The C-7a chiral center has a specific chemical shift, in general with a difference of 3 or 4 ppm [79]. For derivatives of *S* amino alcohols C-7a are presented around 102 ppm for all derivatives, an indication that was formed the expected diastereomer (*3S*, *7aR*). In the next table are presented the chemical shift of C-7a of (*S*)-phenylalaninol and (*S*)-tryptophanol

derivatives. For the other amino alcohols the results were also consistent (see experimental procedure).

Table 5 – Chemical shift (δ) of C-7a in (*S*)-phenylalaninol and (*S*)-tryptophanol derivatives.

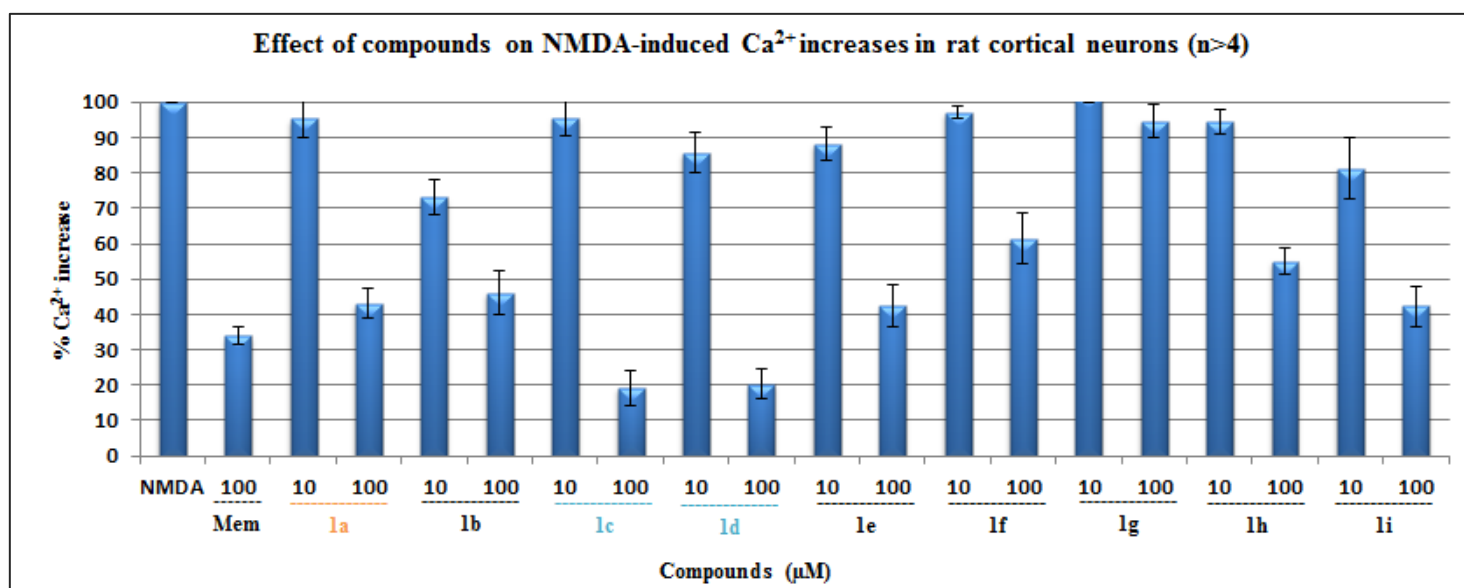
<i>S</i>-phenylalaninol derivatives		<i>S</i>-tryptophanol derivatives	
Reference	δ (ppm)	Reference	δ (ppm)
1b	102.07	3b	102.19
1c	101.96	3c	102.05
1d	102.02	3d	102.12
1e	102.44	3e	102.56
1f	102.32	3f	102.45
1g	103.23	3g	101.83
1h	103.18	3h	102.35

II.2 – Biological evaluation of phenylalaninol-derived bicyclic lactams

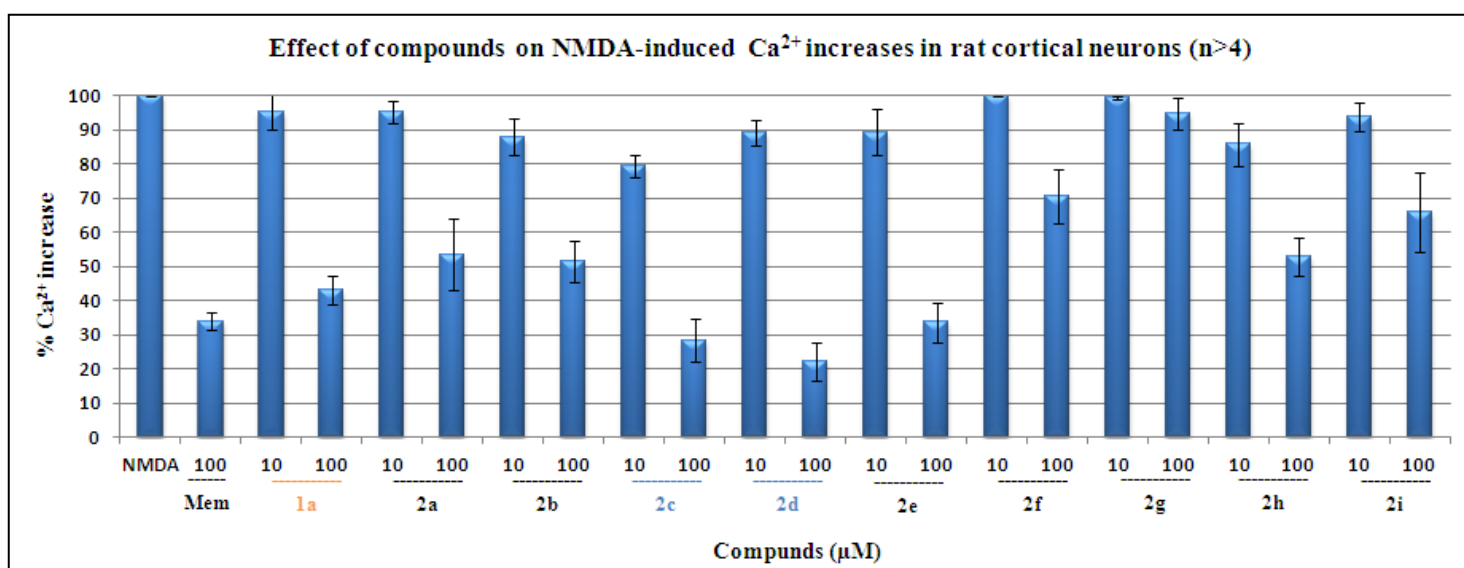
Compounds **1a** – **i** and **2a** – **i**, derived from amino alcohol phenylalaninol, were evaluated as NMDA receptor antagonists.

To measure the activity of compounds for were used cultures of rat cerebellar neurons (granular cells). The test starts with incubation of compounds five minutes before application of the agonist NMDA at 100 μ M of concentration. This addition of amino acid NMDA allows the opening of ion channels and a stable increase of calcium cation influx. So, if the compounds act as antagonists of the NMDA receptor, the influx of calcium will have a proportional decrease with the increase of the concentration of the compounds. In these assays the commercial drug memantine (**40**) was used as positive control. The results of the first screening are presented below (graphs 1 and 2).

Graph 1 – Screening of *S*-phenylalaninol-derived bicyclic lactams **1a** – **i**.



Graph 2 – Screening of *R*-phenylalaninol-derived bicyclic lactams **2a** – **i**.

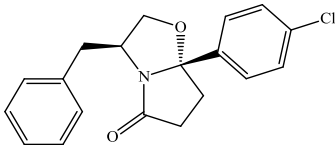
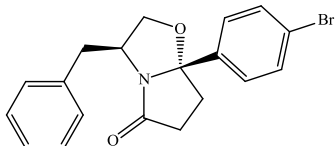
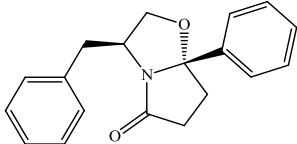
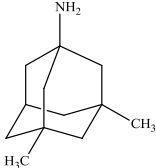


The screening of this library was made using two concentrations. At 10μM the compounds did not show relevant effects on Ca²⁺ increase and comparing positive control **1a** and memantine (**40**) were inactive. At concentrations of 100 μM, four compounds block over 70% the calcium influx: **1c**, **1d**, **2c** and **2d**. These compounds correspond to oxazolopirrolidone lactams with a halogen atom in *para* position of the phenyl group. It is important to highlight that the two (*S*)-phenylalaninol derivatives, compounds **1c** and **1d**, proved to be more active than the

correspondent enantiomers, **2c** and **2d**. Comparing with the hit compound **1a**, the four compounds mentioned before resulting into a substantial optimization as NMDA receptor antagonists. With other substituents in phenyl group there was an effective loss of activity. The compounds with methylsulfonyl (-SO₂CH₃), methoxy (-OCH₃) groups and piperidone ring revealed the lowest impacts into influx of Ca²⁺ (compounds **1f**, **1g**, **2f**, **2g** and **2i**).

IC₅₀ values (table 6) were determined for the most promising compounds. Compounds **1c** and **1d** are 2.3 and 2.5 times more active than the hit compound **1a**. More remarkably, compounds **1c** and **1d** had an IC₅₀ value in the same order of magnitude of memantine (**40**), the positive control used.

Table 6 – IC₅₀ values determined for compounds **1a**, **1c**, **1d** and memantine (**40**).

Reference	Chemical structure	IC ₅₀ (μM)
1c		39±8
1d		36±3
1a		91±6
Memantine (40)		30

The assay used for the evaluation of our compounds only indicates if they act as NMDA receptor antagonists. To know the specific local of action in the NMDA receptor, it is necessary to study each of possible binding sites.

II.2.1 – Hit-to-lead optimization

A hit-to-lead process is defined by methodology where analogues of a hit compound are synthesized with different substitution patterns [97]. In this case, the main goal was to understand which part or substituents of the molecule are important for the activity and if some modifications in the structure results in an increase of biological activity.

So, the next step was the derivatization of the most promising antagonists. Was used a similar amino alcohol with phenylalaninol, the (*S*)-tyrosinol in form of hydrochloride salt (figure 22), which has as hydroxyl group at *para* position of phenyl ring. This amino alcohol was chosen because several compounds identified as NMDA antagonists have one or more hydroxyl groups and was important understand if an increase of polarity resulted into an optimization.

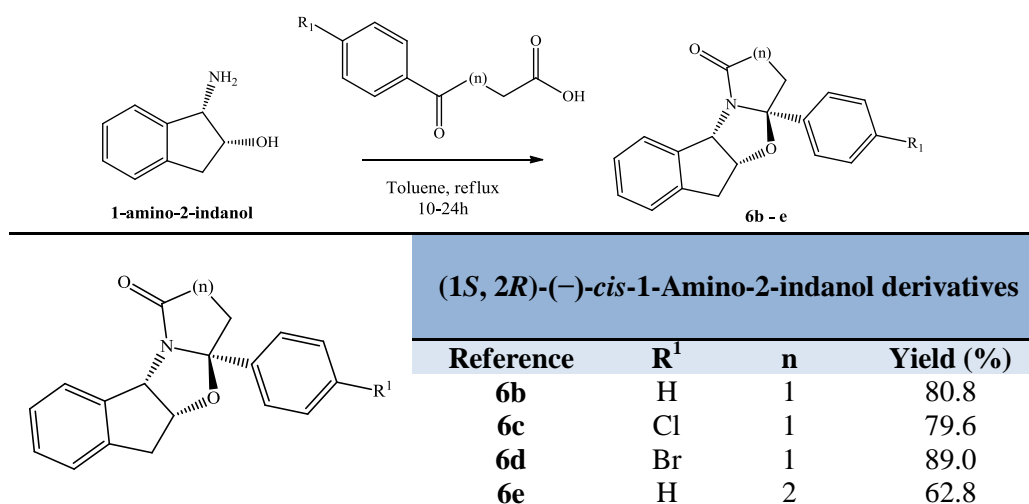
Another aspect taken into account was the flexibility of the oxazopirrolidone lactams synthesized. For example, analyzing the structure of the two commercial drugs amantadine (**39**) and memantine (**40**) is possible to see that they have rigid structures and a little chance of motion. The phenylalaninol derivatives reported previously are flexible structures and to do this parallelism was used a diastereomer of 1-Amino-2-indanol. These two types of enantiopure amino alcohols are commercial available and the methodology was the same: performing cyclocondensation reactions with some selected oxo acids. A small library was constructed and the respective compounds are shown in tables 7 and 8.

Table 7 – (*S*)-tyrosinol derivatives synthesized and respective reaction yields.

The reaction scheme shows the synthesis of *S*-tyrosinol derivatives. The starting material is (*S*)-tyrosinol, which reacts with a substituted oxo acid (R¹-substituted) in toluene at reflux for 10-24 hours to form the bicyclic oxazopirrolidone lactam derivative (5a-b).

<i>S</i> -tyrosinol derivatives		
Reference	R ¹	Yield (%)
5a	Cl	29.1
5b	H	19.4

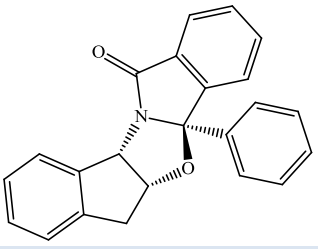
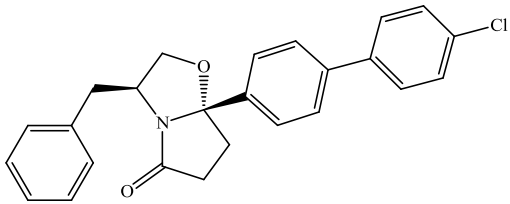
Table 8 – (1*S*, 2*R*)-(-)-*cis*-1-Amino-2-indanol derivatives synthesized and respective reaction yields.



As mentioned before the amino alcohol (*S*)-tyrosinol is commercial available in form of salt, which is not soluble in toluene. Therefore, in literature is described a similar cyclization reaction in toluene performed with this amino alcohol that reports the use of triethylamine (TEA) to hydrolyze the salt and allow the cyclization reaction [98]. However, in this case, the yields of reactions were not good as expected (table 7). Maybe these results are related with the low solubility of (*S*)-tyrosinol. The reaction starts with the addition of (*S*)-tyrosinol and TEA into toluene and with an increase of temperature it is visible the formation of an insoluble yellow oil. So, a large part of the starting material doesn't react resulting in low yields and, because of that, it is necessary to optimize this specific reaction. Two oxazolopirrolidone lactams were synthesized, one with a chlorine atom in *para* position and the other without substituent in phenyl group (compounds **5a** and **5b**). These two compounds were selected to be possible doing a direct comparison with the hit compound **1a** and compound **1c**.

Relatively to (1*S*, 2*R*)-(-)-*cis*-1-Amino-2-indanol derivatives, the library is composed by five compounds, 4 of them oxazolopirrolidone lactams and the other oxazolo-isoindolone (tables 8 and 9) and, in general, the yields of the respective reactions were good/excellent. Compounds **6a** and **6b** were synthesized before the optimization process and tested with the first library (tables 1 and 2), which biological results are shown in graph 3.

Table 9 – Others derivatives of (1*S*, 2*R*)-(-)-*cis*-1-Amino-2-indanol and (*S*)-tyrosinol.

Compound 6a	Compound 7 ^a
	
Yield (%) 98.7	Yield (%) 82.0

About NMR characterization of new compounds, in case of (*S*)-tyrosinol derivatives the ¹H-NMR spectrum is characterized by an additional signal around 3.50 ppm corresponding to hydrogen of hydroxyl group and, also, the disappearance of a proton in aromatic zone, between 6.50 – 7.50ppm. The rest part of the ¹H-NMR spectra are very similar with phenylalaninol derivatives and ¹³C-NMR spectra, as well (see experimental procedure).

In case of indanol derivatives, ¹H-NMR spectrum is characterized by the most deshielding non-aromatic protons in libraries of synthesized compounds. Between 6.00 – 6.20 ppm is presented a doublet representative of CH-N and around 5.20 ppm a double triple doublet of CH-O (figure 22). The deshielding of these two protons is related with the electronegativity of heteroatoms. In upfield there is a signal of CH₂-indanol proton in form of a double doublet around 3.00 ppm (figure 22).

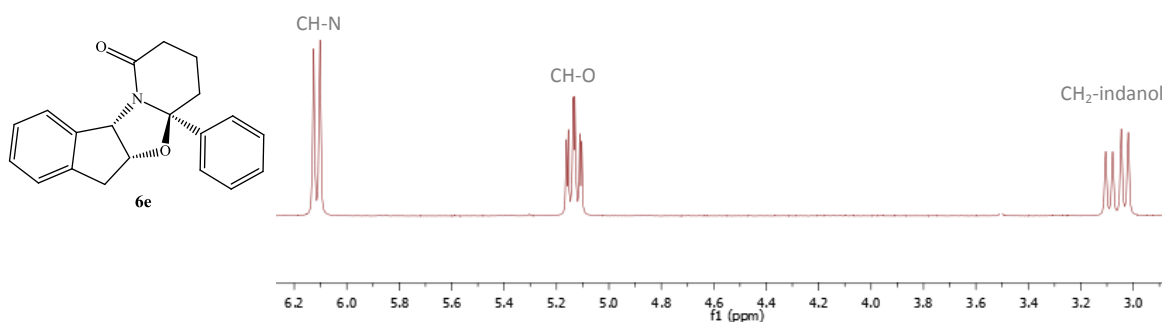


Figure 22 – ¹H-NMR spectra of compound **6e** between 3.00 and 6.20 ppm.

X-ray crystallography of compound **6e**, an indanol derivative, was performed to make sure about the chirality of the new carbon center. The result of the structure's resolution is presented in figure 23 and a screening of several perspectives in figure 24, as well. Analyzing both figures

and considering the phenyl and cyclopentane fused rings the plan it is possible to see nitrogen and phenyl groups behind the plan. In cyclocondensation reactions with indanol amino alcohol was just observed one diastereomer.

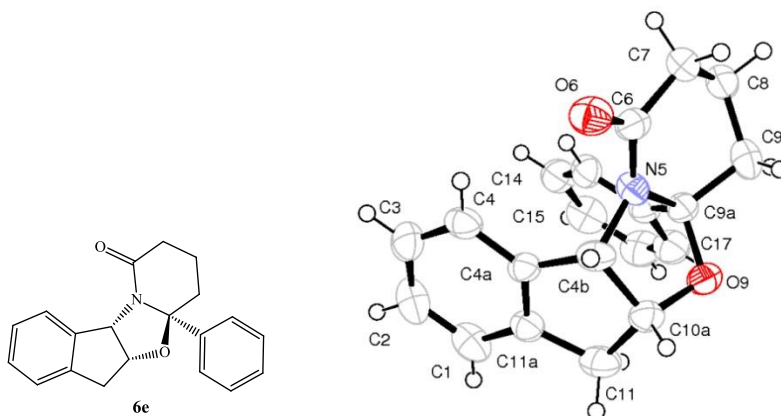


Figure 23 – Chemical structure of compound **6e** and respective crystallographic representation.

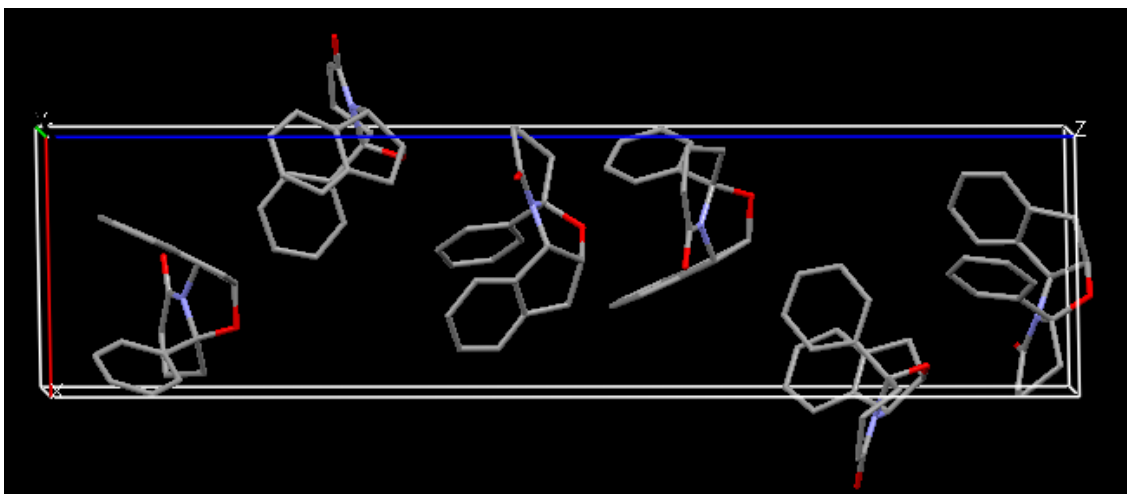
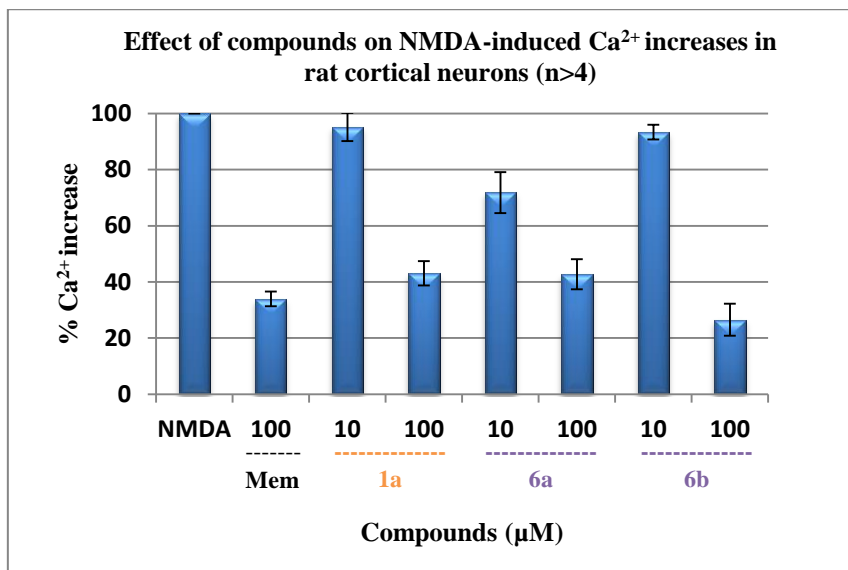


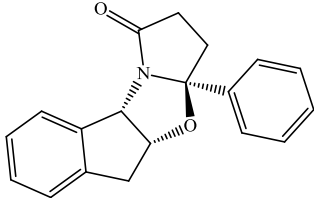
Figure 24 – Several perspectives of compound **6e**.

Graph 3 – Results of inhibition of Ca²⁺ increase by **6a** and **6b** compounds ((1*S*, 2*R*)-(–)-*cis*-1-Amino-2-indanol derivatives).



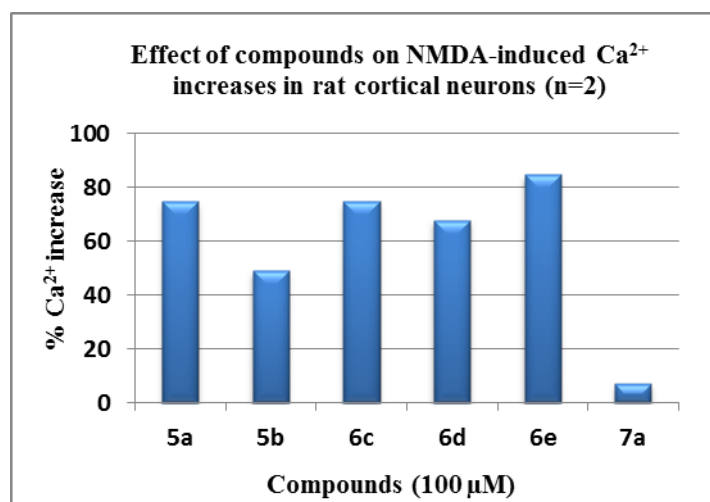
At 100μM, compound **6a** revealed to be more active as **1a**. Compound **6b** shown to be more active than compounds **1a** and **6a** at the same concentration. The structural difference between the two compounds tested is the additional phenyl group fused with pyrrolidone ring in compound **6a**. A larger molecule with the additional ring doesn't bring an increase of activity and, for that reason the IC₅₀ value was only determined for the most active compound, **6b** (table 10).

Table 10 – IC₅₀ values obtained for compound **6b**.

Reference	Chemical structure	IC ₅₀ (μM)
6b		51±8

The remaining compounds of (*S*)-tyrosinol, (*S*)-phenylalaninol and ((1*S*, 2*R*)-(–)-*cis*-1-amino-2-indanol libraries (tables 7-9) were biological evaluated (excepted **6a** and **6b**) and the results are shown on table presented below (graph 4).

Graph 4 – Results of inhibition of Ca^{2+} increase of compounds **5a - b** and **6c - e**.



Compound **6e**, an oxazolopiperidone, was the most active compound from indanol library. Compound **6c**, with a chlorine atom in phenyl group, revealed to be best inhibitor than compound with a bromine atom **6d**.

The (*S*)-tyrosinol derivative **5b** has a similar inhibitory action to compound **1a** and compound **5a** lead to a decrease of Ca^{2+} influx, meaning that has a major inhibitory action. The presence of a hydroxyl group ((*S*)-tyrosinol derivatives) doesn't demonstrate a big difference in Ca^{2+} influx and could be an indication which that an increase of polarity is not important, in this case, for the interaction with NMDA receptor.

Compound **7a** resulted of a Suzuki coupling reaction of **1d** and was synthesized to understand if an expansion of the distance of phenyl group with the halogenated atom brings an increase of activity. The result indicates that this structural modification decreased significantly the action as NMDA receptor antagonist. So, the molecule's size is an important factor for the antagonist activity of oxazolopiperidone and oxazolopiperidone synthesized compounds.

The IC_{50} values of compounds presented in graph 4 are unknown but looking for the values of inhibition is almost right that compounds **5a**, **6c** and **6e** and (table 11) resulted in an optimization of base-structure (**1a** (table 10)).

In general, the presence of a halogen in the phenyl group lead to an increase of activity, while the increase of molecule's size results in loss of activity (compounds **6a** and **7a**). (*S*)-phenylalaninol derivatives were always more active than the corresponding enantiomers. These results confirm the importance of enantioselective synthesis in medicinal chemistry. The new constructed libraries, for the study of NMDA receptor antagonists, resulted in a successful hit-to-lead optimization process with the discovery of new promising compounds, some of them with IC_{50} values very close to memantine, for example compounds **1c** and **1d**. The determination of IC_{50} values of remaining compounds are in progress.

II.3 – Biological evaluation of tryptophanol-derived bicyclic lactams

The (*S*) and (*R*)-tryptophanol-derived bicyclic lactams (compounds **3a – h** and **4a – h**) were evaluated as antitumor agents. (*S*)-tryptophanol-derived oxazolopiperidone lactams were described by Santos's group having an important role in activation of the p53, a tumor suppressor protein, by inhibition of p53 interaction with MDMX and MDM2.

Were selected several cancer cell lines and the screening was made at a concentration of 100µM (table 11). Compounds **3a**, **3g** and **3h** were tested later in another biological screening.

Table 11 – Screening of (*S*) and (*R*)-tryptophanol-derived bicyclic lactams **3b – f** and **4a – h**.

Ref.	Breast adenocarcinoma		Lung carcinoma	Prostate cancer	Gastric adenocarcinoma	Colon adenocarcinoma	Osteosarcoma
	MCF-7	MDA-MB-231	A-549	DU-145	AGS	Caco-2	MG-63
	%CV	%CV	%CV	%CV	%CV	%CV	%CV
3b	24±1	26±6	37±8	51±2	13±10	>50	19±4
3c	25±0	17±2	9±6	9±1	26±20	29±2	6±1
3d	21±1	>50	15±15	23±5	14±12	30±2	6±1
3e	>50	>50	>50	>50	>50	>50	>50
3f	>50	>50	35±4	>50	30±4	>50	38±25
4a	>50	>50	>50	>50	>50	>50	>50
4b	>50	>50	>50	>50	>50	>50	10±1
4c	9±3	11±1	6±3	8±1	4±0	30±3	7±2
4d	28±3	>50	5±1	10±0	8±7	28±1	8±1
4e	19±9	14±5	26±15	17±2	14±2	32±5	16±3
4f	26±6	>50	37±2	>50	18±2	>50	>50
4g	>50	>50	>50	>50	>50	>50	>50
4h	30±7	>50	>50	>50	27±5	>50	40±3

Exp. Time: 48h / n=2

CV – Cell Viability by MTT assay

c=100µM

The most promising compounds were **4c** and **4d** with %CV lower than 10%, in several cancer cell lines. Cell viability (CV) is a practical way to measure the percentage of life in a cellular medium. For Caco-2 cell line (colon adenocarcinoma) all the compounds revealed to be inactive at high concentration (100µM) with a maximum of 28% of cell viability for compound **4d**. Six compounds were selected (table 11 in pink) to be determinate the respective IC₅₀ values and the selection method was based on the compounds which caused lower cell %CV at 100 µM i.e., the most cytotoxic compounds. The respective values of IC₅₀ are shown below (table 12).

Table 12 – IC₅₀ values of selected compounds of (*S*) and (*R*)-tryptophan library.

Ref.	Breast adenocarcinoma		Lung carcinoma	Prostate cancer	Gastric adenocarcinoma	Osteosarcoma
	MCF-7	MDA-MB-231	A-549	DU-145	AGS	MG-63
	IC ₅₀	IC ₅₀	IC ₅₀	IC ₅₀	IC ₅₀	IC ₅₀
3c	81±2	61	60±1	46±4	>100	57±1
3d	84	53±1	45±4	55±6	46±1	56±3
4c	60±2	49±5	59±1	59±1	>100	48±2
4d	71±2	54±1	73±9	66±9	>100	63±3
4e	>100	>100	>100	>100	>100	>100
4f	>100	>100	>100	>100	>100	>100
DOX*	2.6±0.1	6.2±0.1	2.0±0.1	27.8±6.4	1.3±0.2	39.6±2.5

Exp. Time: 48h / n=3

CV – Cell Viability by MTT assay

*Doxorubicin

IC₅₀ (μM)

Compound **4c**, the (*R*)-tryptophan-derived oxazopyrrolidone lactam, which has a chlorine atom in *para* position of phenyl group, seems to be a promising compound. The positive control was doxorubicin, a common drug used in cancer treatment. In next section will be discussed the hit-to-lead optimization process of compound **4c** (figure 25).

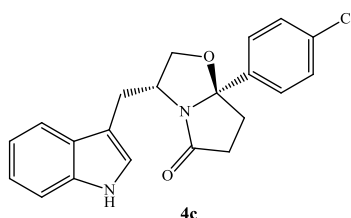


Figure 25 – Chemical structure of the hit compound **4c**, a (*R*)-tryptophan-derived oxazopyrrolidone lactam.

II.3.1 – Hit-to-lead optimization

The hit-to-lead optimization process of compound **4c** was based on possible structural changes as protections of nitrogen atom of the indole group or Suzuki-Miyaura cross-coupling reactions, for example.

The optimization started with nitrogen atom of the indole protections which are represented by compounds **9a**, **9c** and **9f**. Compound **9a** corresponding to a protection with a methyl group, compound **9f** has a *tert*-butyloxycarbonyl (Boc) group and, at last, compound **9c** with a tosyl

(Ts) group in nitrogen atom of the indole group (figure 26). These protecting groups were chosen to have a general ideal if an increase of size has a positive response or if free amine is important for antitumor activity.

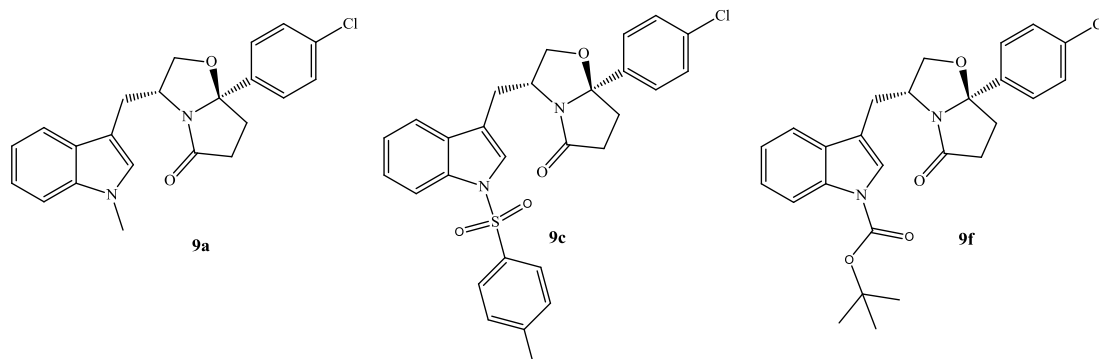
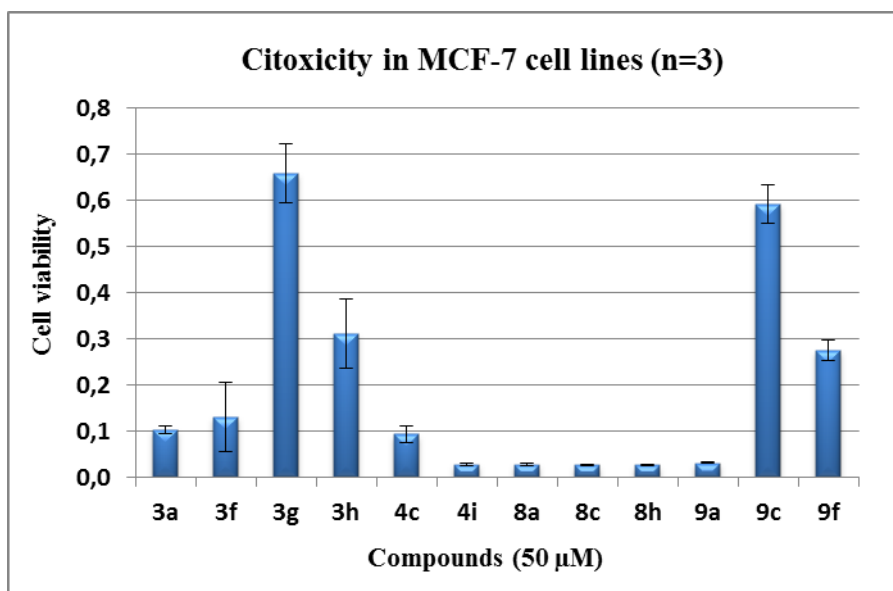


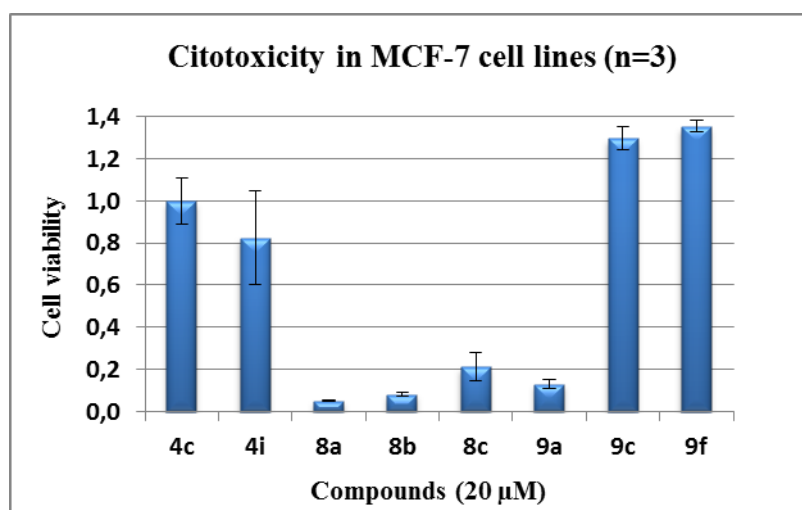
Figure 26 – Compounds **9a**, **9c** and **9f**, corresponding to protections of nitrogen atom of the indole group.

For biological screening was only used one cell line, more precisely MCF-7, a characteristic line of breast adenocarcinoma, the compounds were tested at 50 and 20 μ M and the results are shown in graphs 5 and 6, respectively.

Graph 5 – Screening of optimized compounds at 50 μ M, in MCF-7 cell lines.



Graph 6 – Screening of optimized compounds at 20 μ M, in MCF-7 cell lines.



The increase of protecting group's size has an important impact in antitumor activity: there is a substantial increase of cell viability. **9c**, compound with tosyl group, revealed to be the less active and **9a** more active than reference compound **4c**, showing that methylation has the better positive response in cell viability (graph 5). The reactions of protection were performed with sodium hydride (NaH), a strong base needed to deprotonate the amine of indole. The protections with *tert*-butyloxycarbonyl (**9f**) and tosyl (**9c**) were made in dry THF and the methylation (**9a**) in DMF and respective yields are described in table 13 [99].

In this screening are presented also compounds **3a**, **3g** and **3h**, (*S*)-tryptophanol derivatives which weren't tested in first screening at 100 μ M (table 11). Looking for graph 5, these three compounds were less active than **4c**, at 50 μ M.

Compounds **3a-c** were synthesized using Suzuki-Miyaura cross-coupling reactions (figure 27). The main goal of the synthesis of these compounds is to understand if an extension of the phenyl ring is beneficial and if others substituents in *para* position result in an increase of activity. In Suzuki-Miyaura cross-coupling reactions there is a coupling between a boronic acid derivative and a halide with the help of a catalyst, more precisely a palladium complex. In this case was used Pd(PPh₃)₂Cl₂ as catalyst and the reactions were performed in dry 1,4-dioxane, with good yields which are described below (table 14) [100].

In this first optimization compound **4i** was also synthesized, a compound very similar with **4c**, which has an additional phenyl ring, fused with pyrrolidone lactam i.e., an oxazoloisoindolinone (figure 28). Analyzing the effects in MCF-7 cell lines of these 4 compounds (graph 4), it is possible to see a strong impact in cell viability at 50 μ M. At 20 μ M, compound **4i** loss significantly the activity comparing with compounds **9a** and **8a-c** (graph 5). However, **4i** is even

more active than **4c** and this is an indication that oxazoloisindolinone moiety is responsible for a small increase of cytotoxicity. So the four most active compounds (**9a** and **8a-c**) were considered promising and selected for determining the respective IC₅₀ values (table 13).

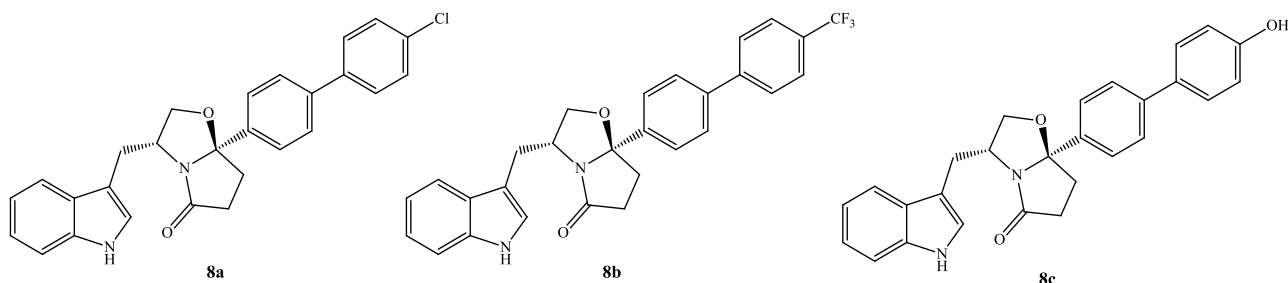


Figure 27 – Chemical structures of compounds **8a-c**.

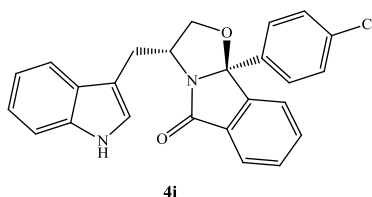


Figure 28 – Chemical structure of compound **4i**.

Table 13 – IC₅₀ values of optimized compounds.

Reference	IC ₅₀ (μM)
8a	10.3±1.1
8b	9.0±1.1
8c	7.3±1.1
9a	11.7±1.1

The assays of IC₅₀ determination revealed values comprised between 7 and 12 μM. Compound with methylation in amine (**9a**) was the less active compound with an IC₅₀ of 11.7 μM. The best result was obtained for compound **8c**, with an IC₅₀ value of 7.3 μM, which means that a hydroxyl group in *para* position is more favorable than a chlorine or trifluoromethyl groups. This is also an indication that a more polar molecule is an important factor, maybe to establish hydrogen bonds or polar interactions. With these small structural variations was possible an

almost ten-fold increase of activity, comparing with **4c** which revealed an IC_{50} value of 60.0 μ M, in the same cell line.

So based on previous positive results were synthesized more derivatives of compound **4c**. This derivatization resulted, primarily in the use of other small protecting groups for indole and also the synthesis of more compounds by Suzuki-Miyaura cross-coupling reactions with several boronic acids. All the compounds are shown in figure 29 and the respective yields in table 14.

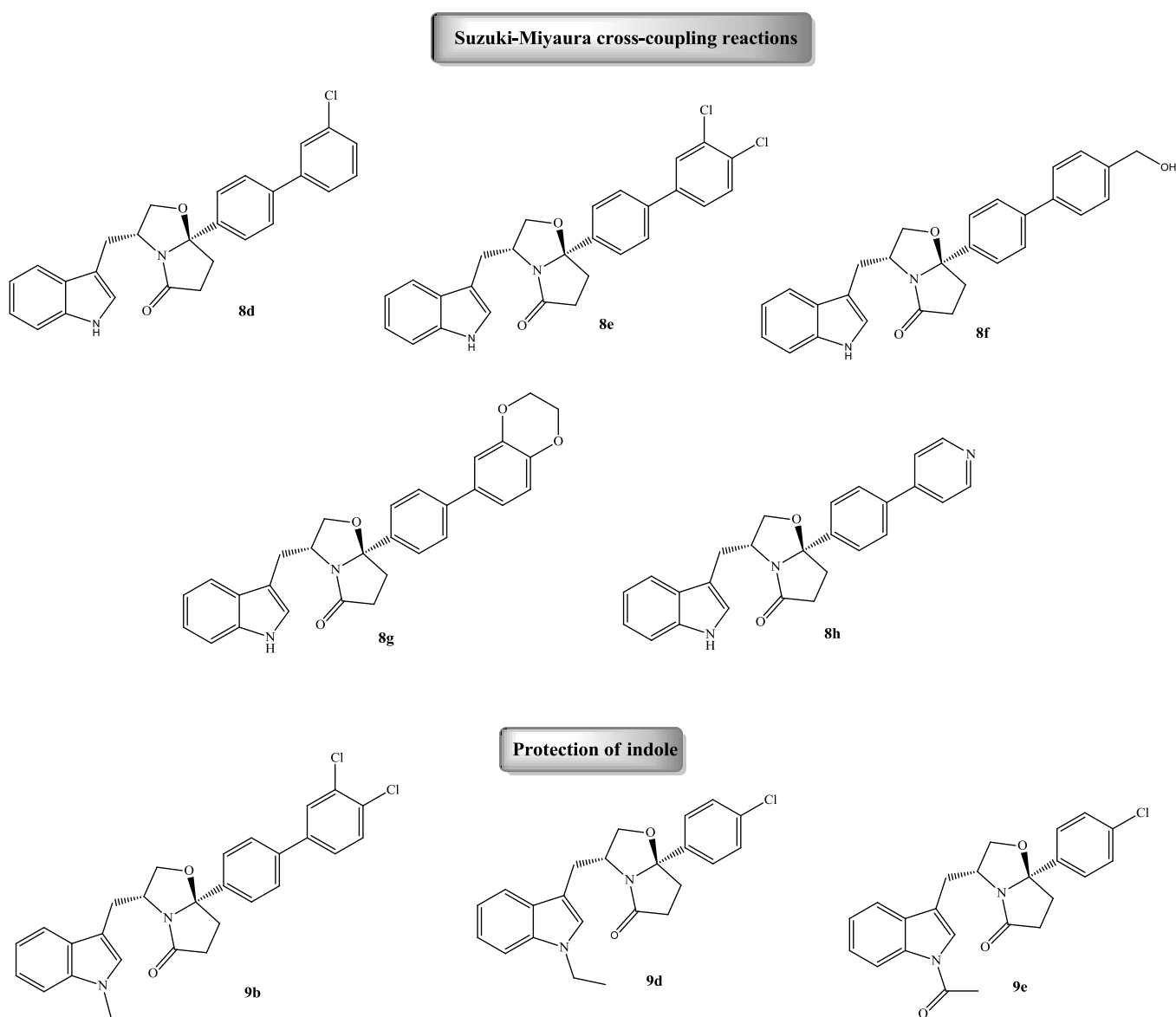


Figure 29 – Compounds presented in second screening of **4c** optimization.

Table 14 – Yields of reactions of optimized compounds.

Reference	Yield (%)
4i	62.5
8a	93.9
8b	86.1
8c	84.9
8d	77.6
8e	85.2
8f	71.0
8g	28.1
8h	97.0
9a	88.8
9b	94.7
9c	85.7
9d	77.8
9e	68.7
9f	65.7

In general, Suzuki-Miyaura cross-coupling reactions had good/excellent yields with the exception of compound **8g** with a benzodioxane ring. This yield is related with the low solubility of respective boronic acid in dioxane, even at high temperature. The indole protections were also easily performed and the lowest yield was 68.7% for **9e** derivative.

The new derivatives were tested in MCF-7 cell lines, firstly with a screening at 20 μ M (graph 7). At this concentration compound **8g**, with benzodioxane ring, revealed to be inactive so, it is possible conclude that this extension of chemical space was unfavorable. Compound with pyridine ring (**8h**) was less active than compounds **8d**, **8e**, **8f**, **9d** and **9e**, reinforcing the idea that to extend the chemical space has a negative effect in antitumor activity. Therefore, the determination of IC₅₀ values were made for the five active compounds and the results are shown in table 15.

Graph 7 – Screening of last optimized compounds at 20 μ M, in MCF-7 cell lines.

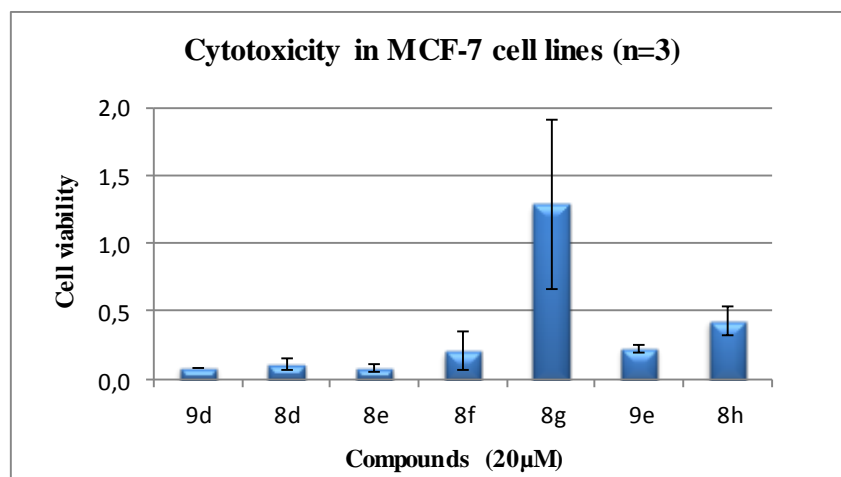


Table 15 – IC₅₀ values of optimized compounds.

Reference	IC ₅₀ (μM)
8d	9.0±1.0
8e	6.7±1.0
8f	7.0±1.1
8h	16.6±1.2
9d	10.4±1.4
9e	17.1±1.1

Protection of indole nitrogen (**9d** and **9e**) revealed a loss of activity, comparing with **9a**, and seems to be a preference for alkyl groups without hetero atoms. About the other compounds, there wasn't a significant increase in activity. **8h** was the compound less active as expected with an IC₅₀ value of 16.6 μM. Compounds **8d-f** have very similar values with **8c**. Addition of a CH₂ between hydroxyl and phenyl groups (**8f**) showed to have no effect.

To understand if *para* position is important for activity was decided to synthesize the correspondent compound of **8a** with a chlorine atom in *meta* position but, in this case the result was almost the same. The second strategy was the synthesis of a compound with chlorine atom in *meta* and *para* positions (**8e**). The gain of activity was small but still an increase of IC₅₀ value for 6.7 μM.

After these results was decided procedure to methylation of indole group in compound **8e** once that protecting group shown good results. The protection was made after Suzuki-Miyaura cross-coupling reaction and the compound **9b** (figure 29) was tested in the same way. However the result was not good and the compound revealed an IC₅₀ value higher than 20 μM, indicating that, in this case, is more favorable the indole in free form. It is likely that these two compounds, **9a** and **8e**, have different interactions or mechanisms of action.

To finish the antitumor activity studies of compounds described in this section were performed biological assays in several cancer cell lines (table 16). The main goal is to see if there is some selectivity between lines. Were tested the compounds that presented IC₅₀ values below 10 μM i.e., compounds **8a-b** and **8d-f**.

Analyzing the results compound **8f** was inactive for all cell lines and the other compounds revealed good selectivity for MCF-7, except AGS cell line (gastric adenocarcinoma) with lower IC₅₀ values.

The last step was the toxicity evaluation of the same compounds in non-tumor cell lines (table 16). This assay was made in human embryonic kidney 293 (HEK 293) cells and the goal was analyzing if the promising compounds would be toxic for normal cells. All compounds were inactive for the tested concentrations.

Table 16 – IC₅₀ values of the most promising compounds in several cell lines.

	Breast adenocarcinoma	Lung adenocarcinoma	Lung carcinoma	Prostate cancer	Gastric adenocarcinoma	Osteosarcoma	Embryonic kidney
	MDA-MB-231	Calu-3	A-549	DU-145	AGS	MG-63	HEK 293
Ref.	IC₅₀						
8b	28.2±1.5	27.3±4.1	62.9±18.0	23.8±5.1	15.4±6.1	26.8±0.4	>50
8c	47.7±3.4	49.1±4.6	72.0±6.3	48.2±4.9	38.1±10.1	49.4±6.2	>50
8d	45.9±1.3	33.1±2.8	64.6±4.9	39.1±2.7	16.5±6.1	30.9±2.3	>100
8e	68.3±5.7	68.5±4.9	87.9±16.6	20.5±12.1	12.6±4.4	55.5±6.8	>50
8f	>100	>100	>100	>100	>100	>100	>50

Exp. Time: 48h / n=6

CV – Cell Viability by MTT assay

IC₅₀ (μM)

Chapter III – Conclusion and Future Work

In this thesis, new libraries of enantiopure phenylalaninol and tryptophanol-derived bicyclic lactams were synthesized.

The phenylalaninol derivatives were evaluated as NMDA receptor antagonists. Compounds **1c** and **1d** revealed to be more active than the hit compound **1a**. (*S*)-phenylalaninol derivatives were more active than (*R*) derivatives as NMDA receptor antagonists. Also, halogenated atoms at the *para* position of phenyl groups are preferred to other groups. In this screening two (1*S*, 2*R*)-(-)-*cis*-1-Amino-2-indanol derivatives were also evaluated leading to the discovery of a new family of NMDA receptor antagonists through the identification of compound **6b** with a IC_{50} value of 51 μ M. Finally, structural optimization of these three promising compounds was developed and the determination of the respective IC_{50} values is in progress.

Further studies must be performed in order to evaluate the exact mechanism of action of these compounds and study the selectivity over other glutamate receptor.

Moreover, a library of tryptophanol-derived bicyclic lactams was tested in several cancer cell lines. The best results obtained were obtained in MCF-7 line derived from breast adenocarcinoma. Enantiomers *R* revealed to be more active. More precisely compound **4c**, a derivative with a chlorine atom at the *para* position of the phenyl group. It was carried out to a hit-to-lead optimization of compound **4c**. More bulky protecting groups are not favorable for activity. Moreover, the presence of chlorine atoms at the *meta* and *para* positions, and the presence of hydroxyl groups are important for activity as antitumor agents. The most promising compounds were **8b-f** with IC_{50} values between 6.7 and 9.0 μ M. Furthermore, these five compounds were selective for MCF-7 cell lines comparing with other cancer lines and were not toxic for normal cells (HEK 293).

Chapter IV - Experimental Procedure

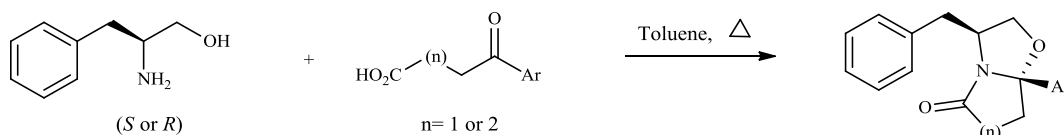
IV.1 – General Methods

All reagents and solvents were obtained from commercial suppliers and were used without further purification. Melting points were determined using a Kofler camera Bock monoscope M. Analysis Merck Silica Gel 60 F254 plates were used as analytical thin layer chromatography and flash chromatography was performed on Merck Silica Gel (200- 400 mesh). ^1H and ^{13}C NMR spectra were recorded on a Bruker 400 Ultra-Shield. ^1H nuclear magnetic resonance spectra were recorded at 300 MHz and ^{13}C nuclear magnetic resonance spectra were recorded at 100 MHz. ^1H and ^{13}C NMR chemical shifts are reported in parts per million (ppm, δ) referenced to the solvent used and the proton coupling constants J in hertz (Hz). Spectras were assigned using appropriate COSY, DEPT, HMQC and HMBC sequences. Microanalysis was performed in a Flash2000 ThermoScientific elemental analyzer and are within $\pm 0.4\%$ of theoretical values

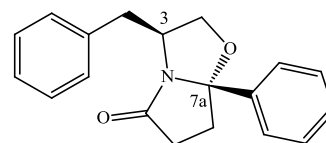
IV.2 - General procedure for cyclocondensation reactions

To a solution of a particular aminoalcohol (0.660mmol) in toluene (5ml) was added the appropriate oxocarboxylic acid (0.730mmol). The mixture was heated at reflux for 10-24h under *Dean-Stark* apparatus, until total consumption of the starting aminoalcohol. The solvent was evaporated and the residue was dissolved in EtOAc. The organic phase was washed with saturated aqueous solutions of NaHCO_3 and NaCl , dried with anhydrous magnesium sulfate, filtered and evaporated. The crude was absorbed on silica and purified by flash chromatography using ethyl AcOEt/*n*-hexane as eluent.

IV.2.1 – (*S*) and (*R*)-phenylalaninol-derived bicyclic lactams

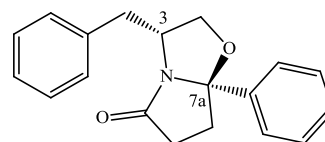


(3*S*,7*aS*)-3-benzyl-7*a*-phenyltetrahydropyrrolo[2,1-*b*]oxazol-5(6*H*)-one (1a): Following the general procedure, to a solution of (*S*)- phenylalaninol (0.100g, 0.661mmol) in toluene (5mL) was added 3-benzoyl propionic acid (0.130g, 0.734mmol). Reaction time: 16h. The compound was purified by flash chromatography (EtOAc/*n*-hexane 1:2) to afford the title compound as a pale yellow oil (0.160g, 82.3%); ^1H -NMR (300 MHz, MeOD) δ 7.53 –



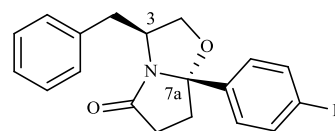
7.46 (m, 2H, ArH), 7.46 – 7.31 (m, 3H, ArH), 7.24 – 7.08 (m, 3H, ArH), 7.07 – 7.01 (m, 2H, ArH), 4.41 – 4.27 (m, 1H, H-3), 4.16 (dd, $J = 8.7, 7.4$ Hz, 1H, H-2), 3.57 (dd, $J = 8.8, 6.8$ Hz, 1H, H-2), 2.93 – 2.76 (m, 1H, CH₂), 2.70 (dd, $J = 13.7, 7.1$ Hz, 1H, ArCH₂), 2.56 – 2.39 (m, 2H, CH₂), 2.37 – 2.12 (m, 2H, ArCH₂+ CH₂), as described in literature [79].

(3R,7aR)-3-benzyl-7a-phenyltetrahydropyrrolo[2,1-b]oxazol-5(6H)-one (2a): Following the general procedure, to a solution of (*R*)- phenylalaninol (0.101g, 0.667mmol) in toluene (5mL) was added 3-benzoyl propionic acid (0.131g, 0.734mmol). Reaction time: 24h. The compound was purified by flash chromatography (EtOAc/*n*-hexane 1:2) to afford the title compound as a pale yellow oil (0.157g, 80.1%); ¹H-NMR spectra was found to be identical to the one obtained for compound **1a** and also described in literature [82].



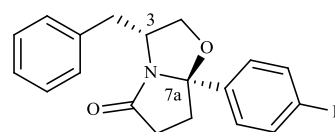
(3S,7aS)-3-benzyl-7a-(4-fluorophenyl)tetrahydropyrrolo[2,1-b]oxazol-5(6H)-one (1b):

Following the general procedure, to a solution of (*S*)-phenylalaninol (0.100g, 0.661mmol) in toluene (5mL) was added 3-(4-fluorobenzoyl) propionic acid (0.143g, 0.728mmol). Reaction time: 23h. The compound was purified by flash chromatography (EtOAc/*n*-hexane 1:2) to afford the title compound as a yellow oil (0.188g, 91.2%); $[\alpha]_D^{25} = +6.0^\circ$ ($c = 0.011, \text{CH}_2\text{Cl}_2$); ¹H-NMR (300 MHz, CDCl₃) δ 7.47 – 7.38 (m, 1H, ArH), 7.24 – 7.10 (m, 2H, ArH), 7.10 – 6.98 (m, 2H, ArH), 4.38 (dq, $J = 9.3, 7.0$ Hz, 1H, H-3), 4.08 (dd, $J = 8.8, 7.4$ Hz, 1H, H-2), 3.51 (dd, $J = 8.8, 7.0$ Hz, 1H), 2.88 (dd, $J = 13.7, 6.2$ Hz, 1H), 2.84 – 2.67 (m, 1H), 2.59 – 2.36 (m, 1H), 2.32 – 2.19 (m, 1H), 2.19 – 2.06 (m, 1H); ¹³C-NMR (100 MHz, CDCl₃) δ 179.98 (C=O), 164.42 (ArC), 161.15 (ArC), 138.60 (ArC), 137.23 (ArC), 129.02 (ArC), 128.67 (ArC), 127.15 (ArC), 127.04 (ArC), 126.81 (ArC), 115.87 (ArC), 115.59 (ArC), 102.07 (C-7a), 72.38 (C-2), 56.64 (C-3), 40.05 (ArCH₂), 35.21, 32.59; Anal. Calcd. (C₁₉H₁₈FNO₂•0.25H₂O): C, 72.30%; H, 5.92%; N, 4.44%. Found C, 71.93%; H, 5.84%; N, 4.31%.



(3R,7aR)-3-benzyl-7a-(4-fluorophenyl)tetrahydropyrrolo[2,1-b]oxazol-5(6H)-one (2b):

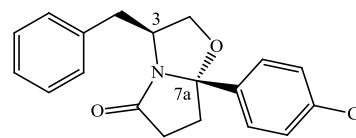
Following the general procedure, to a solution of (*S*)-phenylalaninol (0.101g, 0.667mmol) in toluene (5mL) was added 3-(4-fluorobenzoyl) propionic acid (0.144g, 0.734mmol). Reaction time: 22h. The compound was purified by flash chromatography (EtOAc/*n*-hexane 1:2) to afford the title compound as a yellow oil (0.172g, 82.6%); $[\alpha]_D^{25} = -5.4^\circ$ ($c = 0.011, \text{CH}_2\text{Cl}_2$); ¹H-NMR spectra was found to be identical to the



one obtained for compound **1b**; Anal. Calcd. (C₁₉H₁₈FNO₂): C, 73.29%; H, 5.83%; N, 4.50%. Found C, 72.74%; H, 6.49%; N, 4.94%.

(3*S*,7*aS*)-3-benzyl-7*a*-(4-chlorophenyl)tetrahydropyrrolo[2,1-*b*]oxazol-5(6*H*)-one (1c):

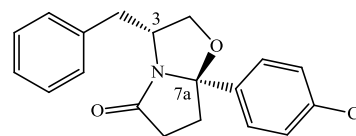
Following the general procedure, to a solution of (*S*)-phenylalaninol (0.100g, 0.661mmol) in toluene (5mL) was added 3-(4-chlorobenzoyl) propionic acid (0.155g, 0.728mmol). Reaction time: 23h. The compound was purified



by flash chromatography (EtOAc/*n*-hexane 1:2) to give the title compound as a yellow oil in (0.205g, 94.9%); $\alpha_D^{25} = +6.0^\circ$ (0.014, CH₂Cl₂); ¹H-NMR (300 MHz, CDCl₃) δ 7.48 – 7.34 (m, 4H, ArH), 7.29 – 7.14 (m, 4H, ArH + CDCl₃), 7.12 – 7.04 (m, 2H, ArH), 4.43 (dq, *J* = 9.3, 7.0 Hz, 1H, *H*-3), 4.13 (dd, *J* = 8.8, 7.4 Hz, 1H, *H*-2), 3.55 (dd, *J* = 8.9, 7.0 Hz, 1H, *H*-2), 2.93 (dd, *J* = 13.7, 6.2 Hz, 1H, ArCH₂), 2.88 – 2.72 (m, 1H), 2.63 – 2.42 (m, 2H), 2.38 – 2.11 (m, 2H); ¹³C-NMR (75 MHz, CDCl₃) δ 179.93 (C=O), 141.39 (ArC), 137.16 (ArC), 134.37 (ArC), 129.04 (ArC), 129.00 (ArC), 128.66 (ArC), 126.81 (ArC), 126.72 (ArC), 101.96 (C-7*a*), 72.41 (C-2), 56.66 (C-3), 40.04 (ArCH₂), 35.07, 32.54; Anal. Calcd. (C₁₉H₁₈ClNO₂•0.05H₂O): C, 69.42%; H, 5.56%; N, 4.26%. Found C, 69.57%; H, 5.51%; N, 4.44%.

(3*R*,7*aR*)-3-benzyl-7*a*-(4-chlorophenyl)tetrahydropyrrolo[2,1-*b*]oxazol-5(6*H*)-one (2c):

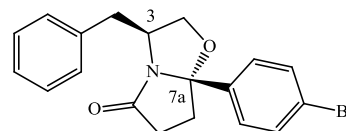
Following the general procedure, to a solution of (*R*)-phenylalaninol (0.100g, 0.661mmol) in toluene (5mL) was added 3-(4-chlorobenzoyl) propionic acid (0.155g, 0.728mmol). Reaction time: 24h. The compound was purified



by flash chromatography (EtOAc/*n*-hexane 1:3) to afford the title compound as a yellow oil (0.180g, 83.1%); $[\alpha]_D^{25} = -5.0^\circ$ (c = 0.014, CH₂Cl₂); ¹H-NMR spectra was found to be identical to the one obtained for compound **1c**; Anal. Calcd. (C₁₉H₁₈ClNO₂): C, 69.62%; H, 5.53%; N, 4.27%. Found C, 69.72%; H, 5.58%; N, 4.39%.

(3*S*,7*aS*)-3-benzyl-7*a*-(4-bromophenyl)tetrahydropyrrolo[2,1-*b*]oxazol-5(6*H*)-one (1d):

Following the general procedure, to a solution of (*S*)-phenylalaninol (0.100g, 0.661mmol) in toluene (5mL) was added 3-(4-bromobenzoyl) propionic acid (0.187g, 0.725mmol). Reaction time: 25h. The compound was purified by flash

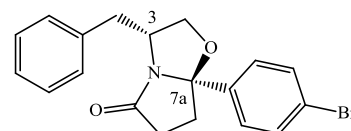


chromatography (EtOAc/*n*-hexane 1:2) to give the title compound as an orange oil (0.246g, 99.8%); $\alpha_D^{25} = +5.4^\circ$ (0.010, CH₂Cl₂); ¹H-NMR (300 MHz, CDCl₃) δ 7.59 – 7.52 (m, 1H, ArH), 7.42 – 7.34 (m, 1H, ArH), 7.29 – 7.14 (m, 2H, ArH), 7.12 – 7.05 (m, 1H, ArH), 4.43 (dq, *J* = 9.3, 7.0 Hz, 1H, *H*-3), 4.17 – 4.09 (m, 1H, *H*-2), 3.55 (dd, *J* = 8.9, 7.0 Hz, 1H, *H*-2), 2.93 (dd, *J*

= 13.7, 6.2 Hz, 1H, ArCH₂), 2.88 – 2.71 (m, 1H), 2.64 – 2.41 (m, 2H), 2.37 – 2.12 (m, 2H); ¹³C-NMR (100 MHz, CDCl₃) δ 179.94 (C=O), 141.96 (ArC), 137.17 (ArC), 132.02 (ArC), 129.02 (ArC), 128.68 (ArC), 127.07 (ArC), 126.83 (ArC), 122.56 (ArC), 102.02 (C-7a), 72.44 (C-2), 56.70 (C-3), 40.06 (ArCH₂), 35.06, 32.55; Anal. Calcd. (C₁₉H₁₈BrNO₂•0.1CH₂Cl₂): C, 60.25%; H, 4.83%; N, 3.68%. Found C, 60.01%; H, 4.90%; N, 4.00%

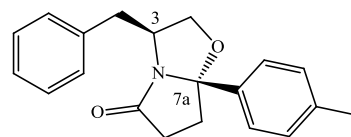
(3R,7aR)-3-benzyl-7a-(4-bromophenyl)tetrahydropyrrolo[2,1-b]oxazol-5(6H)-one (2d)

Following the general procedure, to a solution of (*R*)-phenylalaninol (0.101g, 0.669mmol) in toluene (5mL) was added 3-(4-bromobenzoyl) propionic acid (0.189g, 0.736mmol).



Reaction time: 26h. The compound was purified by flash chromatography (EtOAc/*n*-hexane 1:3) to afford the title compound as a yellow oil (0.189g, 75.2%); $[\alpha]_D^{25} = -4.7^\circ$ (*c* = 0.011, CH₂Cl₂); ¹H-NMR spectra was found to be identical to the one obtained for compound **1d**; Anal. Calcd. (C₁₉H₁₈BrNO₂): C, 61.30%; H, 4.87%; N, 3.76%. Found C, 61.19%; H, 4.94%; N, 3.71%.

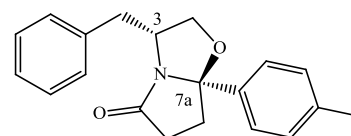
(3S,7aS)-3-benzyl-7a-(*p*-tolyl)tetrahydropyrrolo[2,1-b]oxazol-5(6H)-one (1e): Following the general procedure, to a solution of (*S*)-phenylalaninol (0.100g,



0.661mmol) in toluene (5mL) was added 3-(4-methylbenzoyl) propionic acid (0.140g, 0.728mmol). Reaction time: 25h. The compound was purified by flash chromatography (EtOAc/*n*-hexane 1:2) to give the title compound as a yellow oil (0.189g, 93.2%); $\alpha_D^{25} = +1.4^\circ$ (0.015, CH₂Cl₂); ¹H-NMR (300 MHz, CDCl₃) δ 7.42 – 7.35 (m, 2H, ArH), 7.28 – 7.14 (m, 6H, ArH +CDCl₃), 7.12 – 7.05 (m, 2H, ArH), 4.41 (dq, *J* = 9.3, 7.0 Hz, 1H, *H*-3), 4.17 – 4.07 (m, 1H, *H*-2), 3.57 (dd, *J* = 8.8, 7.0 Hz, 1H, *H*-2), 2.95 (dd, *J* = 13.7, 6.2 Hz, 1H, ArCH₂), 2.90 – 2.72 (m, 1H), 2.62 – 2.42 (m, 2H), 2.40 (s, 3H, ArCH₃), 2.37 – 2.15 (m, 2H). ¹³C-NMR (100 MHz, CDCl₃) δ 179.98 (C=O), 139.73 (ArC), 138.20 (ArC), 137.50 (ArC), 129.49 (ArC), 129.06 (ArC), 128.62 (ArC), 126.71 (ArC), 125.17 (ArC), 102.44 (C-7a), 72.39 (C-2), 56.59 (C-3), 40.07 (ArCH₂), 35.32, 32.74; Anal. Calcd. (C₂₀H₂₁NO₂•0.15H₂O): C, 77.52%; H, 6.94%; N, 4.52%. Found C, 77.35%; H, 6.95%; N, 4.44%.

(3R,7aR)-3-benzyl-7a-(*p*-tolyl)tetrahydropyrrolo[2,1-b]oxazol-5(6H)-one (2e): Following the general procedure, to a solution of (*R*)-phenylalaninol

(0.100g, 0.661mmol) in toluene (5mL) was added 3-(4-methylbenzoyl) propionic acid (0.140g, 0.728mmol). Reaction time: 26h. The compound was purified by flash chromatography

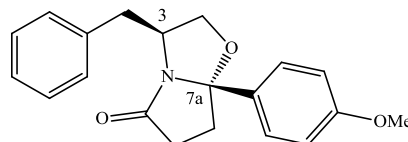


(EtOAc/*n*-hexane 1:2) to give the title compound as a yellow oil (0.152g, 74.6%); $\alpha_D^{25} = -3.2^\circ$

(0.005, CH₂Cl₂); ¹H-NMR spectra was found to be identical to the one obtained for compound **1e**. Anal. Calcd. (C₂₀H₂₁NO₂): C, 64.67%; H, 5.70%; N, 3.77%; S, 8.63%. Found C, 65.01%; H, 5.81%; N, 3.80%; S, 8.40%.

(3*S*,7*aS*)-3-benzyl-7*a*-(4-methoxyphenyl)tetrahydropyrrolo[2,1-*b*]oxazol-5(6*H*)-one (1*f*):

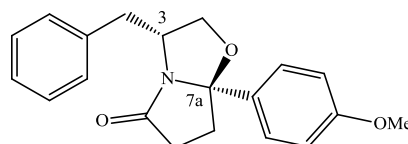
Following the general procedure, to a solution of (*S*)-phenylalaninol (0.100g, 0.661mmol) in toluene (5mL) was added 3-(4-methoxybenzoyl) propionic acid (0.153g, 0.735mmol). Reaction time: 23h. The compound was



purified by flash chromatography (EtOAc/*n*-hexane 1:2) to give the title compound as an yellow oil (0.171g, 79.8%); $\alpha_D^{25} = +1.6^\circ$ (0.005, CH₂Cl₂); ¹H-NMR (300 MHz, CDCl₃) δ 7.45 – 7.38 (m, 2H, Ar*H*), 7.29 – 7.14 (m, 4H, Ar*H*), 7.12 – 7.06 (m, 2H, Ar*H*), 6.98 – 6.90 (m, 2H, Ar*H*), 4.41 (dq, *J* = 9.3, 7.0 Hz, 1H, *H*-3), 4.15 – 4.07 (m, 1H, *H*-2), 3.85 (s, 3H, OCH₃), 3.57 (dd, *J* = 8.8, 7.0 Hz, 1H, *H*-2), 2.96 (dd, *J* = 13.7, 6.2 Hz, 1H, ArCH₂), 2.91 – 2.73 (m, 1H), 2.61 – 2.41 (m, 2H), 2.34 – 2.13 (m, 2H); ¹³C NMR (100 MHz, CDCl₃) δ 179.99 (C=O), 159.67 (ArC), 137.45 (ArC), 134.72 (ArC), 129.04 (ArC), 128.61 (ArC), 126.70 (ArC), 126.52 (ArC), 114.07 (ArC), 102.32 (C-7*a*), 72.34 (C-2), 56.56 (C-3), 55.46 (OCH₃), 40.06 (ArCH₂), 35.31, 32.70; Anal. Calcd. (C₂₀H₂₁NO₃•0.15H₂O): C, 73.66%; H, 6.60%; N, 4.30%. Found C, 73.32%; H, 6.63%; N, 4.32%.

(3*R*,7*aR*)-3-benzyl-7*a*-(4-methoxyphenyl)tetrahydropyrrolo[2,1-*b*]oxazol-5(6*H*)-one (2*f*):

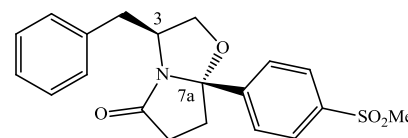
Following the general procedure, to a solution of (*R*)-phenylalaninol (0.102g, 0.675mmol) in toluene (5mL) was added 3-(4-methoxybenzoyl) propionic acid (0.153g, 0.735mmol). Reaction time: 22h. The compound was



purified by flash chromatography (EtOAc/*n*-hexane 1:2) to give the title compound as a yellow oil (0.160g, 73.4%); $\alpha_D^{25} = -2.4^\circ$ (0.005, CH₂Cl₂); ¹H-NMR spectra was found to be identical to the one obtained for compound **1f**; Anal. Calcd. (C₂₀H₂₁NO₃): C, 74.28%; H, 6.55%; N, 4.33%. Found C, 73.97%; H, 6.57%; N, 4.33%.

(3*S*,7*aS*)-3-benzyl-7*a*-(4-(methylsulfonyl)phenyl)tetrahydropyrrolo[2,1-*b*]oxazol-5(6*H*)-one (1*g*):

Following the general procedure, to a solution of (*S*)-phenylalaninol (0.100g, 0.661mmol) in toluene (5mL) was added 3-(4-methylsulfonylbenzoyl) propionic acid (0.186g, 0.727mmol). Reaction time: 22h. The compound was

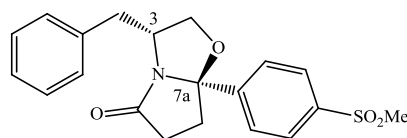


purified by flash chromatography (EtOAc/*n*-hexane 3:1) and recrystallized from AcOEt/*n*-hexane to give the title compound as a white crystalline solid (0.216g, 88.0%); $\alpha_D^{25} = +10.5^\circ$

(0.010 CH₂Cl₂); mp: 150-153 °C; ¹H-NMR (300 MHz, CDCl₃) δ 8.04 – 7.95 (m, 2H, ArH), 7.75 – 7.67 (m, 2H, ArH), 7.29 – 7.15 (m, 3H, ArH), 7.11 – 7.02 (m, 2H, ArH), 4.47 (dq, *J* = 9.1, 6.9 Hz, 1H, *H*-3), 4.17 (dd, *J* = 8.9, 7.3 Hz, 1H, *H*-2), 3.55 (dd, *J* = 8.9, 7.0 Hz, 1H, *H*-2), 3.11 (s, 3H, SO₂CH₃), 2.89 (dd, *J* = 13.7, 6.3 Hz, 1H, ArCH₂), 2.80 (ddd, *J* = 14.9, 9.1, 6.1 Hz, 1H), 2.66 – 2.46 (m, 2H), 2.30 (dt, *J* = 14.6, 7.2 Hz, 1H), 2.26 – 2.11 (m, 1H); ¹³C-NMR (100 MHz, MeOD) δ 182.22 (C=O), 150.16 (ArC), 142.11 (ArC), 138.49 (ArC), 130.08 (ArC), 129.53 (ArC), 129.06 (ArC), 127.69 (ArC), 127.47 (ArC), 103.23 (*C*-7a), 73.45 (*C*-2), 58.22 (*C*-2), 44.29 (SO₂CH₃), 40.56 (ArCH₂), 36.00, 33.21.; Anal. Calcd. (C₂₀H₂₁NO₄S•0.05H₂O): C, 64.51%; H, 5.72%; N, 3.76%. Found C, 64.24%; H, 5.62%; N, 3.89%.

(3*R*,7*aR*)-3-benzyl-7a-(4-(methylsulfonyl)phenyl)tetrahydropyrrolo[2,1-*b*]oxazol-5(6*H*)-one (2*g*):

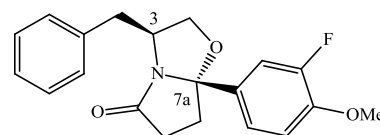
Following the general procedure, to a solution of (*R*)-phenylalaninol (0.101g, 0.665mmol) in toluene (5mL) was added 3-(4-methylsulfonylbenzoyl) propionic acid (0.188g, 0.732mmol). Reaction time: 24h. The compound



was purified by flash chromatography (EtOAc/*n*-hexane 2:1) and recrystallized from AcOEt/*n*-hexane to give white crystalline solid (0.171g, 69.0%); $\alpha_D^{25} = -13.6^\circ$ (0.010 CH₂Cl₂); mp: 160-161 °C; ¹H-NMR spectra was found to be identical to the one obtained for compound **1g**. Anal. Calcd. (C₂₀H₂₁NO₄S): C, 64.67%; H, 5.70%; N, 3.77%. Found C, 65.01%; H, 5.81%; N, 3.80%.

(3*S*,7*aS*)-3-benzyl-7a-(3-fluoro-4-methoxyphenyl)tetrahydropyrrolo[2,1-*b*]oxazol-5(6*H*)-one (1*h*):

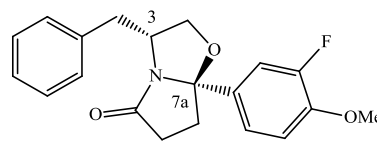
Following the general procedure, to a solution of (*S*)-phenylalaninol (0.100g, 0.661mmol) in toluene (5mL) was added 3-(3-fluoro-4-methoxybenzoyl) propionic acid (0.165g, 0.727mmol). Reaction time: 20h. The compound was



purified by flash chromatography (EtOAc/*n*-hexane 1:2) to give the title compound as a yellow oil (0.198g, 87.6%); $\alpha_D^{25} = +5.1^\circ$ (0.013, CH₂Cl₂); ¹H-NMR (300 MHz, CDCl₃) δ 7.29 – 7.17 (m, 5H, ArH), 7.13 – 7.06 (m, 2H, ArH), 7.03 – 6.94 (m, 1H, ArH), 4.41 (dq, *J* = 9.3, 7.1 Hz, 1H, *H*-3), 4.18 – 4.07 (m, 1H, *H*-2), 3.93 (s, 3H, OCH₃), 3.57 (dd, *J* = 8.8, 7.0 Hz, 1H, *H*-2), 2.95 (dd, *J* = 13.7, 6.2 Hz, 1H, ArCH₂), 2.89 – 2.71 (m, 1H), 2.64 – 2.40 (m, 2H), 2.33 (dd, *J* = 13.7, 9.4 Hz, 1H, ArCH₂), 2.27 – 2.12 (m, 1H); ¹³C-NMR (100 MHz, MeOD) δ 182.24 (C=O), 155.27 (ArC), 149.16 (ArC), 149.02 (ArC), 138.70 (ArC), 136.86 (ArC), 136.79 (ArC), 130.02 (ArC), 129.51 (ArC), 127.62 (ArC), 122.32 (ArC), 122.27 (ArC), 114.65 (ArC), 114.21 (ArC), 113.95 (ArC), 103.18 (*C*-7a), 73.36 (*C*-2), 58.05 (OCH₃), 56.75 (*C*-3), 40.76 (ArCH₂), 36.05, 33.22; Anal. Calcd. (C₂₀H₂₀FNO₃•0.1CH₂Cl₂): C, 69.00%; H, 5.83%; N, 4.00%. Found C, 69.04%; H, 5.77%; N, 4.21%.

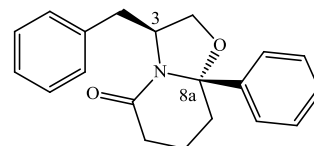
(3*R*,7*aR*)-3-benzyl-7*a*-(3-fluoro-4-methoxyphenyl)tetrahydropyrrolo[2,1-*b*]oxazol-5(6*H*)-

one (2*h*): Following the general procedure, to a solution of (*R*)- phenylalaninol (0.100g, 0.661mmol) in toluene (5mL) was added 3-(3-fluoro-4-methoxybenzoyl) propionic acid (0.165g, 0.727mmol). Reaction time: 24h. The compound was



purified by flash chromatography (EtOAc/*n*-hexane 2:3) to give the title compound as a yellow oil (0.184g, 81.5%); $\alpha_D^{25} = -4.2^\circ$ (0.013, CH₂Cl₂); ¹H-NMR spectra was found to be identical to the one obtained for compound **1h**. Anal. Calcd. (C₂₀H₂₀FNO₃): C, 70.37%; H, 5.91%; N, 4.10%. Found C, 70.14%; H, 6.44%; N, 4.22%.

(3*S*,8*aS*)-3-benzyl-8*a*-phenylhexahydro-5*H*-oxazolo[3,2-*a*]pyridin-5-one (1*i*): Following the general procedure, to a solution of (*S*)- phenylalaninol (0.100g,

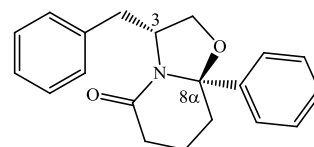


0.661mmol) in toluene (5mL) was added 4-benzoylbutyric acid (0.140g, 0.728mmol). Reaction time: 23h. The compound was purified by flash chromatography (EtOAc/*n*-hexane 1:2) and

recrystallized from AcOEt/*n*-hexane to give white crystalline solid (0.176g, 86.6%); $\alpha_D^{25} = -5.2^\circ$ (0.012 CH₂Cl₂); mp: 137-140 °C; ¹H-NMR (300 MHz, CDCl₃) δ 7.32 – 7.17 (m, 5H, *ArH*), 7.10 – 6.95 (m, 3H, *ArH*), 6.93 – 6.86 (m, 2H, *ArH*), 4.40 – 4.23 (m, 1H, *H*-3), 3.73 (dd, *J* = 9.0, 7.7 Hz, 1H, *H*-2), 3.41 (dd, *J* = 12.9, 3.6 Hz, 1H, *H*-2), 3.14 (t, *J* = 8.9 Hz, 1H), 2.47 (dd, *J* = 18.6, 6.9 Hz, 1H, *ArCH*₂), 2.26 (ddd, *J* = 18.6, 11.1, 7.7 Hz, 1H), 2.10 – 1.95 (m, 2H), 1.81 – 1.64 (m, 1H), 1.64 – 1.49 (m, 2H), 1.47 – 1.23 (m, 1H); ¹³C-NMR (100 MHz, CDCl₃) δ 170.19 (C=O), 141.77 (*ArC*), 137.86 (*ArC*), 128.97 (*ArC*), 128.63 (*ArC*), 128.43 (*ArC*), 126.74 (*ArC*), 126.64 (*ArC*), 96.47 (*C*-8*a*), 68.63 (*C*-2), 57.60 (*C*-3), 39.20 (*ArCH*₂), 36.49 (*CH*₂), 31.06 (*CH*₂), 15.91 (*CH*₂); Anal. Calcd. (C₂₀H₂₁NO₂•0.05H₂O): C, 77.91%; H, 6.91%; N, 4.54%. Found C, 77.81%; H, 6.97%; N, 4.53%.

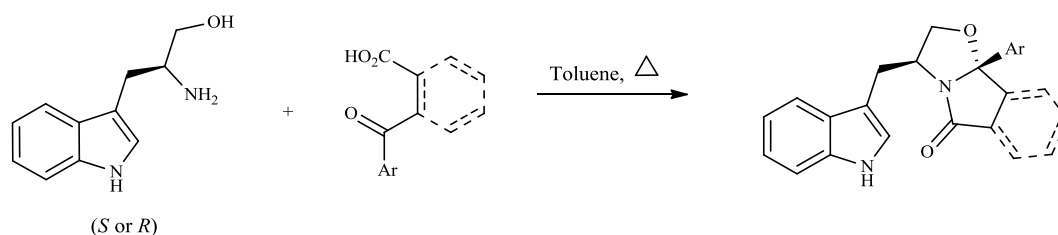
(3*R*,8*aR*)-3-benzyl-8*a*-phenyltetrahydro-2*H*-oxazolo[3,2-*a*]pyridin-5(3*H*)-one (2*i*):

Following the general procedure, to a solution of (*R*)- phenylalaninol (0.100g, 0.661mmol) in toluene (5mL) was added 4-benzoylbutyric acid (0.140g, 0.728mmol). Reaction time: 23h. The compound was purified by flash chromatography (EtOAc/*n*-



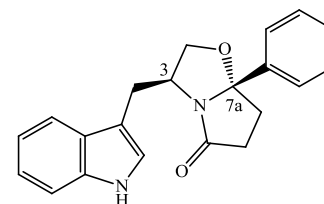
hexane 2:3) and recrystallized from AcOEt/*n*-hexane to give white crystalline solid (0.138g, 67.6%); $\alpha_D^{25} = +7.1^\circ$ (0.012, CH₂Cl₂); mp: 142-144 °C; ¹H-NMR spectra was found to be identical to the one obtained for compound **1i**. Anal. Calcd. (C₂₀H₂₁NO₂): C, 78.15%; H, 6.89%; N, 4.56%. Found C, 78.53%; H, 6.90 %; N, 4.66%.

IV.2.2 – (S) and (R)-tryptophan-derived bicyclic lactams



(3S,7aS)-3-((1H-indol-3-yl)methyl)-7a-phenyltetrahydropyrrolo[2,1-b]oxazol-5(6H)-one

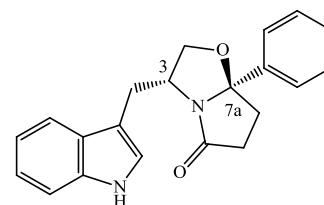
(3a): Following the general procedure, to a solution of (S)-tryptophan (0.101g, 0.529mmol) in toluene (5mL) was added 3-benzoyl propionic acid (0.104g, 0.582mmol). Reaction time: 24h. The compound was purified by flash chromatography (EtOAc/*n*-hexane 1:1) and recrystallized from AcOEt/*n*-hexane to give pale



pink crystalline solid (0.127g, 71.8%); $\alpha_D^{25} = +40.4$ °C (c=0.002, MeOH); mp: 153-156 °C; $^1\text{H-NMR}$ (300 MHz, CDCl_3) δ 7.99 (s, 1H, NH), 7.50 (d, $J = 6.0$ Hz, 2H, ArH), 7.46 – 7.29 (m, 5H, ArH), 7.17 (t, $J = 7.5$ Hz, 1H, ArH), 7.10-7.05 (m, 2H, ArH), 4.62 – 4.52 (m, 1H, H-3), 4.16 (t, $J = 8.1$ Hz, 1H, H-2), 3.63 – 3.58 (m, 1H, H-2), 3.07 (dd, $J = 14.3, 6.2$ Hz, 1H, indole-CH₂), 2.96 – 2.75 (m, 1H, H-6), 2.68 – 2.35 (m, 3H, H-7 H-6 indole-CH₂), 2.34 – 2.14 (m, 1H, H-7) ppm. $^{13}\text{C-RMN}$ (100 MHz, CDCl_3) δ 180.15 (C=O), 142.67 (ArC), 136.07 (ArC), 128.69 (ArC), 128.27 (ArC), 127.35 (ArC), 125.07 (ArC), 122.08 (ArC), 122.03 (ArC), 119.39 (ArC), 118.75 (ArC), 111.62 (ArC), 111.06 (ArC), 102.35 (C-7a), 72.69 (C-2), 55.53 (C-3), 35.01 (C-7), 32.62 (C-6), 29.62 (indole-CH₂) ppm; Anal. Calcd. ($\text{C}_{21}\text{H}_{20}\text{N}_2\text{O}_2$): C, 75.88%; H, 6.06%; N, 8.43%. Found C, 75.95%; H, 5.76%; N, 8.36%.

(3R,7aR)-3-((1H-indol-3-yl)methyl)-7a-phenyltetrahydropyrrolo[2,1-b]oxazol-5(6H)-one

(4a): Following the general procedure, to a solution of (R)-tryptophan (0.102g, 0.536mmol) in toluene (5mL) was added 3-benzoyl propionic acid (0.105g, 0.590mmol). Reaction time: 19h.

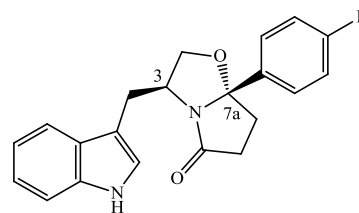


The compound was purified by flash chromatography (EtOAc/*n*-hexane 1:1) and recrystallized from AcOEt/*n*-hexane to give pale pink crystalline solid (0.166g, 95.1%); $\alpha_D^{25} = -54.7$ °C (c=0.002,

MeOH); mp: 155-157 °C, $^1\text{H-NMR}$ spectra was found to be identical to the one obtained for compound **3a**. Anal. Calcd. ($\text{C}_{21}\text{H}_{20}\text{N}_2\text{O}_2$): C, 75.88%; H, 6.06%; N, 8.43%. Found C, 75.22%; H, 5.87%; N, 8.23%.

(3*S*,7*aS*)-3-((1*H*-indol-3-yl)methyl)-7*a*-(4-fluorophenyl)tetrahydropyrrolo[2,1-*b*]oxazol-

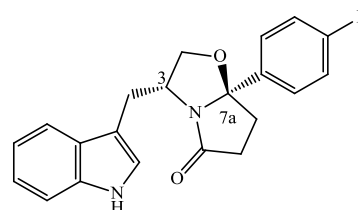
5(6*H*)-one (3*b*): Following the general procedure, to a solution of (*S*)-tryptophanol (0.102g, 0.535mmol) in toluene (5mL) was added 3-(4-fluorobenzoyl) propionic acid (0.115g, 0.588mmol). Reaction time: 21h. The compound was purified by flash chromatography (EtOAc/*n*-hexane 1:1) and recrystallized from AcOEt/*n*-hexane to give orange crystalline solid (0.156g, 83.3%);



$\alpha_D^{25} = +39.5$ °C ($c=0.002$, MeOH); mp: 197-198 °C; $^1\text{H-NMR}$ (300 MHz, CDCl_3) δ 8.00 (s, 1H, NH), 7.51-7.41 (m, 3H, ArH), 7.33 (d, $J= 8.1$ Hz, 1H, ArH), 7.21-7.15 (m, 1H, ArH), 7.11–7.03 (m, 4H, ArH), 4.62–4.53 (m, 1H, H-3), 4.17 (dd, $J= 8.8\text{Hz}, 7.4\text{Hz}$, 1H, H-2), 3.59 (dd, $J= 8.8$ Hz, 6.9Hz, 1H, H-2), 3.05 (dd, $J= 14.7\text{Hz}, 6.2\text{Hz}$, 1H, indole- CH_2), 2.90–2.78 (m, 1H, H-6), 2.65-2.43 (m, 3H, H-7 H-6 indole- CH_2), 2.24-2.15 (m, 1H, H-7) ppm. $^{13}\text{C-RMN}$ (100 MHz, CDCl_3) δ 180.32 (C=O), 164.43/161.16 (ArC-F), 138.78 (ArC), 136.27 (ArC), 127.51 (ArC), 127.17 (ArC), 127.06 (ArC), 122.31 (ArC), 122.24 (ArC), 119.63 (ArC), 118.85 (ArC), 115.87 (ArC), 115.58 (ArC), 111.62 (ArC), 111.28 (ArC), 102.19 (C-7*a*), 72.84 (C-2), 55.78 (C-3), 35.21 (C-7), 32.69 (C-6), 29.79 (indole- CH_2). Anal. Calcd. ($\text{C}_{21}\text{H}_{19}\text{FN}_2\text{O}_2$): C, 71.98%; H, 5.47%; N, 8.00%. Found C, 72.48%; H, 5.37%; N, 8.03%.

(3*R*,7*aR*)-3-((1*H*-indol-3-yl)methyl)-7*a*-(4-fluorophenyl)tetrahydropyrrolo[2,1-*b*]oxazol-

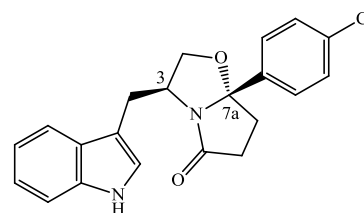
5(6*H*)-one (4*b*): Following the general procedure, to a solution of (*R*)-tryptophanol (0.100g, 0.526mmol) in toluene (5mL) was added 3-(4-fluorobenzoyl) propionic acid (0.114g, 0.581mmol). Reaction time: 19h. The compound was purified by flash chromatography (EtOAc/*n*-hexane 1:1) and recrystallized from AcOEt/*n*-hexane to give pale yellow



crystalline solid (0.1129g, 69.7%); $\alpha_D^{25} = -48.8$ °C ($c=0.002$, MeOH); mp: 194-196 °C; $^1\text{H-NMR}$ spectra was found to be identical to the one obtained for compound **3b**. Anal. Calcd. ($\text{C}_{21}\text{H}_{19}\text{FN}_2\text{O}_2$): C, 71.98%; H, 5.47%; N, 8.00%. Found C, 72.09%; H, 5.49%; N, 7.94%.

(3*S*,7*aS*)-3-((1*H*-indol-3-yl)methyl)-7*a*-(4-chlorophenyl)tetrahydropyrrolo[2,1-*b*]oxazol-

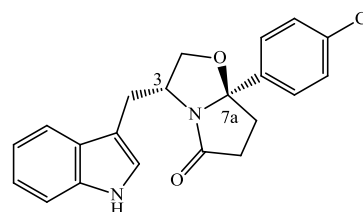
5(6*H*)-one (3*c*): Following the general procedure, to a solution of (*S*)-tryptophanol (0.104g, 0.545mmol) in toluene (5mL) was added 3-(4-chlorobenzoyl) propionic acid (0.128g, 0.600mmol). Reaction time: 23h. The compound was purified by flash chromatography (EtOAc/*n*-hexane 1/1) and recrystallized from AcOEt/*n*-hexane to give pale pink crystalline solid (0.164g,



81.9%); $\alpha_D^{25} = +54.5$ °C (c=0.002, MeOH); mp: 206-208 °C; $^1\text{H-NMR}$ (300 MHz, CDCl_3) δ 7.98 (s, 1H, NH), 7.47-7.32 (m, 6H, ArH), 7.21-7.16 (m, 1H, ArH), 7.12-7.06 (m, 2H, ArH), 4.62-4.52 (m, 1H, H-3), 4.17 (dd, J= 8.8Hz, 7.5Hz, 1H, H-2), 3.59 (dd, J= 8.8Hz, 6.9Hz, 1H, H-2), 3.05 (dd, J= 15.1Hz, 7.5Hz, 1H, indole-CH₂), 2.89-2.78 (m, 1H, H-6), 2.65-2.44 (m, 3H, m, 3H, H-7 H-6 indole-CH₂), 2.22-2.14 (m, 1H, H-7) ppm. $^{13}\text{C-RMN}$ (100 MHz, CDCl_3) δ 180.26 (C=O), 141.45 (ArC), 136.25 (ArC), 134.27 (ArC), 129.00 (ArC), 127.43 (ArC), 126.70 (ArC), 122.29 (ArC), 122.21 (ArC), 119.54 (ArC), 118.80 (ArC), 111.37 (ArC), 111.29 (ArC), 102.05 (C-7a), 72.85 (C-2), 55.78 (C-3), 35.07 (C-7), 32.64 (C-6), 29.77 (indole-CH₂). Anal. Calcd. ($\text{C}_{21}\text{H}_{19}\text{ClN}_2\text{O}_2$): C, 68.76%; H, 5.22%; N, 7.62%. Found C, 68.94%; H, 5.06%; N, 7.60%.

(3R,7aR)-3-((1H-indol-3-yl)methyl)-7a-(4-chlorophenyl)tetrahydropyrrolo[2,1-b]oxazol-5(6H)-one (4c):

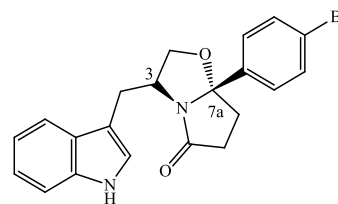
Following the general procedure, to a solution of (*R*)-tryptophan (0.103g, 0.541mmol) in toluene (5mL) was added 3-(4-chlorobenzoyl) propionic acid (0.127g, 0.596mmol). Reaction time: 18h. The compound was purified by flash chromatography (EtOAc/*n*-hexane 1:1) and recrystallized from AcOEt/*n*-hexane to give pale yellow



crystalline solid (0.133g, 66.7%); $\alpha_D^{25} = -63.1$ °C (c=0.002, MeOH); mp: 204-206 °C; $^1\text{H-NMR}$ spectra was found to be identical to the one obtained for compound **3c**. Anal. Calcd. ($\text{C}_{21}\text{H}_{19}\text{ClN}_2\text{O}_2$): C, 68.76%; H, 5.18%; N, 7.62%. Found C, 68.76%; H, 5.22%; N, 7.64%.

(3S,7aS)-3-((1H-indol-3-yl)methyl)-7a-(4-bromophenyl)tetrahydropyrrolo[2,1-b]oxazol-5(6H)-one (3d):

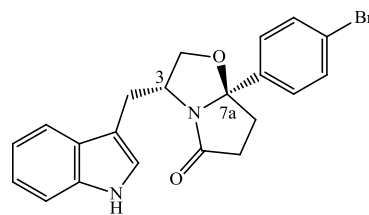
Following the general procedure, to a solution of (*S*)-tryptophan (0.102g, 0.536mmol) in toluene (5mL) was added 3-(4-bromobenzoyl) propionic acid (0.151g, 0.589mmol). Reaction time: 18h. The compound was purified by flash chromatography (EtOAc/*n*-hexane 1:1) and recrystallized from



AcOEt/*n*-hexane to give pale yellow crystalline solid (0.159g, 72.3%); $\alpha_D^{25} = +52.3$ °C (c=0.002, MeOH); mp: 207-210 °C. $^1\text{H NMR}$ (300 MHz, CDCl_3) δ 7.97 (s, 1H, NH), 7.52-7.45 (m, 3H, ArH), 7.37-7.32 (m, 3H, ArH), 7.21-7.05 (m, 3H, ArH), 4.62-4.52 (m, 1H, H-3), 4.17 (dd, J= 8.8Hz, 7.4Hz, 1H, H-2), 3.59 (dd, J= 8.8Hz, 6.9Hz, 1H, H-2), 3.05 (dd, J= 14.7Hz, 6.1Hz, 1H, indole-CH₂), 2.89-2.78 (m, 1H, H-6), 2.65-2.44 (m, 3H, H-7 H-6 indole-CH₂), 2.22-2.14 (m, 1H, H-7) ppm. $^{13}\text{C-RMN}$ (100 MHz, CDCl_3) δ 180.26 (C=O), 142.07 (ArC), 136.27 (ArC), 132.01 (ArC), 127.49 (ArC), 127.07 (ArC), 122.51 (ArC), 122.34 (ArC), 122.25 (ArC), 119.67 (ArC), 118.92 (ArC), 111.57 (ArC), 111.28 (ArC), 102.12 (C-7a), 72.91 (C-2), 55.79 (C-3), 35.09 (C-7), 32.68 (C-6), 29.81 (indole-CH₂). Anal. Calcd. ($\text{C}_{21}\text{H}_{19}\text{BrN}_2\text{O}_2$): C, 61.33%; H, 4.66%; N, 6.81%. Found C, 61.26%; H, 4.48%; N, 6.76%.

(3*R*,7*aR*)-3-((1*H*-indol-3-yl)methyl)-7*a*-(4-bromophenyl)tetrahydropyrrolo[2,1-*b*]oxazol-5(6*H*)-one (4*d*):

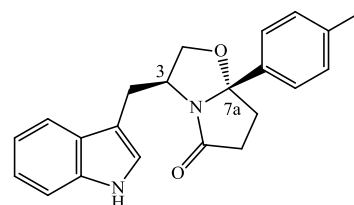
Following the general procedure, to a solution of (*R*)-tryptophan (0.102g, 0.536mmol) in toluene (5mL) was added 3-(4-bromobenzoyl) propionic acid (0.153g, 0.590mmol). Reaction time: 18h. The compound was purified by flash chromatography (EtOAc/*n*-hexane 1:1) and recrystallized from AcOEt/*n*-hexane to give pale pink



crystalline solid (0.182g, 82.5%); $\alpha_D^{25} = -53.6$ °C ($c=0.002$, MeOH); mp: 204-206 °C; $^1\text{H-NMR}$ spectra was found to be identical to the one obtained for compound **3d**. Anal. Calcd. ($\text{C}_{21}\text{H}_{19}\text{BrN}_2\text{O}_2$): C, 61.33%; H, 4.66%; N, 6.81%. Found C, 60.47%; H, 4.55%; N, 6.55%.

(3*S*,7*aS*)-3-((1*H*-indol-3-yl)methyl)-7*a*-(*p*-tolyl)tetrahydropyrrolo[2,1-*b*]oxazol-5(6*H*)-one (3*e*):

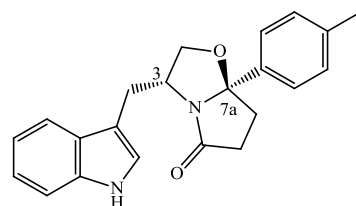
Following the general procedure, to a solution of (*S*)-tryptophan (0.100g, 0.526mmol) in toluene (5mL) was added 3-(4-methylbenzoyl) propionic acid (0.112g, 0.583mmol). Reaction time: 18h. The compound was purified by flash chromatography (EtOAc/*n*-hexane 1:1) and recrystallized from AcOEt/*n*-hexane to give pale pink crystalline solid (0.097g, 53%); $\alpha_D^{25} = +45.1$ °C



($c=0.002$, MeOH); mp: 210-213 °C. $^1\text{H-NMR}$ (300 MHz, (CDCl_3)) δ 8.00 (s, 1H, *NH*), 7.47-7.32 (m, 4H, *ArH*), 7.21-7.06 (m, 5H, *ArH*), 4.60-4.50 (m, 1H, *H*-3), 4.15 (dd, $J=8.7\text{Hz}$, 7.4Hz, 1H, *H*-2), 3.61 (dd, $J=8.8\text{Hz}$, 6.9Hz, 1H, *H*-2), 3.09 (dd, $J=14.7\text{Hz}$, 6.1Hz, 1H, indole- CH_2), 2.90-2.79 (m, 1H, *H*-6), 2.64-2.43 (m, 3H, *H*-7 *H*-6 indole- CH_2), 2.39 (s, 3H, CH_3), 2.26-2.17 (m, 1H, *H*-7) ppm. $^{13}\text{C-RMN}$ (100 MHz, CDCl_3) δ 180.30 (C=O), 139.88 (ArC), 138.21 (ArC), 136.28 (ArC), 129.53 (ArC), 127.54 (ArC), 125.21 (ArC), 122.26 (ArC), 122.21 (ArC), 119.55 (ArC), 118.98 (ArC), 111.91 (ArC), 111.24 (ArC), 102.56 (*C*-7*a*), 72.89 (*C*-2), 55.68 (*C*-3), 35.35 (*C*-7), 32.85 (*C*-6), 29.86 (indole- CH_2), 21.36 (CH_3). Anal. Calcd. ($\text{C}_{22}\text{H}_{22}\text{N}_2\text{O}_2$): C, 76.28%; H, 6.40%; N, 8.09%. Found C, 76.49%; H, 6.27%; N, 8.16%.

(3*R*,7*aR*)-3-((1*H*-indol-3-yl)methyl)-7*a*-(*p*-tolyl)tetrahydropyrrolo[2,1-*b*]oxazol-5(6*H*)-one (4*e*):

Following the general procedure, to a solution of (*R*)-tryptophan (0.103g, 0.541mmol) in toluene (5mL) was added 3-(4-methylbenzoyl) propionic acid (0.114g, 0.596mmol). Reaction time: 19h. The compound was purified by flash chromatography (EtOAc/*n*-hexane 1:1) and recrystallized from

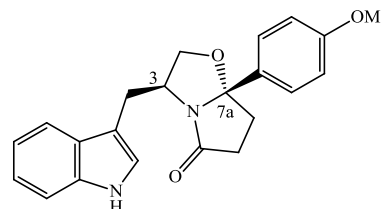


AcOEt/*n*-hexane to give pale pink crystalline solid (0.160g, 85.5%); $\alpha_D^{25} = -58.7$ °C ($c=0.002$, MeOH); mp: 211-212 °C; $^1\text{H-NMR}$ spectra was found to be identical to the one obtained for

compound **3e**. Anal. Calcd. (C₂₂H₂₂N₂O₂): C, 76.28%; H, 6.40%; N, 8.09%. Found C, 75.87%; H, 6.23%; N, 8.06%.

(3*S*,7*aS*)-3-((1*H*-indol-3-yl)methyl)-7*a*-(4-methoxyphenyl)tetrahydropyrrolo[2,1-*b*]oxazol-

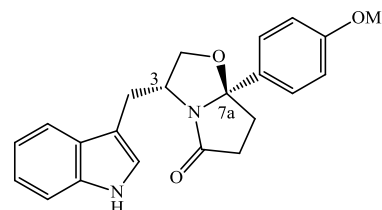
5(6*H*)-one (3*f*): Following the general procedure, to a solution of (*S*)-tryptophanol (0.101g, 0.533mmol) in toluene (5mL) was added 3-(4-methoxybenzoyl) propionic acid (0.122g, 0.586mmol). Reaction time: 25h. The compound was purified by flash chromatography (EtOAc/*n*-hexane 1:1) and recrystallized from AcOEt/*n*-hexane to give pale yellow crystalline solid



(0.134g, 69.3%); $\alpha_D^{25} = +45.6$ °C (c=0.002, MeOH); mp: 185-187 °C. ¹H-NMR (300 MHz, (CDCl₃)) δ 8.00 (s, 1H, NH), 7.47-7.32 (m, 4H, ArH), 7.20-7.05 (m, 3H, ArH), 6.92-6.89 (m, 2H, ArH), 4.61-4.50 (m, 1H, H-3), 4.15 (dd, J= 8.4Hz, 7.7Hz, 1H, H-2), 3.84 (s, 3H, O-CH₃), 3.61 (dd, J= 8.7Hz, 7.0Hz, 1H, H-2), 3.08 (dd, J= 14.7Hz, 6.2Hz, 1H, indole-CH₂), 2.90-2.79 (m, 1H, H-6), 2.64-2.44 (m, 3H, H-7 H-6 indole-CH₂), 2.25-2.17 (m, 1H, H-7) ppm. ¹³C-RMN (100 MHz, CDCl₃) δ 180.15 (C=O), 142.67 (ArC), 159.65 (ArC), 136.26 (ArC), 134.88 (ArC), 127.53 (ArC), 126.57 (ArC), 122.24 (ArC), 119.54 (ArC), 118.97 (ArC), 114.10 (ArC), 111.83 (ArC), 111.24 (ArC), 102.45 (C-7*a*), 72.84 (C-2), 55.66 (OCH₃), 55.53 (C-3), 35.33 (C-7), 32.83 (C-6), 29.83 (indole-CH₂). Anal. Calcd. (C₂₂H₂₂N₂O₃): C, 72.91%; H, 6.12%; N, 7.73%. Found C, 72.73%; H, 5.76%; N, 7.73%.

(3*R*,7*aR*)-3-((1*H*-indol-3-yl)methyl)-7*a*-(4-methoxyphenyl)tetrahydropyrrolo[2,1-*b*]oxazol-

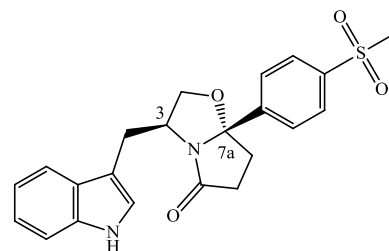
5(6*H*)-one (4*f*): Following the general procedure, to a solution of (*R*)-tryptophanol (0.100g, 0.526mmol) in toluene (5mL) was added 3-(4-methoxybenzoyl) propionic acid (0.121g, 0.581mmol). Reaction time: 24h. The compound was purified by flash chromatography (EtOAc/*n*-hexane 1/1) and recrystallized from AcOEt/*n*-hexane to give pale yellow



crystalline solid (0.106g, 55.6%); $\alpha_D^{25} = -55.8$ °C (c=0.002, MeOH); mp: 181-184 °C. ¹H-NMR spectra was found to be identical to the one obtained for compound **3f**. Anal. Calcd. (C₂₂H₂₂N₂O₃•0.1AcOEt): C, 72.47%; H, 6.20%; N, 7.55%. Found C, 72.22%; H, 6.21%; N, 7.53%.

(3*S*,7*aS*)-3-((1*H*-indol-3-yl)methyl)-7*a*-(4-(methylsulfonyl)phenyl)tetrahydropyrrolo[2,1-*b*]oxazol-5(6*H*)-one (3*g*):

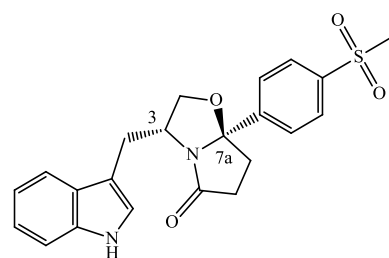
Following the general procedure, to a solution of (*S*)-tryptophanol (0.100g, 0.526mmol) in toluene (5mL) was added 3-(4-methylsulfonylbenzoyl) propionic acid (0.148g, 0.578mmol). Reaction time: 23h. The compound was purified by flash chromatography (EtOAc/*n*-hexane 7:3) and recrystallized from AcOEt/*n*-hexane to give yellow crystalline solid (0.131g, 60.5%); α_D^{25}



= +66.9 °C (c=0.002, MeOH); mp: 205-207 °C. ¹H-NMR (300 MHz, (CDCl₃)) δ 8.01 (s, 1H, *NH*), 7.90-7.88 (m, 2H, *ArH*), 7.62-7.59 (m, 2H, *ArH*), 7.43 (d, *J*= 7.9Hz, 1H, *ArH*), 7.33 (d, *J*= 8.1Hz, 1H, *ArH*), 7.21-7.16 (m, 1H, *ArH*), 7.11-7.06 (m, 1H, *ArH*), 7.00 (d, *J*= 2.3Hz, 1H, *ArH*), 4.66-4.56 (m, 1H, *H*-3), 4.22 (dd, *J* = 8.9, 7.4 Hz, 1H, *H*-2), 3.61 (dd, *J* = 8.9, 7.0 Hz, 1H, *H*-2), 3.10 (s, 1H, SO₂-CH₃), 3.00 (dd, *J* = 15.5, 5.9 Hz, 1H, indole-CH₂), 2.92–2.75 (m, 1H, *H*-6), 2.70–2.45 (m, 3H, *H*-7 *H*-6 indole-CH₂), 2.21–2.13 (m, 1H, *H*-7) ppm. ¹³C-RMN (100 MHz, CDCl₃) δ 180.09 (C=O), 149.23 (*ArC*), 140.51 (*ArC*), 136.25 (*ArC*), 128.00 (*ArC*), 127.49 (*ArC*), 126.23 (*ArC*), 122.35 (*ArC*), 119.66 (*ArC*), 118.73 (*ArC*), 111.40 (*ArC*), 111.10 (*ArC*), 101.83 (*C*-7*a*), 72.94 (*C*-2), 55.95 (*C*-3), 44.57 (SO₂CH₃), 35.08 (*C*-7), 32.64 (*C*-6), 29.48 (indole-CH₂). Anal. Calcd. (C₂₂H₂₂N₂O₄S): C, 64.37%; H, 5.40%; N, 6.82%. Found C, 64.59%; H, 5.51%; N, 6.69%.

(3*R*,7*aR*)-3-((1*H*-indol-3-yl)methyl)-7*a*-(4-(methylsulfonyl)phenyl)tetrahydropyrrolo[2,1-*b*]oxazol-5(6*H*)-one (4*g*):

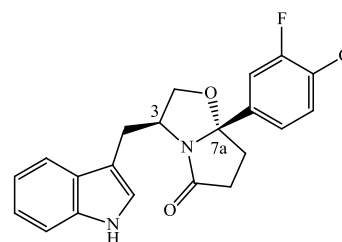
Following the general procedure, to a solution of (*R*)-tryptophanol (0.106g, 0.557mmol) in toluene (5mL) was added 3-(4-methylsulfonylbenzoyl) propionic acid (0.157g, 0.613mmol). Reaction time: 22h. The compound was purified by flash chromatography (EtOAc/*n*-hexane 7:3) and recrystallized from AcOEt/*n*-



hexane to give a pale yellow crystalline solid (0.171g, 74.9%); α_D^{25} = -57.2 °C (c=0.002, MeOH); mp: 205-207 °C. ¹H-NMR spectra was found to be identical to the one obtained for compound **3g**. Anal. Calcd. (C₂₂H₂₂N₂O₄S): C, 64.37%; H, 5.40%; N, 6.82%. Found C, 64.31%; H, 5.32%; N, 6.81%.

(3*S*,7*aS*)-3-((1*H*-indol-3-yl)methyl)-7*a*-(3-fluoro-4-methoxyphenyl)tetrahydropyrrolo[2,1-*b*]oxazol-5(6*H*)-one (3*h*):

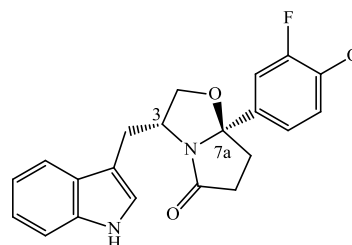
Following the general procedure, to a solution of (*S*)-tryptophanol (0.101g, 0.530mmol) in toluene (5mL) was added 3-(3-fluoro-4-methoxybenzoyl) propionic acid (0.120g, 0.530mmol). Reaction time: 23h. The compound was purified by flash chromatography (EtOAc/*n*-hexane 1:1) and



recrystallized from AcOEt/*n*-hexane to give yellow crystalline solid (0.136g, 67.4%); $\alpha_D^{25} = +43.9$ °C (*c*=0.002, MeOH); mp: 134-136 °C. ¹H-NMR (300 MHz, (CDCl₃) δ 8.01 (s, 1H, NH), 7.47 (d, *J* = 7.9 Hz, 1H, ArH), 7.33 (d, *J* = 8.0 Hz, 1H, ArH), 7.23 – 7.04 (m, 4H, ArH), 6.93 (t, *J* = 8.4 Hz, 1H, ArH), 4.61 – 4.41 (m, 1H, H-3), 4.16 (dd, *J* = 8.7, 7.4 Hz, 1H, H-2), 3.92 (s, 3H, O-CH₃), 3.61 (dd, *J* = 8.8, 6.9 Hz, 1H, H-2), 3.08 (dd, *J* = 13.9, 6.0 Hz, 1H, indole-CH₂), 2.90-2.83 (m, 1H, H-6), 2.64 – 2.43 (m, 3H, H-7 H-6 indole-CH₂), 2.24-2.15 (m, 1H, H-7) ppm. ¹³C-RMN (100 MHz, CDCl₃) δ 180.22 (C=O), 154.09 (ArC), 150.82 (ArC), 147.70 (ArC), 136.28 (ArC), 135.97/135.90 (ArC-F), 127.44 (ArC), 122.30 (ArC), 122.21 (ArC), 119.52 (ArC), 118.82 (ArC), 113.44 (ArC), 113.18 (ArC), 111.49 (ArC), 111.29 (ArC), 101.86 (C-7*a*), 72.93 (C-2), 56.45 (C-3), 55.79 (OCH₃), 35.17 (C-7), 32.89 (C-6), 29.82 (indole-CH₂). Anal. Calcd. (C₂₂H₂₁FN₂O₃): C, 69.46%; H, 5.56%; N, 7.36%. Found C, 69.13%; H, 5.10%; N, 7.62%.

(3*R*,7*aR*)-3-((1*H*-indol-3-yl)methyl)-7*a*-(3-fluoro-4-methoxyphenyl)tetrahydropyrrolo[2,1-*b*]oxazol-5(6*H*)-one (4*h*):

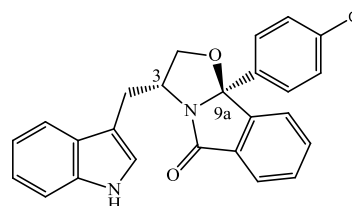
Following the general procedure, to a solution of (*R*)-tryptophanol (0.100g, 0.526mmol) in toluene (5mL) was added 3-(3-fluoro-4-methoxybenzoyl) propionic acid (0.131g, 0.578mmol). Reaction time: 22h. The compound was purified by flash chromatography (EtOAc/*n*-hexane 1:1) and recrystallized from AcOEt/*n*-hexane to give a pale yellow



crystalline solid (0.139g, 69.3%); $\alpha_D^{25} = -51.3$ °C (*c*=0.002, MeOH); mp: 131-132 °C. ¹H-NMR spectra was found to be identical to the one obtained for compound **3h**. Anal. Calcd. (C₂₂H₂₁FN₂O₃): C, 69.46%; H, 5.56%; N, 7.36%. Found C, 69.49%; H, 5.76%; N, 7.12%.

(3*R*,9*bS*)-3-((1*H*-indol-3-yl)methyl)-9*b*-(4-chlorophenyl)-2,3-dihydrooxazolo[2,3-*a*]isoindol-5(9*bH*)-one (4*i*):

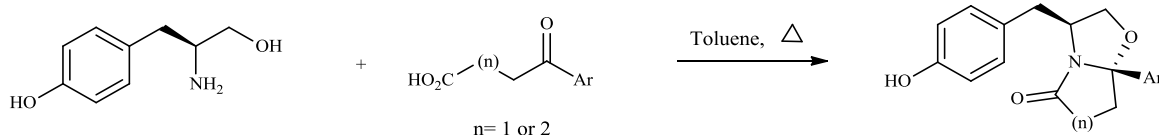
Following the general procedure, to a solution of (*R*)-tryptophanol (0.077g, 0.403mmol) in toluene (5mL) was added 2-(4-chlorobenzoyl) benzoic acid (0.126g, 0.484mmol). Reaction time: 22h. The compound was purified by flash chromatography (EtOAc/*n*-hexane 1:1) and



recrystallized from AcOEt/*n*-hexane to give a white crystalline solid (0.105g, 62.5%); ¹H-NMR

(300 MHz, CDCl₃) δ 8.08 (s, 1H, NH), 7.84 – 7.77 (m, 1H, ArH), 7.56 – 7.51 (m, 3H, ArH), 7.51 – 7.46 (m, 2H, ArH), 7.38 – 7.30 (m, 3H, ArH), 7.23 – 7.16 (m, 2H, ArH), 7.16 – 7.07 (m, 2H, ArH), 4.72 (dq, $J = 8.7, 6.6$ Hz, 1H, H-3), 4.47 (dd, $J = 8.7, 7.5$ Hz, 1H, H-2), 3.98 (dd, $J = 8.8, 6.7$ Hz, 1H, H-2), 3.22 – 3.10 (m, 1H, ArCH₂), 2.70 (dd, $J = 14.8, 8.8$ Hz, 1H, ArCH₂); ¹³C-NMR (100 MHz, CDCl₃) δ 174.70 (C=O), 146.92 (ArC), 137.67 (ArC), 136.23 (ArC), 134.71 (ArC), 133.55 (ArC), 131.01 (ArC), 130.41 (ArC), 129.08 (ArC), 127.49 (ArC), 127.35 (ArC), 124.54 (ArC), 123.46 (ArC), 122.31 (ArC), 122.21 (ArC), 119.55 (ArC), 118.79 (ArC), 111.57 (ArC), 111.27 (ArC), 100.66 (C-9b), 76.36 (C-2), 55.91 (C-3), 30.15 (ArCH₂); Anal. Calcd. (C₂₅H₁₉ClN₂O₂•0.25CH₂Cl₂): C, 69.53%; H, 4.52%; N, 6.42%. Found C, 69.18%; H, 4.63%; N, 6.21%.

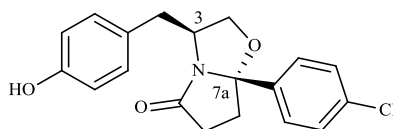
IV.2.3 – (S)-tyrosinol-derived oxazolopyrrolidone lactams



(3S,7aS)-7a-(4-chlorophenyl)-3-(4-hydroxybenzyl)tetrahydropyrrolo[2,1-b]oxazol-5(6H)-

one (5a): Following the general procedure, to a solution of

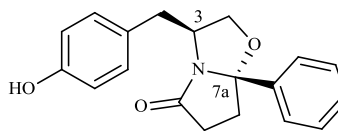
(S)-tyrosinol (0.032g, 0.156mmol) in toluene (2mL) was added TEA anhydrous (24.0 μ L, 0.172mmol). At 60°C was added 3-(4-chlorobenzoyl) propionic acid (0.040g,



0.187mmol). Reaction time: 24h. The compound was purified by flash chromatography (EtOAc/*n*-hexane 1:2) to afford the title compound as a white powder (0.016g, 29.1%); mp: 186-187 °C; ¹H-NMR (300 MHz, CDCl₃) δ 7.44 – 7.34 (m, 4H, ArH), 6.94 (d, $J = 8.4$ Hz, 2H, ArH), 6.73 (d, $J = 8.4$ Hz, 2H, ArH), 4.44 – 4.34 (m, 1H, H-3), 4.17 (dd, $J = 8.8, 7.4$ Hz, 1H, H-2), 3.56 (dd, $J = 8.8, 7.0$ Hz, 1H, H-2), 3.49 (s, 1H, OH), 2.89 – 2.69 (m, 2H, ArCH₂, CH₂), 2.62 – 2.44 (m, 2H), 2.31 – 2.14 (m, 2H); ¹³C-NMR (100 MHz, CDCl₃) δ 180.49 (C=O), 155.07 (ArC), 141.26 (ArC), 134.52 (ArC), 130.17 (ArC), 129.14 (ArC), 128.87 (ArC), 126.76 (ArC), 115.65 (ArC), 102.17 (C-7a), 72.60 (C-2), 56.97 (C-3), 39.18 (ArCH₂), 35.16, 32.71; Anal. Calcd. (C₁₉H₁₈ClNO₃): C, 66.38%; H, 5.28%; N, 4.07%. Found C, 66.19%; H, 5.22%; N, 3.94%.

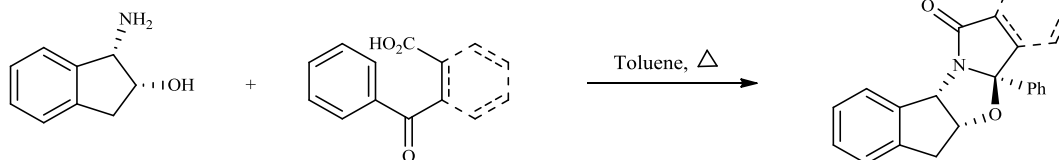
(3*S*,7*aS*)-3-(4-hydroxybenzyl)-7*a*-phenyltetrahydropyrrolo[2,1-*b*]oxazol-5(6*H*)-one (5*b*):

Following the general procedure, to a solution of (*S*)-tyrosinol (0.061g, 0.299mmol) in toluene (3mL) was added TEA anhydrous (45.9μL, 0.329mmol). At 60°C was added 3-benzoylpropionic acid (0.064g, 0.359mmol). Reaction



time: 25h. The compound was purified by flash chromatography (EtOAc/*n*-hexane 1:2) to afford the title compound as a white powder (0.018g, 19.4%); mp: 163-164 °C; ¹H-NMR (300 MHz, CDCl₃) δ 7.51 – 7.34 (m, 4H, Ar*H*), 6.95 (d, *J* = 8.5 Hz, 2H, Ar*H*), 6.73 (d, *J* = 8.5 Hz, 2H, Ar*H*), 4.45 – 4.35 (m, 1H, *H*-3), 4.18 (dd, *J* = 8.7, 7.5 Hz, 1H, *H*-2), 3.58 (dd, *J* = 8.7, 6.8 Hz, 1H, *H*-2), 2.91 – 2.80 (m, 1H, ArCH₂), 2.77 – 2.69 (m, 1H, CH₂), 2.64 – 2.45 (m, 2H), 2.35 – 2.19 (m, 2H); ¹³C-NMR (100 MHz, CDCl₃) δ 180.40 (C=O), 154.92 (ArC), 142.33 (ArC), 129.99 (ArC), 128.79 (ArC), 128.74 (ArC), 128.39 (ArC), 125.03 (ArC), 115.43 (ArC), 102.42 (C-7*a*), 72.41 (C-2), 56.71 (C-3), 38.97 (ArCH₂), 35.07, 32.67; Anal. Calcd. (C₁₉H₁₉NO₃): C, 73.77%; H, 6.19%; N, 4.53%. Found C, 73.88%; H, 6.57%; N, 4.68%.

IV.2.4 - Indanol-derived bicyclic lactams

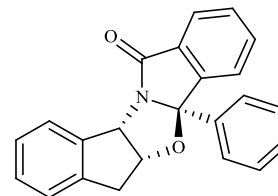


(4*bR*,5*aS*,10*bS*)-4*b*-phenyl-5*a*,10*b*-dihydro-6*H*-indeno[1',2':4,5]oxazolo[2,3-*a*]isoindol-

12(4*bH*)-one (6*a*): Following the general procedure, to a solution of

(1*S*, 2*R*)-(-)-*cis*-1-Amino-2-indanol (0.100g, 0.670mmol) in toluene (5mL) was added 2-benzoylbenzoic acid (0.167g, 0.737mmol).

Reaction time: 23h. The compound was purified by flash chromatography (EtOAc/*n*-hexane 1:2) to give white crystalline

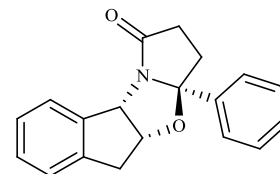


solid (0.225g, 98.7%); mp: 150-153 °C; ¹H-NMR (300 MHz, MeOD) δ 7.81 – 7.72 (m, 1H, Ar*H*), 7.59 – 7.45 (m, 1H, Ar*H*), 7.31 (d, *J* = 7.3 Hz, 1H, Ar*H*), 7.27 – 7.15 (m, 1H, Ar*H*), 7.06 – 6.89 (m, 2H, Ar*H*), 6.84 (d, *J* = 7.2 Hz, 1H,), 5.87 (d, *J* = 6.2 Hz, 1H, CH-N), 5.40 (td, *J* = 6.2, 2.0 Hz, 1H, CH-O), 3.23 – 3.01 (m, 2H, CH₂-indanol); ¹³C-NMR (100 MHz, CDCl₃) δ 173.83 (C=O), 148.29, 141.30 (ArC), 139.44 (ArC), 138.66 (ArC), 133.65 (ArC), 130.35 (ArC), 130.01 (ArC), 128.51 (ArC), 127.89 (ArC), 127.66 (ArC), 127.14 (ArC), 125.94 (ArC), 125.45

(ArC), 124.58 (ArC), 124.50 (ArC), 123.48 (ArC), 101.49 (C-9b), 87.43 (CH-N), 64.28 (CH-O), 39.62 (CH₂-indanol); Anal. Calcd. (C₂₀H₁₃NO₂•0.05H₂O): C, 81.17%; H, 5.08%; N, 4.12%. Found C, 81.35%; H, 4.94%; N, 4.24%.

(3aS,4aS,9bS)-3a-phenyl-3,3a,4a,9b-tetrahydro-5H-indeno[1,2-d]pyrrolo[2,1-b]oxazol-

1(2H)-one (6b): Following the general procedure, to a solution of (1S, 2R)-(-)-*cis*-1-Amino-2-indanol (0.100g, 0.670mmol) in toluene (5mL) was added 3-benzoyl propionic acid (0.131g, 0.737mmol).

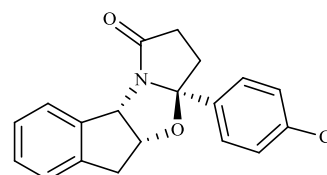


Reaction time: 24h. The compound was purified by flash chromatography (EtOAc/*n*-hexane 1:2) to give white crystalline

solid (0.184g, 80.8%); mp: 116-119 °C; ¹H-NMR (300 MHz, CDCl₃) δ 7.38 (d, *J* = 7.7 Hz, 1H, ArH), 7.08 (dd, *J* = 9.8, 4.8 Hz, 3H, ArH), 7.03 – 6.89 (m, 4H, ArH), 6.71 (d, *J* = 7.5 Hz, 1H, ArH), 5.82 (d, *J* = 6.5 Hz, 1H, CH-N), 5.19 – 5.08 (m, 1H, CH-O), 3.09 (dd, *J* = 18.0, 7.5 Hz, 1H, CH₂-indanol), 2.90 – 2.69 (m, 2H, CH₂), 2.69 – 2.42 (m, 2H, CH₂), 2.29 – 2.12 (m, 1H, CH₂); ¹³C-NMR (100 MHz, CDCl₃) δ 179.45 (C=O), 143.42 (ArC), 141.52 (ArC), 138.80 (ArC), 128.55 (ArC), 127.58 (ArC), 127.42 (ArC), 127.14 (ArC), 125.84 (ArC), 124.71 (ArC), 124.44 (ArC), 102.99 (C-9b), 82.70 (CH-N), 64.53 (CH-O), 39.48 (CH₂-indanol) 36.43 (CH₂), 32.22 (CH₂); Anal. Calcd. (C₁₉H₁₇NO₂•0.05H₂O): C, 78.08%; H, 5.91%; N, 4.79%. Found C, 78.19%; H, 5.77%; N, 4.92%.

(3aS,4aR,9bS)-3a-(4-chlorophenyl)-2,3,3a,4a,5,9b-hexahydro-1H-indeno[1,2-d]pyrrolo[2,1-

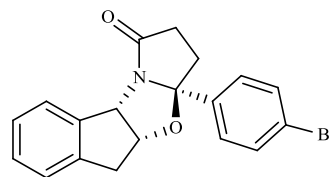
b]oxazol-1-one (6c): Following the general procedure, to a solution of (1S, 2R)-(-)-*cis*-1-Amino-2-indanol (0.070g, 0.469mmol) in toluene (3.5mL) was added 3-(4-chlorobenzoyl) propionic acid (0.120g, 0.563mmol). Reaction time: 23h. The compound was purified by flash chromatography (EtOAc/*n*-



hexane 1:1) to give white crystalline solid (0.122g, 79.6%); mp: 149-151 °C; ¹H-NMR (300 MHz, CDCl₃) δ 7.36 (d, *J* = 7.5 Hz, 1H, ArH), 7.10 (t, *J* = 7.4 Hz, 1H, ArH), 7.04 – 6.90 (m, 5H, ArH), 6.75 (d, *J* = 7.5 Hz, 1H, ArH), 5.81 (d, *J* = 6.5 Hz, 1H, CH-N), 5.18 – 5.05 (m, 1H, CH-O), 3.10 (dd, *J* = 17.9, 7.3 Hz, 1H, CH₂-indanol), 2.83 – 2.45 (m, 4H, CH₂), 2.18 – 2.10 (m, 1H, CH₂); ¹³C-NMR (75 MHz, CDCl₃) δ 179.47 (C=O), 142.12 (ArC), 141.39 (ArC), 138.61 (ArC), 133.24 (ArC), 130.29 (ArC), 129.19 (ArC), 128.76 (ArC), 127.73 (ArC), 127.33 (ArC), 127.05 (ArC), 126.83 (ArC), 126.21 (ArC), 125.77 (ArC), 124.60 (ArC), 102.52 (C-9b), 87.77 (CH-N), 64.68 (CH-O), 39.53 (CH₂-indanol), 36.21 (CH₂), 32.08 (CH₂); Anal. Calcd. (C₁₉H₁₆ClNO₂): C, 70.05%; H, 4.95%; N, 4.30%. Found C, 70.35%; H, 4.99%; N, 4.37%.

(3aS,4aR,9bS)-3a-(4-bromophenyl)-2,3,3a,4a,5,9b-hexahydro-1H-indeno[1,2-d]pyrrolo[2,1-b]oxazol-1-one (6d):

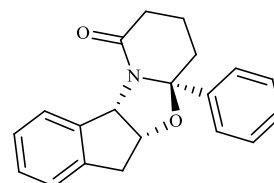
Following the general procedure, to a solution of (1*S*, 2*R*)-(-)-*cis*-1-Amino-2-indanol (0.060g, 0.402mmol) in toluene (3.0mL) was added 3-(4-bromobenzoyl) propionic acid (0.114g, 0.442mmol). Reaction



time: 15h. The compound was purified by flash chromatography (EtOAc/*n*-hexane 1/1) to give white crystalline solid (0.133g, 89.0%); mp: 169-171 °C; ¹H-NMR (300 MHz, CDCl₃) δ 7.29 (d, *J* = 7.0 Hz, 1H, Ar*H*), 7.03 – 6.87 (m, 6H, Ar*H*), 6.69 (d, *J* = 7.0 Hz, 1H, Ar*H*), 5.75 (d, *J* = 5.9 Hz, 1H, CH-N), 5.05 (t, *J* = 5.8 Hz, 1H, CH-O), 3.04 (dd, *J* = 17.9, 7.1 Hz, 1H, CH₂-indanol), 2.76 – 2.43 (m, 4H, CH₂), 2.11 – 2.03 (m, 1H, CH₂); ¹³C NMR (100 MHz, CDCl₃) δ 179.48 (C=O), 142.66 (ArC), 141.40 (ArC), 138.60 (ArC), 130.70 (ArC), 128.79 (ArC), 127.36 (ArC), 126.56 (ArC), 125.78 (ArC), 124.64 (ArC), 121.48 (ArC), 102.56 (C-9b), 82.80 (CH-N), 64.71 (CH-O), 39.51 (CH₂-indanol), 36.18 (CH₂), 32.09 (CH₂); Anal. Calcd. (C₁₉H₁₆BrNO₂): C, 61.64%; H, 4.36%; N, 3.78%. Found C, 61.58%; H, 4.51%; N, 3.81%.

(4bS,9aS,10aR)-9a-phenyl-7,8,9,9a,10a,11-hexahydroindeno[1',2':4,5]oxazolo[3,2-a]pyridin-6(4bH)-one (6e):

Following the general procedure, to a solution of (1*S*, 2*R*)-(-)-*cis*-1-Amino-2-indanol (0.103g, 0.689mmol) in toluene (5mL) was added 4-benzoylbutyric acid (0.159g, 0.827mmol). Reaction time: 23h. The compound was purified by

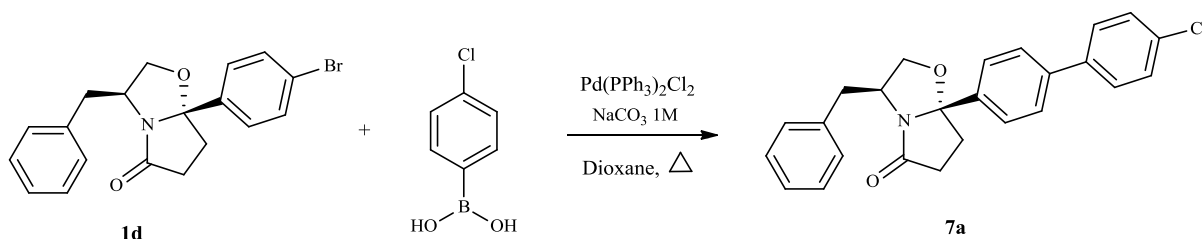


flash chromatography (EtOAc/*n*-hexane 1:1) to give white crystalline solid (0.132g, 62.8%); mp: 166-167 °C; ¹H-NMR (300 MHz, CDCl₃) δ 7.65 (d, *J* = 7.6 Hz, 1H, Ar*H*), 7.14 (t, *J* = 7.5 Hz, 1H, Ar*H*), 7.05 – 6.93 (m, 5H, Ar*H*), 6.64 (d, *J* = 7.6 Hz, 1H, Ar*H*), 6.11 (d, *J* = 7.3 Hz, 1H, CH-N), 5.13 (td, *J* = 7.9 Hz, *J* = 2.3 Hz, 1H, CH-O), 3.06 (dd, *J* = 17.9, 8.0 Hz, 1H, CH₂-indanol), 2.68 – 2.42 (m, 3H, CH₂), 2.26 (dt, *J* = 7.0, 3.1 Hz, 1H, CH₂), 1.77 – 1.67 (m, 1H, CH₂), 1.45 – 1.28 (m, 1H, CH₂); ¹³C-NMR (75 MHz, CDCl₃) δ 168.92 (C=O), 142.41 (ArC), 141.12 (ArC), 140.32 (ArC), 128.51 (ArC), 127.61 (ArC), 127.22 (ArC), 127.14 (ArC), 126.47 (ArC), 126.40 (ArC), 124.13 (ArC), 96.47 (C-9b), 79.71 (CH-N), 64.29 (CH-O), 39.53 (CH₂), 37.62 (CH₂), 30.77 (CH₂), 15.96 (CH₂); Anal. Calcd. (C₂₀H₁₉NO₂): C, 78.66%; H, 6.27%; N, 4.59%. Found C, 78.84%; H, 6.34%; N, 4.68%.

IV.3 - General procedure for Suzuki Coupling reactions

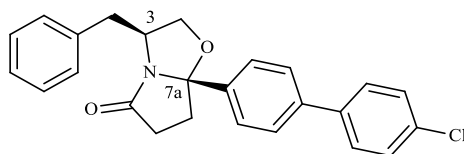
To a solution of the appropriate tryptophan-derived oxazolopiperidones or phenylalaninol-derived oxazolopyrrolidone lactams (0.23 mmol) in dioxane (2.3 mL) was added Pd(PPh₃)₂Cl₂ (0.023 mmol) and Na₂CO₃ 1 M (690 μL) followed by the proper boronic acid (0.28 mmol). The resulting mixture was degassed and stirred at 100°C between 2 and 5h under N₂ atmosphere. After cooling to room temperature, the reaction mixture was diluted with CH₂Cl₂, filtered under celite and concentrated under pressure to give the crude product. The crude was absorbed on silica and purified by flash chromatography using a mixture of EtOAc/n-hexane as eluent.

IV.3.1 – (S)-phenylalaninol-derived oxazolopiperidone lactams



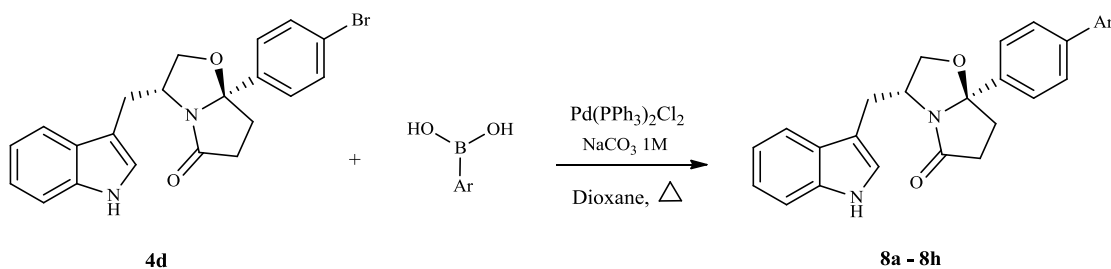
(3*S*,7*aS*)-3-benzyl-7*a*-(4'-chloro-[1,1'-biphenyl]-4-yl)tetrahydropyrrolo[2,1-*b*]oxazol-5(6*H*)-

one (7a): Following the general procedure, to a solution of **1d** (0.051g, 0.137mmol) in dioxane (1.6mL) was added Pd(PPh₃)₂Cl₂ (5mg, 16.3μmol), Na₂CO₃ 1 M (420μL) and 4-chlorophenylboronic acid (0.027g, 0.173mmol) Reaction time: 4h. The



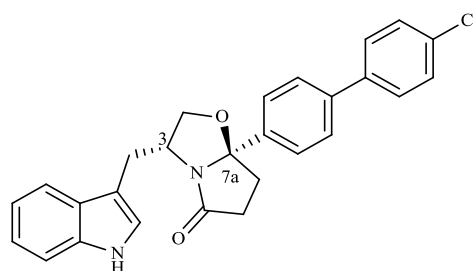
compound was purified by flash chromatography (EtOAc/*n*-hexane 2:3) to afford the title compound as a colorless oil (0.045g, 82.0%); ¹H-NMR (300 MHz, CDCl₃) δ 7.49 – 7.41 (m, 6H, ArH), 7.30 – 7.27 (m, 2H, ArH), 7.13 – 7.04 (m, 3H, ArH), 6.98 – 6.05 (m, 2H, ArH), 4.31 (dq, *J* = 13.6, 7.0 Hz, 1H, *H*-3), 4.02 (dd, *J* = 8.7, 7.5 Hz, 1H, *H*-2), 3.47 (dd, *J* = 8.8, 7.1 Hz, 1H, *H*-2), 2.84 (dd, *J* = 13.7, 6.2 Hz, 1H, ArCH₂), 2.77 – 2.64 (m, 1H), 2.50 – 2.33 (m, 2H), 2.26 – 2.08 (m, 2H); ¹³C-NMR (100 MHz, CDCl₃) δ 180.02 (C=O), 142.15 (ArC), 140.13 (ArC), 139.03 (ArC), 137.38 (ArC), 133.88 (ArC), 132.05 (ArC), 129.21 (ArC), 129.09 (ArC), 128.69 (ArC), 128.52 (ArC), 127.43 (ArC), 127.11 (ArC), 126.88 (ArC), 125.88 (ArC), 102.32 (C-7a), 72.52 (C-2), 56.72 (C-3), 40.12 (ArCH₂), 35.28 (CH₂), 32.74 (CH₂); Anal. Calcd. (C₂₅H₂₂ClNO₂): C, 74.34%; H, 5.49%; N, 3.47%. Found C, 74.66%; H, 5.58%; N, 3.47%.

IV.3.2 – (R)-tryptophan-derived oxazolopiperidone lactams



(3R,7aR)-3-((1H-indol-3-yl)methyl)-7a-(4'-chloro-[1,1'-biphenyl]-4-yl)tetrahydropyrrolo[2,1-b]oxazol-5(6H)-one

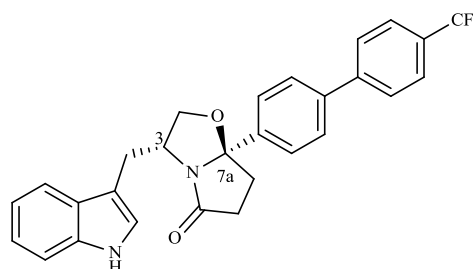
(8a): Following the general procedure, to a solution of **4d** (0.036g, 0.088mmol) in dioxane (1.0mL) was added Pd(PPh₃)₂Cl₂ (2.7mg, 8.8μmol), Na₂CO₃ 1 M (266μL) and 4-chlorophenylboronic acid (0.017g, 0.107mmol) Reaction time: 4h. The compound was purified by flash chromatography (EtOAc/*n*-hexane



2:3) to afford the title compound as a white solid (0.036g, 93.9%); mp: 201-204 °C; ¹H-NMR (300 MHz, CDCl₃) δ 8.08 (s, 1H, *NH*), 7.63 – 7.50 (m, 6H, *ArH*), 7.48 – 7.39 (m, 3H, *ArH*), 7.33 (d, *J* = 8.1 Hz, 1H, *ArH*), 7.22 – 7.12 (m, 1H, *ArH*), 7.12 – 7.01 (m, 2H, *ArH*), 4.70 – 4.52 (m, 1H, *H*-3), 4.20 (dd, *J* = 8.7, 7.4 Hz, 1H, *H*-2), 3.66 (dd, *J* = 8.8, 6.8 Hz, 1H), 3.11 (dd, *J* = 15.1, 6.6 Hz, 1H), 3.01 – 2.78 (m, 1H), 2.73 – 2.44 (m, 3H), 2.38 – 2.17 (m, 1H); ¹³C-NMR (100 MHz, CDCl₃) δ 180.32 (C=O), 142.27 (ArC), 140.05 (ArC), 139.09 (ArC), 136.27 (ArC), 133.85 (ArC), 133.22 (ArC), 129.22 (ArC), 128.53 (ArC), 127.54 (ArC), 127.41 (ArC), 125.87 (ArC), 122.29 (ArC), 122.24 (ArC), 119.59 (ArC), 118.92 (ArC), 111.76 (ArC), 111.27 (ArC), 102.40 (*C*-7a), 72.95 (*C*-2), 55.75 (*C*-3), 35.24 (ArCH₂), 32.80, 29.85; Anal. Calcd. (C₂₇H₂₃ClN₂O₂•0.2Hex): C, 73.60%; H, 5.66%; N, 6.09%. Found C, 73.56%; H, 5.83%; N, 5.92%.

(3R,7aR)-3-((1H-indol-3-yl)methyl)-7a-(4'-(trifluoromethyl)-[1,1'-biphenyl]-4-yl)tetrahydropyrrolo[2,1-b]oxazol-5(6H)-one

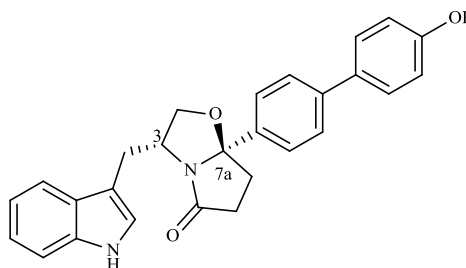
(8b): Following the general procedure, to a solution of **4d** (0.050g, 0.122mmol) in dioxane (1.4mL) was added Pd(PPh₃)₂Cl₂ (3.7mg, 12.2μmol), Na₂CO₃ 1 M (370μL) and 4-(trifluoromethyl)phenylboronic acid (0.028g, 0.148mmol) Reaction time: 3h. The



compound was purified by flash chromatography (EtOAc/*n*-hexane 2:3) to afford the title compound as a white solid (0.050g, 86.1%); mp: 201-203 °C; ¹H-NMR (300 MHz, CDCl₃) δ 7.99 (s, 1H, *NH*), 7.72 (s, 4H, *ArH*), 7.64 – 7.55 (m, 4H, *ArH*), 7.43 (d, *J* = 7.5 Hz, 1H, *ArH*), 7.33 (d, *J* = 8.1 Hz, 1H, *ArH*), 7.21 – 7.14 (m, 1H, *ArH*), 7.12 – 7.03 (m, 2H, *ArH*), 4.67 – 4.53 (m, 1H, *H*-3), 4.20 (dd, *J* = 8.8, 7.4 Hz, 1H, *H*-2), 3.65 (dd, *J* = 8.8, 6.8 Hz, 1H), 3.10 (dd, *J* = 15.0, 6.5 Hz, 1H), 2.91 – 2.83 (m, 1H), 2.67 – 2.48 (m, 3H), 2.33 – 2.22 (m, 1H); ¹³C-NMR (100 MHz, CDCl₃) δ 180.34 (C=O), 144.16 (ArC), 143.18 (ArC), 142.08 (ArC), 139.77 (ArC), 136.42 (ArC), 132.02 (ArC), 127.76 (ArC), 127.59 (ArC), 127.08 (ArC), 126.09 (ArC), 126.04 (ArC), 125.98 (ArC), 122.33 (ArC), 122.23 (ArC), 119.61 (ArC), 118.09 (ArC), 111.65 (ArC), 111.17 (ArC), 102.36 (C-7a), 72.92 (C-2), 55.78 (C-3), 35.23 (ArCH₂), 32.79, 29.85; Anal. Calcd. (C₂₈H₂₃F₃N₂O₂): C, 70.58%; H, 4.87%; N, 5.88%. Found C, 70.09%; H, 5.19%; N, 5.83%.

(3R,7aR)-3-((1H-indol-3-yl)methyl)-7a-(4'-hydroxy-[1,1'-biphenyl]-4-yl)tetrahydropyrrolo[2,1-b]oxazol-5(6H)-one

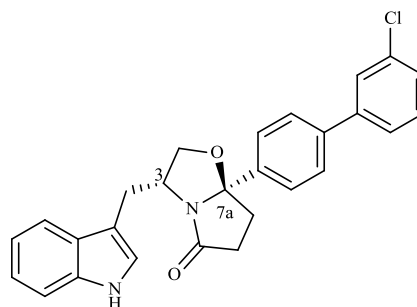
(8c): Following the general procedure, to a solution of **4d** (0.050g, 0.122mmol) in dioxane (1.4mL) was added Pd(PPh₃)₂Cl₂ (3.7mg, 12.2μmol), Na₂CO₃ 1 M (370μL) and 4-hydroxyphenylboronic acid (0.021g, 0.148mmol) Reaction time: 2h. The compound was purified by flash chromatography



(EtOAc/*n*-hexane 3:2) to afford the title compound as a white solid (0.044g, 84.9%); mp: 223-225 °C; ¹H-NMR (300 MHz, CDCl₃) δ 7.98 (s, 1H, *NH*), 7.62 – 7.43 (m, 7H, *ArH*), 7.34 (d, *J* = 7.8 Hz, 1H, *ArH*), 7.18 (t, *J* = 7.6 Hz, 1H, *ArH*), 7.10 – 7.05 (m, 2H, *ArH*), 6.95 (d, *J* = 8.5 Hz, 2H, *ArH*), 5.21 (s, 1H, *OH*), 4.68 – 4.51 (m, 1H, *H*-3), 4.20 (dd, *J* = 8.5, 7.8 Hz, 1H, *H*-2), 3.66 (dd, *J* = 8.6, 6.8 Hz, 1H), 3.13 (dd, *J* = 14.9, 6.3 Hz, 1H), 2.98 – 2.76 (m, 1H), 2.75 – 2.46 (m, 3H), 2.33 – 2.24 (m, 1H); ¹³C-NMR (100 MHz, DMSO) δ 179.53 (C=O), 157.19 (ArC), 140.75 (ArC), 140.18 (ArC), 136.02 (ArC), 130.07 (ArC), 127.73 (ArC), 126.93 (ArC), 126.03 (ArC), 125.51 (ArC), 122.87 (ArC), 118.31 (ArC), 117.85 (ArC), 115.78 (ArC), 111.39 (ArC), 109.88 (ArC), 101.66 (C-7a), 72.28 (C-2), 55.28 (C-3), 40.41 (ArCH₂), 32.75, 29.84; Anal. Calcd. (C₂₇H₂₄N₂O₃•0.1AcOEt): C, 75.95%; H, 5.78%; N, 6.47%. Found C, 75.74%; H, 5.85%; N, 6.57%.

(3R,7aR)-3-((1H-indol-3-yl)methyl)-7a-(3'-chloro-[1,1'-biphenyl]-4-yl)tetrahydropyrrolo[2,1-b]oxazol-5(6H)-one (8d):

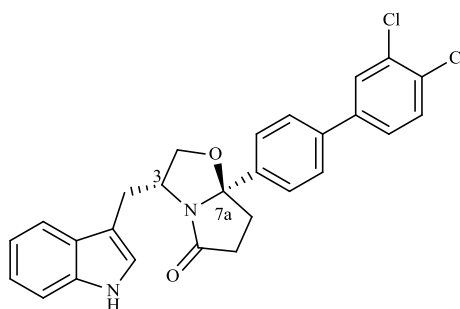
Following the general procedure, to a solution of **4d** (0.070g, 0.170mmol) in dioxane (2.0mL) was added Pd(PPh₃)₂Cl₂ (5.2mg, 17.0μmol), Na₂CO₃ 1 M (520μL) and 3-chlorophenylboronic acid (0.033g, 0.208mmol) Reaction time: 4h. The compound was purified by flash chromatography (EtOAc/*n*-hexane 1:1) to afford the



title compound as a pale yellow solid (0.059g, 77.6%); mp: 204-206 °C; ¹H-NMR (300 MHz, CDCl₃) δ 7.98 (s, 1H, *NH*), 7.47 (t, 1.6 Hz, 1H, *ArH*), 7.43 (s, 4H, *ArH*), 7.36 (dt, *J* = 7.4 Hz, 1.6 Hz, 1H, *ArH*), 7.30 (d, 7.7 Hz, 1H, *ArH*), 7.25 – 7.17 (m, 3H, *ArH*), 7.06 – 7.00 (m, 1H, *ArH*), 6.95 – 6.91 (m, 2H, *ArH*), 4.51 – 4.42 (m, 1H, *H*-3), 4.05 (dd, *J* = 8.9, 6.9 Hz, 1H, *H*-2), 3.51 (dd, *J* = 8.8, 6.8 Hz, 1H), 2.95 (dd, *J* = 14.4, 6.6 Hz, 1H), 2.80 – 2.66 (m, 1H), 2.53 – 2.34 (m, 3H), 2.22 – 2.08 (m, 1H); ¹³C-NMR (100 MHz, CDCl₃) δ 180.33 (C=O), 142.54 (*ArC*), 142.49 (*ArC*), 139.88 (*ArC*), 136.26 (*ArC*), 134.93 (*ArC*), 130.29 (*ArC*), 127.72 (*ArC*), 127.56 (*ArC*), 127.45 (*ArC*), 125.85 (*ArC*), 125.43 (*ArC*), 122.26 (*ArC*), 119.57 (*ArC*), 118.89 (*ArC*), 111.67 (*ArC*), 111.27 (*ArC*), 102.36 (*C*-7a), 72.93 (*C*-2), 55.74 (*C*-3), 35.20 (*ArCH*₂), 32.78, 29.82; Anal. Calcd. (C₂₇H₂₃ClN₂O₂): C, 73.21%; H, 5.23%; N, 6.32%. Found C, 72.91%; H, 5.70%; N, 6.24%.

(3R,7aR)-3-((1H-indol-3-yl)methyl)-7a-(3',4'-dichloro-[1,1'-biphenyl]-4-yl)tetrahydropyrrolo[2,1-b]oxazol-5(6H)-one (8e):

Following the general procedure, to a solution of **4d** (0.070g, 0.170mmol) in dioxane (2.0mL) was added Pd(PPh₃)₂Cl₂ (5.2mg, 17.0μmol), Na₂CO₃ 1 M (520μL) and 3,4-dichlorophenylboronic acid (0.040g, 0.208mmol) Reaction time: 4h. The compound was purified by flash chromatography

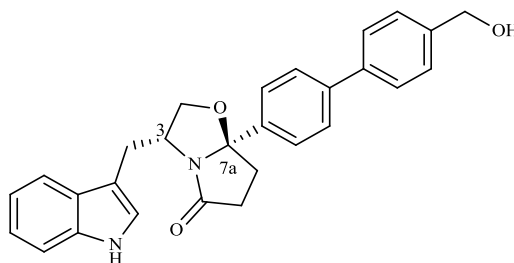


(EtOAc/*n*-hexane 1:1) to afford the title compound as a pale yellow solid (0.069g, 85.2%); mp: 176-178 °C; ¹H-NMR (300 MHz, CDCl₃) δ 7.98 (s, 1H, *NH*), 7.49 (s, 5H, *ArH*), 7.38 (dd, *J* = 8.4 Hz, 2.2 Hz, 2H, *ArH*), 7.27 (d, 8.1 Hz, 1H, *ArH*), 7.11 (d, 8.1 Hz, 1H, *ArH*), 7.06 – 6.97 (m, 2H, *ArH*), 4.65 – 4.45 (m, 1H, *H*-3), 4.14 (dd, *J* = 8.7, 7.4 Hz, 1H, *H*-2), 3.58 (dd, *J* = 8.8, 6.8 Hz, 1H), 3.02 (dd, *J* = 15.0, 6.6 Hz, 1H), 2.87 – 2.76 (m, 1H), 2.65 – 2.38 (m, 3H), 2.26 – 2.15 (m, 1H); ¹³C-NMR (100 MHz, CDCl₃) δ 180.32 (C=O), 142.89 (*ArC*), 140.73 (*ArC*), 138.88 (*ArC*), 136.22 (*ArC*), 133.16 (*ArC*), 131.97 (*ArC*), 130.99 (*ArC*), 129.15 (*ArC*), 127.53 (*ArC*), 127.44 (*ArC*), 126.51 (*ArC*), 125.98 (*ArC*), 122.34 (*ArC*), 122.22 (*ArC*), 119.61 (*ArC*), 118.75 (*ArC*), 111.68 (*ArC*), 111.28 (*ArC*), 102.29 (*C*-7a), 72.83 (*C*-2), 55.76 (*C*-3), 35.21 (*ArCH*₂),

32.85, 29.85; Anal. Calcd. (C₂₇H₂₂Cl₂N₂O₂): C, 67.93%; H, 4.65%; N, 5.87%. Found C, 67.96%; H, 4.90%; N, 5.73%.

(3R,7aR)-3-((1H-indol-3-yl)methyl)-7a-(4'-(hydroxymethyl)-[1,1'-biphenyl]-4-yl)tetrahydropyrrolo[2,1-b]oxazol-5(6H)-one

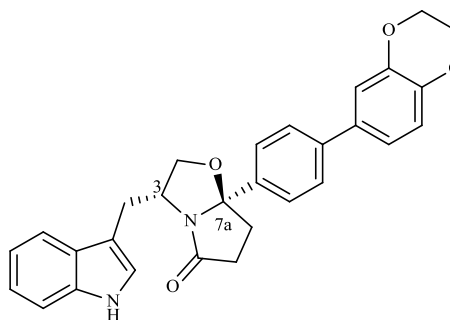
(8f): Following the general procedure, to a solution of **4d** (0.070g, 0.170mmol) in dioxane (2.0mL) was added Pd(PPh₃)₂Cl₂ (5.2mg, 17.0μmol), Na₂CO₃ 1 M (520μL) and 4-(hydroxymethyl)phenylboronic acid (0.032g, 0.208mmol) Reaction time: 3h. The compound was purified by flash chromatography



(EtOAc/*n*-hexane 3:2) to afford the title compound as a pale yellow solid (0.053g, 71.0%); mp: 213-215 °C; ¹H-NMR (300 MHz, CDCl₃) δ 8.00 (s, 1H, *NH*), 7.65 – 7.44 (m, 9H, *ArH*), 7.33 (d, *J* = 8.0 Hz, 1H, *ArH*), 7.17 (t, *J* = 7.3 Hz, 1H, *ArH*), 7.11 – 7.02 (m, 2H, *ArH*), 4.77 (s, 2H, *CH*₂), 4.67 – 4.53 (m, 1H, *H*-3), 4.19 (t, *J* = 8.0 Hz, 1H, *H*-2), 3.66 (t, *J* = 8.0 Hz, 1H), 3.11 (dd, *J* = 14.7, 6.0 Hz, 1H), 2.95 – 2.78 (m, 1H), 2.69 – 2.47 (m, 3H), 2.38 – 2.20 (m, 1H).; ¹³C-NMR (100 MHz, CDCl₃) δ 180.33 (C=O), 141.95 (ArC), 140.93 (ArC), 140.42 (ArC), 140.05 (ArC), 136.28 (ArC), 127.75 (ArC), 127.62 (ArC), 127.51 (ArC), 127.48 (ArC), 125.80 (ArC), 122.32 (ArC), 122.24 (ArC), 119.63 (ArC), 118.99 (ArC), 111.85 (ArC), 111.25 (ArC), 102.48 (C-7a), 72.95 (C-2), 65.27 (CH₂), 55.75 (C-3), 35.28 (ArCH₂), 32.84, 29.85; Anal. Calcd. (C₂₈H₂₆N₂O₃•0.10CH₂Cl₂): C, 75.50%; H, 5.92%; N, 6.27%. Found C, 75.18%; H, 6.21%; N, 6.14%.

(3R,7aR)-3-((1H-indol-3-yl)methyl)-7a-(4-(2,3-dihydrobenzo[*b*][1,4]dioxin-6-yl)phenyl)tetrahydropyrrolo[2,1-b]oxazol-5(6H)-one (8g):

Following the general procedure, to a solution of **4d** (0.070g, 0.170mmol) in dioxane (2.0mL) was added Pd(PPh₃)₂Cl₂ (5.2mg, 17.0μmol), Na₂CO₃ 1 M (520μL) and 1,4-benzodioxane-6-boronic acid (0.037g, 0.208mmol) Reaction time: 5h. The compound was purified by flash chromatography (EtOAc/*n*-hexane 1:1) to

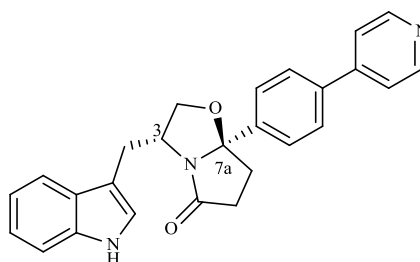


afford the title compound as a pale yellow solid (0.022g, 28.1%); mp: 286-288 °C; ¹H-NMR (300 MHz, CDCl₃) δ 7.97 (s, 1H, *NH*), 7.56 – 7.44 (m, 5H, *ArH*), 7.33 (d, *J* = 8.0 Hz, 1H, *ArH*), 7.19 – 7.08 (m, 5H, *ArH*), 6.95 (d, *J* = 8.3 Hz, 1H, *ArH*), 4.64 – 4.54 (m, 1H, *H*-3), 4.31 (s, 4H, *CH*₂), 4.18 (dd, *J* = 8.7, 7.5 Hz, 1H, *H*-2), 3.65 (dd, *J* = 8.8, 6.9 Hz, 1H), 3.11 (dd, *J* = 14.7, 6.1 Hz, 1H), 2.93 – 2.82 (m, *IH*), 2.67 – 2.45 (m, 3H), 2.37 – 2.19 (m, 1H); ¹³C-NMR (100 MHz,

CDCl₃) δ 180.36 (C=O), 143.89 (ArC), 143.59 (ArC), 141.41 (ArC), 140.68 (ArC), 136.28 (ArC), 134.24 (ArC), 127.60 (ArC), 127.12 (ArC), 125.56 (ArC), 122.33 (ArC), 122.23 (ArC), 120.44 (ArC), 119.66 (ArC), 119.04 (ArC), 117.95 (ArC), 115.95 (ArC), 111.81 (ArC), 111.22 (ArC), 102.43 (C-7a), 72.92 (C-2), 64.70 (CH₂), 55.73 (C-3), 35.22 (ArCH₂), 32.93, 29.91; Anal. Calcd. (C₂₉H₂₆N₂O₄): C, 74.66%; H, 5.68%; N, 6.00%. Found C, 74.65%; H, 5.70%; N, 5.67%.

(3R,7aR)-3-((1H-indol-3-yl)methyl)-7a-(4-(pyridin-4-yl)phenyl)tetrahydropyrrolo[2,1-b]oxazol-5(6H)-one (8h): Following the general

procedure, to a solution of **4d** (0.070g, 0.170mmol) in dioxane (2.0mL) was added Pd(PPh₃)₂Cl₂ (5.2mg, 17.0 μ mol), Na₂CO₃ 1 M (520 μ L) and 4-pyridinylboronic acid (0.026g, 0.208mmol) Reaction time: 2h. The compound was purified by flash chromatography (EtOAc/*n*-hexane 3:1) to



afford the title compound as a pale yellow solid (0.068g, 97.0%); mp: 214-215 °C; ¹H-NMR (300 MHz, CDCl₃) δ 8.69 (d, *J* = 5.6 Hz, 2H, ArH), 8.23 (s, 1H, NH), 7.63 (q, *J* = 8.4 Hz, 4H, ArH), 7.54 (d, *J* = 5.9 Hz, 2H, ArH), 7.43 (d, *J* = 7.8 Hz, 1H, ArH), 7.32 (d, *J* = 8.0 Hz, 1H, ArH), 7.17 (t, *J* = 7.4 Hz, 1H, ArH), 7.12 – 7.01 (m, 2H, ArH), 4.71 – 4.55 (m, 1H, H-3), 4.21 (t, *J* = 8.1 Hz, 1H, H-2), 3.65 (dd, *J* = 8.6, 7.0 Hz, 1H), 3.09 (dd, *J* = 14.7, 6.1 Hz, 1H), 2.88 (ddd, *J* = 24.1, 12.1, 6.3 Hz, 1H), 2.72 – 2.45 (m, 3H), 2.37 – 2.20 (m, 1H); ¹³C-NMR (100 MHz, CDCl₃) δ 180.28 (C=O), 150.50 (ArC), 147.88 (ArC), 144.01 (ArC), 138.20 (ArC), 136.31 (ArC), 127.53 (ArC), 126.11 (ArC), 122.27 (ArC), 121.79 (ArC), 119.57 (ArC), 118.85 (ArC), 111.64 (ArC), 111.30 (ArC), 102.28 (C-7a), 72.97 (C-2), 55.81 (C-3), 35.19 (ArCH₂), 32.75, 29.85; Anal. Calcd. (C₂₆H₂₃N₃O₂•0.35H₂O): C, 75.10%; H, 5.76%; N, 10.11%. Found C, 74.90%; H, 5.81%; N, 9.73%.

IV.4 - General procedure for Indole Protection reactions

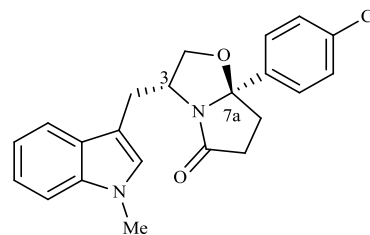
IV.4.1 – Method 1 for indole protection of (*R*)-tryptophanol-derived oxazolopyrrolidone lactams

The respective (*R*)-tryptophanol-derived oxazolopyrrolidone lactam (0.129 mmol) was dissolved in THF or DMF (5 mL) and the solution was cooled to 0 °C under an atmosphere of nitrogen. Sodium hydride (NaH) in 60% dispersion in mineral oil (0.250 mmol) was added in one portion and the mixture stirred for 15 minutes. The appropriate protecting agent

(0.320mmol) was added and the reaction mixture stirred between 3 and 6h, at room temperature. After reaction completion was added distilled water (10mL), for quenching, and EtOAc (10mL). The aqueous phase was washed with EtOAc (2 x 10mL) and the combined organic phases were also washed with brine (10mL), dried with MgSO₄, concentrated *in vacuo* and the residue was purified by flash chromatography using ethyl AcOEt/n-hexane as eluent.

(3R,7aR)-7a-(4-chlorophenyl)-3-((1-methyl-1H-indol-3-yl)methyl)tetrahydropyrrolo[2,1-b]oxazol-5(6H)-one (9a):

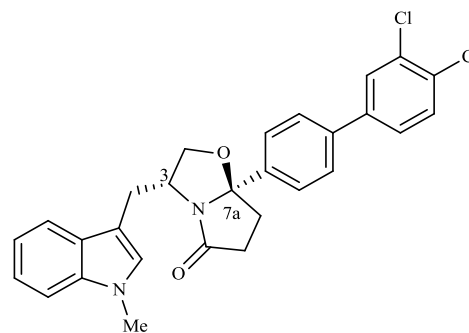
Following the general procedure, to a solution of **4c** (0.070g, 0.191mmol) in DMF (7.0mL) was added NaH (9.2mg, 0.382mmol) and methyl iodide (MeI) (29.7μL, 0.477mmol). Reaction time: 5h. The compound was purified by flash chromatography (EtOAc/n-hexane 2:3) to afford the title compound as a pale yellow oil (0.065g,



88.8%); ¹H-NMR (300 MHz, CDCl₃) δ 7.37 – 7.22 (m, 5H, ArH), 7.18 – 7.09 (m, 2H, ArH), 6.99 (t, *J* = 7.2 Hz, 1H, ArH), 6.78 (s, 1H, ArH), 4.54 – 4.36 (m, 1H, H-3), 4.07 (t, *J* = 8.1 Hz, 1H, H-2), 3.60 (s, 3H, CH₃), 3.51 (dd, *J* = 8.6, 7.2 Hz, 1H), 2.97 (dd, *J* = 14.6, 5.7 Hz, 1H), 2.87 – 2.65 (m, 1H), 2.54 – 2.25 (m, 3H), 2.32 – 2.19 (m, 1H), 2.19 – 2.00 (m, 1H); ¹³C-NMR (100 MHz, CDCl₃) δ 180.13 (C=O), 141.56 (ArC), 137.01 (ArC), 134.22 (ArC), 128.95 (ArC), 127.96 (ArC), 127.02 (ArC), 126.69 (ArC), 121.84 (ArC), 119.09 (ArC), 119.00 (ArC), 109.87 (ArC), 109.30 (ArC), 102.02 (C-7a), 72.85 (C-2), 55.90 (C-3), 35.16 (ArCH₂), 32.77 (CH₃), 32.69, 29.60; Anal. Calcd. (C₂₂H₂₁ClN₂O₂): C, 69.38%; H, 5.56%; N, 7.36%. Found C, 69.49%; H, 5.70%; N, 7.21%.

(3R,7aR)-7a-(3',4'-dichloro-[1,1'-biphenyl]-4-yl)-3-((1-methyl-1H-indol-3-yl)methyl)tetrahydropyrrolo[2,1-b]oxazol-5(6H)-one (9b):

Following the general procedure, to a solution of **8e** (0.060g, 0.126mmol) in DMF (7.5mL) was added NaH (6.0mg, 0.251mmol) and methyl iodide (MeI) (19.6μL, 0.314mmol). Reaction time: 3h. The compound was purified by flash chromatography (EtOAc/n-hexane 2:3) to afford the title compound as a pale yellow powder (0.059g, 94.7%); mp: 74-76 °C; ¹H-NMR (300 MHz, CDCl₃) δ 7.54 (s, 4H,

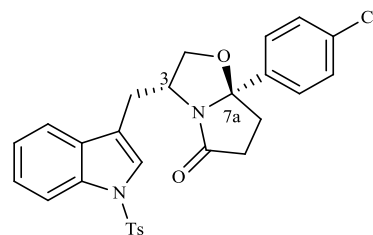


ArH), 7.45 – 7.40 (m, 3H, ArH), 7.24 – 7.15 (m, 2H, ArH), 7.05 (ddd, 7.9 Hz, 6.7 Hz, 1.3 Hz, 1H, ArH), 6.90 (s, 1H, ArH), 4.61 – 4.51 (m, 1H, H-3), 4.17 (dd, *J* = 8.7, 7.4 Hz, 1H, H-2), 3.68 (s, 3H, CH₃), 3.63 (dd, *J* = 8.8, 6.9 Hz, 1H), 3.08 (dd, *J* = 15.1, 5.9 Hz, 1H), 2.93 – 2.78 (m, 1H), 2.66 – 2.45 (m, 3H), 2.27 – 2.17 (m, 1H); ¹³C-NMR (100 MHz, CDCl₃) δ 180.24 (C=O), 142.95 (ArC), 140.70 (ArC), 138.83 (ArC), 137.03 (ArC), 133.16 (ArC), 131.91 (ArC), 130.99

(ArC), 129.15 (ArC), 127.98 (ArC), 127.41 (ArC), 127.03 (ArC), 126.50 (ArC), 125.98 (ArC), 121.86 (ArC), 119.06 (ArC), 119.03 (ArC), 110.05 (ArC), 109.33 (ArC), 102.30 (C-7a), 72.98 (C-2), 55.89 (C-3), 35.25 (ArCH₂), 32.84 (CH₃), 32.79, 29.85; Anal. Calcd. (C₂₈H₂₄Cl₂N₂O₂): C, 68.44%; H, 4.92%; N, 5.70%. Found C, 68.24%; H, 5.36%; N, 5.43%.

(3R,7aR)-7a-(4-chlorophenyl)-3-((1-tosyl-1H-indol-3-yl)methyl)tetrahydropyrrolo[2,1-b]oxazol-5(6H)-one (9c):

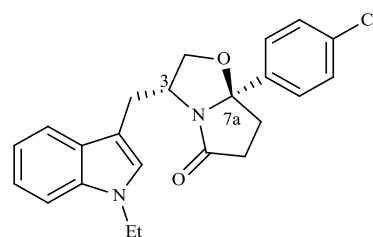
Following the general procedure, to a solution of **4c** (0.036g, 0.098mmol) in THF (1.5mL) was added NaH (3.5mg, 0.147mmol) and *p*-toluenesulfonyl chloride (0.024g, 0.128mmol). Reaction time: 3h. The compound was purified by flash chromatography (EtOAc/*n*-hexane 2:3) to afford the title compound as a pale yellow oil



(0.044g, 85.7%); ¹H-NMR (300 MHz, CDCl₃), 7.95 (d, *J* = 8.2 Hz, 1H, ArH), 7.72 (d, *J* = 8.4 Hz, 2H, ArH), 7.43 – 7.27 (m, 7H, ArH), 7.25 – 7.16 (m, 3H, ArH), 4.61 – 4.44 (m, 1H, H-3), 4.20 – 4.13 (m, 1H, H-2), 3.53 (dd, *J* = 8.8, 6.8 Hz, 1H), 2.97 – 2.75 (m, 2H), 2.69 – 2.44 (m, 2H), 2.42 – 2.33 (m, 1H), 2.32 (s, 3H, CH₃), 2.25 – 2.12 (m, 1H). ¹³C-NMR (100 MHz, CDCl₃) δ 180.31 (C=O), 145.04 (ArC), 141.30 (ArC), 135.40 (ArC), 135.34 (ArC), 134.54 (ArC), 130.71 (ArC), 130.00 (ArC), 129.17 (ArC), 127.02 (ArC), 126.64 (ArC), 125.10 (ArC), 123.82 (ArC), 123.43 (ArC), 119.53 (ArC), 118.38 (ArC), 113.96 (ArC), 102.12 (C-7a), 72.62 (C-2), 54.91 (C-3), 35.02 (ArCH₂), 32.53, 29.65; 21.77 (CH₃); Anal. Calcd. (C₂₈H₂₅ClN₂O₄S): C, 64.55%; H, 4.84%; N, 5.38%. Found C, 64.43%; H, 4.97%; N, 5.32%.

(3R,7aR)-7a-(4-chlorophenyl)-3-((1-ethyl-1H-indol-3-yl)methyl)tetrahydropyrrolo[2,1-b]oxazol-5(6H)-one (9d):

Following the general procedure, to a solution of **4c** (0.120g, 0.327mmol) in DMF (13.5mL) was added NaH (15.7mg, 0.654mmol) and ethyl iodide (65.4μL, 0.818mmol). Reaction time: 3h. The compound was purified by flash chromatography (EtOAc/*n*-hexane 1:2) to afford the title compound as a pale yellow oil (0.101g,

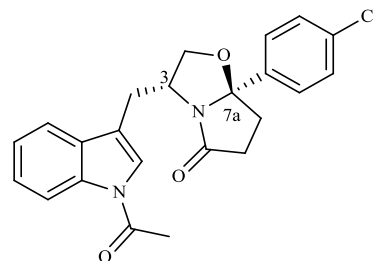


77.8%); ¹H-NMR (300 MHz, CDCl₃) δ 7.39 (d, *J* = 7.9 Hz, 1H, ArH), 7.36 – 7.17 (m, 5H, ArH), 7.16 – 7.08 (m, 1H, ArH), 7.04 – 6.97 (m, 1H, ArH), 6.87 (s, 1H, ArH), 4.48 (m, 1H, H-3), 4.08 (dd, *J* = 8.8, 7.5 Hz, 1H, H-2), 4.01 (q, *J* = 7.3 Hz, 2H, CH₂), 3.52 (dd, *J* = 8.8, 7.0 Hz, 1H), 3.01 (dd, *J* = 14.6, 5.3 Hz, 1H), 2.84 – 2.70 (m, 1H), 2.58 – 2.36 (m, 3H), 2.15 – 2.07 (m, 1H), 1.33 (t, *J* = 7.3 Hz, 3H, CH₃). ¹³C-NMR (100 MHz, CDCl₃) δ 180.15 (C=O), 141.58 (ArC), 136.07 (ArC), 134.28 (ArC), 129.01 (ArC), 128.09 (ArC), 126.75 (ArC), 125.27 (ArC), 121.73 (ArC), 119.16 (ArC), 119.08 (ArC), 109.98 (ArC), 109.41 (ArC), 102.07 (C-7a), 72.93 (C-2), 55.91 (C-3), 40.94 (CH₂), 35.21, 32.75, 29.74, 15.63 (CH₃); Anal. Calcd.

(C₂₃H₂₃ClN₂O₂•0.10Hex): C, 70.24%; H, 6.11%; N, 6.94%. Found C, 70.12%; H, 6.40%; N, 6.95%.

(3R,7aR)-3-((1-acetyl-1H-indol-3-yl)methyl)-7a-(4-chlorophenyl)tetrahydropyrrolo[2,1-b]oxazol-5(6H)-one (9e): Following the general procedure,

to a solution of **4c** (0.094g, 0.256mmol) in DMF (9.5mL) was added NaH (12.3mg, 0.512mmol) and acetic anhydride (60.6μL, 0.641mmol). Reaction time: 6h. The compound was purified by flash chromatography (EtOAc/*n*-hexane 1:1) to afford the title compound as a white powder (0.072g, 68.7%); mp: 66-67 °C; ¹H-NMR (300 MHz, CDCl₃) δ 8.32



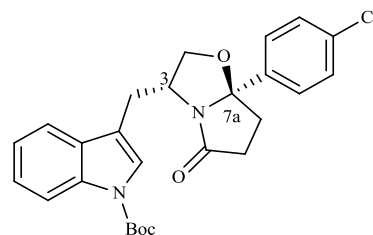
(d, *J* = 7.8 Hz, 1H, *ArH*), 7.56 (s, 1H, *ArH*), 7.28 – 7.11 (m, 7H, *ArH*), 4.61 – 4.45 (m, 1H, *H*-3), 4.20 (dd, *J* = 8.7, 7.6 Hz, 1H, *H*-2), 3.49 (dd, *J* = 8.7, 6.5 Hz, 2H), 2.80 – 2.52 (m, 3H), 2.52 (s, 3H, *CH*₃), 2.48 – 2.35 (m, 2H), 2.16 – 2.02 (m, 1H); ¹³C-NMR (100 MHz, CDCl₃) δ 180.93 (*C*=O), 168.94 (*C*=O), 141.23 (*ArC*), 135.89 (*ArC*), 134.50 (*ArC*), 130.60 (*ArC*), 129.12 (*ArC*), 126.62 (*ArC*), 125.54 (*ArC*), 123.70 (*ArC*), 123.28 (*ArC*), 123.22 (*ArC*), 118.71 (*ArC*), 118.30 (*ArC*), 116.84 (*ArC*), 102.39 (*C*-7a), 72.56 (*C*-2), 54.86 (*C*-3), 34.67 (*ArCH*₂), 32.40, 29.57, 24.23 (*CH*₃); Anal. Calcd. (C₂₃H₂₁ClN₂O₃): C, 67.56%; H, 5.18%; N, 6.85%. Found C, 67.37%; H, 5.47%; N, 6.72%.

IV.4.2 - Method 2 for indole protection of (*R*)-tryptophanol-derived oxazolopyrrolidone lactams

To a solution of *R*-tryptophanol-derived oxazolopyrrolidone lactam (0.13 mmol) in dry THF (5mL) was added TEA anhydrous (2.87mmol) and DMAP (0.33mmol), under an atmosphere of nitrogen. After 15 minutes of stirred, Boc₂O (1.74mmol) was added and reaction mixture stirred, at room temperature, until consumption of starting material. After reaction completion the mixture was concentrated in vacuo and the crude was dissolved in EtOAc (20mL). The organic phase was washed with a saturated solution of NH₄Cl (2 x 15mL), a saturated solution of NaHCO₃ (2 x 15mL) and, finally, with brine (15mL). The combined organic phases were dried with MgSO₄, concentrated *in vacuo* and the residue was purified by flash chromatography using ethyl AcOEt/*n*-hexane as eluent.

Tert-butyl 3-(((3R,7aR)-7a-(4-chlorophenyl)-5-oxohexahydropyrrolo[2,1-b]oxazol-3-yl)methyl)-1H-indole-1-carboxylate (9f):

Following the general procedure, to a solution of **4c** (0.070g, 0.191mmol) in THF (7.0mL) was added TEA anhydrous (58.6μL, 0.420mmol), DMAP (5.8mg, 0.048mmol) and Boc₂O (0.054g, 0.248mmol). Reaction time: 3h. The compound was purified by flash chromatography (EtOAc/*n*-hexane 2:3) to



afford the title compound as a pale yellow powder (0.059g, 65.7%); mp: 163-165 °C; ¹H-NMR (300 MHz, CDCl₃) δ 8.01 (d, *J* = 7.6 Hz, 1H, Ar*H*), 7.37 – 7.30 (m, 4H, Ar*H*), 7.29 – 7.18 (m, 3H, Ar*H*), 7.14 (td, *J* = 7.5, 1.1 Hz, 1H, Ar*H*), 4.57 – 4.40 (m, 1H, *H*-3), 4.14 (dd, *J* = 8.8, 7.5 Hz, 1H, *H*-2), 3.51 (dd, *J* = 8.9, 7.0 Hz, 1H), 2.90 (ddd, *J* = 14.7, 5.7, 1.2 Hz, 1H), 2.85 – 2.70 (m, 1H), 2.59 – 2.30 (m, 3H), 2.16 – 2.05 (m, 1H), 1.58 (s, 9H, CH₃); ¹³C-NMR (100 MHz, CDCl₃) δ 180.26 (C=O), 149.82 (C=O), 141.39 (ArC), 134.39 (ArC), 130.44 (ArC), 129.06 (ArC), 126.57 (ArC), 124.70 (ArC), 123.53 (ArC), 122.74 (ArC), 119.10 (ArC), 116.12 (ArC), 115.40 (ArC), 102.07 (C-7a), 83.82, 72.76 (C-2), 55.16 (C-3), 35.15 (ArCH₂), 32.65, 29.54, 28.40 (CH₃); Anal. Calcd. (C₂₆H₂₇ClN₂O₄): C, 66.88%; H, 5.83%; N, 6.00%. Found C, 66.90%; H, 6.16%; N, 5.89%.

IV.5 – Cytotoxicity assay in human cell lines

Cytotoxicity was assessed using 3-(4,5-dimethyl-2-thiazolyl)-2,5-diphenyl-2H-tetrazolium bromide (MTT), a yellow, water soluble tetrazolium dye that is converted by mitochondrial dehydrogenases in viable cells to a water-insoluble, purple formazan [101, 102]. The day before experiments cells obtained from the American Type Culture Collection HEK 293T – human embryonic kidney epithelial cell line (ATCC HBT-22TM), two breast cancer cell lines MCF-7 (ATCC HTB-22TM) (estrogen receptor positive (ER+) and human epidermal growth factor receptor 2 negative (HER2-) and MDA-MB-231 (ATCC HTB-26TM) (ER-, and HER2-), osteosarcoma cell line MG-63 (ATCC CRL-1427TM), colon adenocarcinoma cell line Caco-2 (ATCC HTB-37TM), gastric adenocarcinoma cell line AGS (ATCC CRL-1739TM), prostate cancer cell line DU-145 (ATCC HTB-81TM) and lung carcinoma cell line A549 (ATCC CCL-185TM) were seeded at 2×10^4 cells and 5×10^3 cells for A549 cell line per well in 96 well tissue culture plates, in 100 μ l of RPMI 1640 culture medium supplemented with 10% fetal bovine serum, 100 units of penicillin G (sodium salt), 100 μ g of streptomycin sulfate and 2 mM L-glutamine, at a concentration that allows cells to grow exponentially during the assay.

Tested compounds were dissolved in dimethyl sulfoxide (DMSO) serially diluted in the culture medium and added to the cells. The final concentration of DMSO in culture medium during treatment did not exceed 0.5% (v/v), and the same concentration of DMSO was added to the control. Each compound concentration was tested in triplicate in a single experiment which was repeated at least 3 times, controls contained equivalent concentrations of DMSO. Cells were incubated at 37°C in humidified 5% CO₂ atmosphere. After 48 h, cell media was removed and replaced with fresh medium containing the MTT dye at 0.5mg/mL and after 3 h of incubations the media was removed and intracellular formazan crystals were solubilized and extracted with 100 μ l of DMSO. After 15 minutes at room temperature absorbance was measured at 570 nm in a microplate reader (FLUOstar Omega, BMG Labtech, Germany), and the percentage of viable cells was determined for each compound concentration as described previously [95]. IC₅₀s were determined by non-linear regression using GraphPad PRISM software. Statistical analysis of the experimental data was performed by applying one-way ANOVA tests using the software package GraphPad PRISM. Differences were considered to be significant when $P < 0.05$.

Chapter V –References

- [1] <http://goldbook.iupac.org/E02069.html> (accessed on 27.07.2015).
- [2] Rouf A, Taneja S., Synthesis of single-enantiomer bioactive molecules: a brief overview. *Chirality* 2014, 26: 63-78.
- [3] Blaser H., The chiral pool as a source of enantioselective catalysts and auxiliaries. *Chem. Rev.* 1992, 92: 835-852.
- [4] Pérez M., Espadinha M., Santos M. M. M., Indolo[2,3-*a*]quinolizidines and derivatives: bioactivity and asymmetric synthesis. *Curr. Pharm. Design*, 2015, 21 (in press).
- [5] Juaristi E., Recent advances in the enantioselective synthesis of chiral drugs. *Anales de Química* 1997, 93: 135-142.
- [6] Escolano C., Amat M., Bosch J., Chiral oxazolopiperidone lactams: versatile intermediates for the enantioselective synthesis of piperidine-containing natural products. *Chem. Eur. J.*, 2006, 12: 8198 – 8207.
- [7] Schrittwieser J., Resch V., The role of biocatalysis in the asymmetric synthesis of alkaloids. *RSC Adv.*, 2013, 3: 17602–17632.
- [8] Caldwell J., Do single enantiomers have something special to offer?. *Human Psychopharmacology Clin. Exp.*, 2001, 16: S67-S71.
- [9] Nguyen L., He H., Pham-Huy C., Chiral Drugs: An Overview. *Int. J. Biomed. Sci.*, 2006, 2 (2): 85–100.
- [10] Mansfield P., Henry D., Tonkin A., Single-enantiomer drugs. Elegant science, disappointing effects. *Clin. Pharmacokinet.* 2004; 43 (5): 287-290.
- [11] Meyers A., Burgess L., A simple asymmetric synthesis of 2-substituted pyrrolidines from 3-acylpropionic acids. *J. Org. Chem.*, 1991, 56(7): 2294–2296.
- [12] Romo D., Meyers A., Chiral non-racemic bicyclic lactams. Vehicles for the construction of natural and unnatural products containing quaternary carbon centers. *Tetrahedron*, 1991, 47(46): 9503-9569.
- [13] Olofsson B., Khamrai U., Somfai P., A regio- and stereodivergent synthesis of vic-amino alcohols. *Org. Lett.*, 2000, 2(25): 4087–4089.
- [14] Bergmeier S., Stanchina D., Synthesis of vicinal amino alcohols via a tandem acylnitrene aziridination-aziridine ring opening. *J. Org. Chem.*, 1997, 62: 4449-4456.
- [15] Kivelä H., Klika K., Szabó A., Stájer G., Pihlaja K., Structures of saturated 5*H*-Pyrrolo[1,2-*a*][3,1]benzoxazin-1(2*H*)-ones prepared from 4-oxopentanoic acid and cyclic amino alcohols. *Eur. J. Org. Chem.*, 2003, 10: 1879-1886.
- [16] Burgess L., Meyers A., A simple asymmetric synthesis of 2-substituted pyrrolidines and 5-substituted pyrrolidinones. *J. Org. Chem.*, 1992, 57(6): 1992.
- [17] Burgess L., Meyers A., Asymmetric synthesis of γ,γ -dialkyl- γ -aminobutyric acid analogues and 2,2-disubstituted pyrrolidines. Control of stereochemistry in amination ring opening by varying the extent of allylic 1,3-strain. *J. Am. Chem. Soc.*, 1991, 113: 9858-9859.

- [18] Meyers A., Downing S., Weiser M., Asymmetric synthesis of 2-alkyl-perhydroazepines from [5,3,0]-bicyclic lactams. *J. Org. Chem.*, 2001, 66: 1413-1419.
- [19] Amat M., Bassas O., Llor N., Cantó M., Pérez M., Molins E., Bosch J., Dynamic kinetic resolution and desymmetrization processes: a straightforward methodology for the enantioselective synthesis of piperidines. *Chem. Eur. J.*, 2006, 12: 7872 – 7881.
- [20] Bencsik J., Kercher T., O’Sullivan M., Josey J., Efficient, stereoselective synthesis of oxazolo[3,2-*a*]pyrazin-5-ones: novel bicyclic lactam scaffolds from the bicyclocondensation of 3-aza-1,5-ketoacids and amino alcohols. *Org. Lett.*, 2003, 5(15): 2727-2730.
- [21] Soueidan M., Jida M., Bousquet T., Niedercorna F., Péliniski L., Efficient access to new chiral ferrocenyl γ -lactams from amino alcohols. *New J. Chem.*, 2011, 35: 991-993.
- [22] Aydogana F., Demira A., Synthesis and photooxygenation of homochiral 2-methylpyrrole derivatives of chiral amino alcohols: simple, selective access to chiral bicyclic lactams. *Tetrahedron: Asymmetry*, 2004, 15: 259-265.
- [23] Meyers A., Bienz S., Kwon H., Wallace R., The asymmetric synthesis of fused cyclopentenone ring systems: a formal asymmetric total synthesis of (-)-isocomene. *Helvetica Chimica Acta*, 1996, 79:1026-1046.
- [24] Sayed M., Devine P., Burgess L., Meijere A., Meyers A., An asymmetric synthesis of novel aminocyclopropyl carboxylic acids (ACC). *J. Chem. Soc., Chem. Commun.*, 1995, 141-142.
- [25] Tähtinen P., Sillanpää R., Stájer G., Szabó A., Pihlaja K., NMR and X-ray structural study of saturated (*p*-chlorophenyl)-pyrrolo[1,2-*a*][3,1]benzoxazin-1-ones prepared from aroylisobutyric acid and cyclic amino alcohols. High energy barriers for hindered rotation of bridgehead phenyl groups. *J. Chem. Soc., Perkin Trans.* 1999, 2: 2011–2021.
- [26] Skovronsky D., Lee V., Trojanowski J., Neurodegenerative diseases: new concepts of pathogenesis and their therapeutic implications. *Annu. Rev. Pathol. Mech. Dis.*, 2006, 1: 151–170.
- [27] Brown R., Lockwood A., and Sonawane B., Neurodegenerative diseases: an overview of environmental risk factors. *Environmental Health Perspectives*, 2005, 113: 1250-1256.
- [28] Sloane P., Zimmerman S., Suchindran C., Reed P., Wang L., Boustani M., Sudha S., The public health impact of alzheimer’s disease, 2000–2050: potential implication of treatment advances. *Annu. Rev. Public Health*, 2002, 23: 213-31.
- [29] Strong K., Jing Y., Prosser A., Traynelis S., Liotta D., NMDA receptor modulators: an updated patent review (2013-2014). *Expert Opin. Ther. Patents*, 2014, 24(12): 1349-1366.
- [30] Mayer M., Armstrong N., Structure and function of glutamate receptor ion channel. *Annu. Rev. Physiol.*, 2004, 66: 161–81.
- [31] Ghasemi M., Schachter S., The NMDA receptor complex as a therapeutic target in epilepsy: a review. *Epilepsy & Behavior*, 2011, 22: 617-640.
- [32] Jansson L., Akerman K., The role of glutamate and its receptors in the proliferation, migration, differentiation and survival of neural progenitor cells. *J. Neural Transm.*, 2014, 121:819-836.

- [33] Majdi M., Chen H., NMDA-gated ion channel research and its therapeutic potentials in neurodegenerative diseases: a review. *Journal of Receptor, Ligand and Channel Research*, 2009, 2: 59-73.
- [34] Lau C., Zukin R., NMDA receptor trafficking in synaptic plasticity and neuropsychiatric disorders. *Nature*, 2007, 8: 413-427.
- [35] Calì T., Ottolinib D., Brini M., Mitochondrial Ca²⁺ and neurodegeneration. *Neuropharmacology*, 1995, 34(10): 1219-1237.
- [36] Mori H., Mishina M., Structure and function of the NMDA receptor channel. *Neuropharmacology*, 1995, 34(10): 1219-1237.
- [37] Heresco-Levy U., Javittb D., The role of N-Methyl-D-Aspartate (NMDA) receptor-mediated neurotransmission in the pathophysiology and therapeutics of psychiatric syndromes. *European Neuropsychopharmacology*, 1998, 8: 141-152.
- [38] Kemp J., Mckernan R., NMDA receptor pathways as drug targets. *Nature*, 2002, 5: 1039-1042.
- [39] Monyer H., Sprengel R., Schoepfer R., Herb A., Higuchi M., Lomeli H., Burnashev N., Sakmann B., Seeburg P., Heteromeric NMDA receptors: molecular and functional distinction of subtypes. *Science*, 1992, 256: 1217-1221.
- [40] Cull-Candy S., Leszkiewicz D., Role of distinct NMDA receptor subtypes at central synapses. *Sci STKE.*, 2004, 255: re16.
- [41] Paoletti P., Bellone C., Zhou Q., NMDA receptor subunit diversity: impact on receptor properties, synaptic plasticity and disease. *Nat. Rev. Neurosci.*, 2013, (6): 383-400.
- [42] Karakas E., Furukawa H., Crystal structure of a heterotetrameric NMDA receptor ion channel. *Science*, 2014, 344(6187): 992-997.
- [43] Lee C., Lu W., Michel J., Goehring A., Du J., Song X., Gouaux E., NMDA receptor structures reveal subunit arrangement and pore architecture. *Nature*, 2014, 511: 191-197.
- [44] Lipton S., Failures and successes of NMDA receptor antagonists: molecular basis for the use of open-channel blockers like memantine in the treatment of acute and chronic neurologic insults. *NeuroRx*, 2004, 1(1): 101-110.
- [45] Parsons C., Danysz W., Quack G., Memantine is a clinically well tolerated N-methyl-D-aspartate (NMDA) receptor antagonist - a review of preclinical data. *Neuropharmacology*, 1999, 38: 735-767.
- [46] Santangelo R., Acker T., Zimmerman1 S., Katzman B., Strong K., Traynelis S., Liotta D., Novel NMDA receptor modulators: an update. *Expert Opin. Ther. Pat.*, 2012, 22(11): 1337-1352.
- [47] Koek W., Colpaert F., Selective blockade of N-methyl-D-aspartate (NMDA)-induced convulsions by NMDA antagonists and putative glycine antagonists: relationship with phencyclidine-like behavioral effects. *J. Pharmacol. Exp. Ther.*, 1990; 252(1): 349-57.
- [48] Danysz W., Parsons C., Glycine and N-methyl-D-aspartate receptors: physiological significance and possible therapeutic applications. *Pharmacol. Rev.*, 1998; 50(4): 597-664.

- [49] Evans R., Francis A., Watkins J., Mg^{2+} -like selective antagonism of excitatory amino acid-induced responses by α,ϵ -diaminopimelic acid, D- α -aminoadipate and HA-966 in isolated spinal cord of frog and immature rat. *Brain Research*, 1978, 148: 536-542.
- [50] Leeson P., Williams B., Rowley M., Moore K., Baker R., Kemp J., Priestley T., Foster A., Donald A., Derivatives of 1-hydroxy-3-aminopyrrolidin-2-one (HA-966). Partial agonists at the glycine site of the NMDA receptor. *Bioor. Med. Chem. Letters*, 1993, 3(1): 71-76.
- [51] Kessler M., Terramani T., Lynch G., Baudry M., A glycine site associated with N-Methyl-D-Aspartic acid receptors: characterization and identification of a new class of antagonists. *J. Neurochem.*, 1989, 52(4): 1319-1328.
- [52] Leeson P. *et al.*, Kynurenic acid derivatives. Structure-activity relationships for excitatory amino acid antagonism and identification of potent and selective antagonists at the glycine site on the N-Methyl-D-aspartate receptor. *J. Med. Chem.*, 1991, 34: 1243-1252.
- [53] Leeson P. *et al.*, 4-Amido-2-carboxytetrahydroquinolines. Structure-activity relationships for antagonism at the glycine site of the NMDA receptor. *J. Med. Chem.*, 1992, 35: 1954-1968.
- [54] Kulagowski J. *et al.*, 3'-(arylmethyl)- and 3'-(aryloxy)-3-phenyl-4-hydroxyquinolin-2(1H)-ones: orally active antagonists of the glycine site on the NMDA receptor. *J. Med. Chem.*, 1994, 37: 1402-1405.
- [55] Fabio R. *et al.*, Substituted indole-2-carboxylates as *in vivo* potent antagonists acting as the strychnine-insensitive glycine binding site. *J. Med. Chem.* 1997, 40, 841-850.
- [56] Cai S. *et al.*, Structure-activity relationships of alkyl- and alkoxy-substituted 1,4-dihydroquinoxaline-2,3-diones: potent and systemically active antagonists for the glycine site of the NMDA receptor. *J. Med. Chem.*, 1997, 40: 730-738.
- [57] Bare T. *et al.*, Pyridazinoquinolinetriones as NMDA glycine-site antagonists with oral antinociceptive activity in a model of neuropathic pain. *J. Med. Chem.*, 2007, 50: 3113-3131.
- [58] Koller M., Urwyler S., Novel N-methyl-D-aspartate receptor antagonists: a review of compounds patented since 2006. *Expert Opin. Ther. Patents*, 2010, 20(12): 1683-1702.
- [59] Henrich M. *et al.*, Glycine b antagonists. Patent, 08 2010, US 20110190342.
- [60] Khan A., Moskal J., NMDA receptor modulators and uses thereof. Patent, 09 2013, US 20130035292
- [61] Paoletti P., Neyton J., NMDA receptor subunits: function and pharmacology. *Current Opinion in Pharmacology*, 2007, 7: 39-47.
- [62] Evans R., Francis A., Jones A., Smith D., Watkins J., The effects of a series of ω -phosphonic α -carboxylic amino acids on electrically evoked and excitant amino acid-induced responses in isolated spinal cord preparations. *Br. J. Pharmac.*, 1982, 75: 65-75.
- [63] Jane D.; Olverman, H.; Watkins J., Agonists and competitive antagonists: structure-activity and molecular modeling studies. In the NMDA receptor, 2nd ed.; Collingridge G., Watkins J., Eds.; *Oxford University Press: Oxford, U.K.*, 1994.
- [64] Lehmann J. *et al.*, CGS 19755, a selective and competitive N-methyl-D-aspartate-type excitatory amino acid receptor antagonist. *J. Pharmacol. Exp. Ther.*, 1988, 246(1): 65-75.

- [65] Urwyler S., Laurie D., Lowe D., Meier C., Müller W., Biphenyl-derivatives of 2-amino-7-phosphonoheptanoic acid, a novel class of potent competitive N-Methyl-D-Aspartate receptor antagonists - I. Pharmacological characterization *in vitro*. *Neuropharmacology*, 1996, 35(6): 643-654.
- [66] Gaoni Y., Chapman A., Parvez N., Pook P., Jane D., Watkins J., Synthesis, NMDA receptor antagonist activity, and anticonvulsant action of 1-aminocyclobutanecarboxylic acid derivatives. *J. Med. Chem.*, 1994, 37: 4288-4296.
- [67] Moghaddam B., Adams B., Verma A., Daly D., Activation of glutamatergic neurotransmission by ketamine: a novel step in the pathway from NMDA receptor blockade to dopaminergic and cognitive disruptions associated with the prefrontal cortex. *J. Neurosci.*, 1997, 17(8): 2921-2927.
- [68] Kapur S., Seeman P., NMDA receptor antagonists ketamine and PCP have direct effects on the dopamine D₂ and serotonin 5-HT₂ receptors - implications for models of schizophrenia. *Mol. Psychiatry*, 2002, 7: 837-844.
- [69] Muir W., Skarda R., Milne D., Evaluation of xylazine and ketamine hydrochloride for anesthesia in horses. *Am. J. Vet. Res.*, 1977, 38(2): 195-201.
- [70] Clineschmidt B., Martin G., Bunting P., Anticonvulsant activity of (+)-5-methyl-10, 11-dihydro-5H-dibenzo[a,d]cyclohepten-5,10-imine (MK-801), a substance with potent anticonvulsant, central sympathomimetic, and apparent anxiolytic properties. *Drug Development Research*, 1982, 2: 123-134.
- [71] Mark D. Tricklebank *, Lakhbir Singh, Ryszard J. Oles, Cliff Preston and Susan D. Iversen, The behavioural effects of MK-801: a comparison with antagonists acting non-competitively and competitively at the NMDA receptor. *European Journal of Pharmacology*, 167 (1989) 127-135.
- [72] Parsons C., Stöffler A., Danysz W., Memantine: a NMDA receptor antagonist that improves memory by restoration of homeostasis in the glutamatergic system - too little activation is bad, too much is even worse. *Neuropharmacology*, 2007, 53: 699-723.
- [73] Parsons C., Panchenko V., Pinchenko V., Tsyndrenko A., Krishtal O., Comparative patch-clamp studies with freshly dissociated rat hippocampal and striatal neurons on the NMDA receptor antagonistic effects of amantadine and memantine. *Eur. J. Neurosc.*, 1996, 8: 446-454.
- [74] Parsons C., Danysz W., Quack G., Glutamate in CNS disorders as a target for drug development: an update. *Drug News & Perspectives*, 1998, 11(9): 523-569.
- [75] Williams K., Ifenprodil discriminates subtypes of the N-methyl-D-aspartate receptor: selectivity and mechanisms at recombinant heteromeric receptors. *Mol. Pharmacol.*, 1993, 44(4): 851-859.
- [76] Fischer G, Mutel V., Trube G., Malherbe P., Kew J., Mohacsi E., Heitz M., Kemp J., Ro 25-6981, a highly potent and selective blocker of N-methyl-D-aspartate receptors containing the NR2B subunit. Characterization *in vitro*. *J. Pharmacol. Exp. Ther.*, 1997, 283(3): 1285-1292.
- [77] Layton M., Kelly M., Rodzinak K., Recent advances in the development of NR2B subtype-selective NMDA receptor antagonists. *Current Topics in Medicinal Chemistry*, 2006, 6: 697-709.

- [78] Chui-Fun Ip F. et al, Oxazolidine derivatives as NMDA antagonists. Patent, 07 2009, US 20110144168.
- [79] Pereira N., Sureda F., Turch M., Amat M., Bosch J., Santos M.M.M., Synthesis of phenylalaninol-derived oxazolopyrrolidone lactams and evaluation as NMDA receptor antagonists. *Monatsh. Chem.*, 2013, 144: 473-477.
- [80] Jemal A., Bray F., Center M., Ferlay J., Ward E., Forman D., Global cancer statistics. *CA Cancer J. Clin.*, 2011; 61: 69-90.
- [81] Soerjomataram I., Lortet-Tieulent J., Parkin D., Ferlay J., Mathers C., Forman D., Bray F., Global burden of cancer in 2008: a systematic analysis of disability-adjusted life-years in 12 world regions. *Lancet Oncol.*, 2012; 380: 1840-1850.
- [82] Bray F., Jemal A., Grey N., Ferlay J., Forman D., Global cancer transitions according to the human development index (2008–2030): a population-based study. *Lancet Oncol.*, 2012; 13: 790-801.
- [83] Rastogi T., Hildesheim A., Sinha R., Opportunities for cancer epidemiology in developing countries. *Nature Reviews Cancer*, 2004, 4: 909-917.
- [84] Thun M., DeLancey J., Center M., Jemal A., Ward E., The global burden of cancer: priorities for prevention. *Carcinogenesis*, 2010, 31(1): 100-110.
- [85] Wong R., Apoptosis in cancer: from pathogenesis to treatment. *J. Exp. Clin. Cancer Research*, 2011, 30: 87-101.
- [86] Ghobrial I., Witzig T., Adjei A., Targeting apoptosis pathways in cancer therapy. *CA Cancer J. Clin.*, 2005; 55: 178-194.
- [87] Kamb A., Wee S., Lengauer C., Why is cancer drug discovery so difficult?. *Nature Reviews Drug Discovery*, 2007, 6: 115-120.
- [88] Biswal S., Sahoo U., Sethy S., Kumari H., Banerjee M., Indole: the molecule of diverse biological activities. *Asian J. Pharm. Clin. Res.*, 2012, 5(1): 1-6.
- [89] Kaushik N., Kaushik N., Attri P., Kumar N., Kim C., Verma A., Choi E., Biomedical importance of indole. *Molecules*, 2013, 18(6): 6620-62.
- [90] Patil S., Patil R., Miller D., Indole molecules as inhibitors of tubulin polymerization: potential new anticancer agents. *Future Med. Chem.*, 2012, 4(16): 2085-2115.
- [91] Sharma V., Kumar P., Pathak D., Biological importance of the indole nucleus in recent years: a comprehensive review. *J. Heterocyclic Chem.*, 2010, 491-502.
- [92] Reddy Y., Reddy P., Koduru S., Damodaran C., Crooks P., Aplysinopsin analogs: synthesis and anti-proliferative activity of substituted (Z)-5-(N-benzylindol-3-ylmethylene)imidazolidine-2,4-diones. *Bioorg. Med. Chem.*, 2010, 18(10): 3570-3574.
- [93] Asgatay S., Synthesis and evaluation of analogues of N-Phthaloyl-L-tryptophan (RG108) as inhibitors of DNA methyltransferase 1. *J. Med. Chem.*, 2014, 57: 421-434.
- [94] Khalaf R., Abdula A., Mubarak M., Taha M., Tryptophan and thiosemicarbazide derivatives: design, synthesis, and biological evaluation as potential β -D-galactosidase and β -D-glucosidase inhibitors. *Med. Chem. Res.*, 2015, 24: 2529-2550.

- [95] Soares J., Raimundo L., Pereira N. A. L., Santos D. J. V. A., Pérez M., Queiroz G., Leão M., Santos M. M. M., Saraiva L., A tryptophanol-derived oxazolopiperidone lactam is cytotoxic against tumors via inhibition of p53 interaction with murine double minute proteins. *Pharmacol. Res.*, 2015, 95-96: 42-52.
- [96] Pereira N. A. L., Sureda F. X., Espuglas R., Pérez M., Amat M., Santos M. M. M., Tryptophanol-derived oxazolopiperidone lactams: identification of a hit compound as NMDA receptor antagonist. *Bioorg. Med. Chem. Lett.*, 2014, 24: 3333-3336.
- [97] Keserú G., Makara G., Hit discovery and hit-to-lead approaches. *Drug Discovery Today*, 2006, 11(15-16): 742 – 748.
- [98] Cruz A., Rivero I., Preparation and supporting on solid phase of chiral auxiliary (S)-4-(4-hydroxybenzyl)oxazolidin-2-one from *L*-tyrosinol assisted by Microwaves. *J. Mex. Chem. Soc.*, 2009, 53(3): 120-125.
- [99] Parsons T., Spencer N., Tsang C., Grainger R., Total synthesis of kottamide E. *Chem. Commun.*, 2013, 49: 2296-2298.
- [100] Carrasco M. *et al.*, Probing the aurone scaffold against *Plasmodium falciparum*: design, synthesis and antimalarial activity. *Eur. J. Med. Chem.*, 2014, 80: 523-534.
- [101] Mosmann T., Rapid colorimetric assay for cellular growth and survival: application to proliferation and cytotoxicity assays. *Journal of Immunological Methods*, 1983, 65: 55-63.
- [102] Cadete A., Figueiredo L., Lopes R., Calado C., Almeida A., Gonçalves L. M. D., Development and characterization of a new plasmid delivery system based on chitosan-sodium deoxycholate nanoparticles. *Eur. J. Pharm. Sci.*, 2012, 45: 451-458.

Chapter VI –Annex

VI.1 – Measurement of cytosolic Ca²⁺ concentrations increases induced by NMDA receptor

Pregnant rats (18 days) were decapitated and embryos were immediately extracted from the womb by caesarean section and their brains were carefully dissected out. Meninges were removed and a portion of total cortex was isolated after the dissection of the brain. The fragments obtained from several embryos were subjected to mechanic digestion for 5 min. Cells were resuspended in Neurobasal medium with 2% B-27 and seeded in 96-well black plates at a density of 30.000 cells/well. Neuronal cultures were allowed to grow for 8 – 10 days and when the microscope showed the existence of a dense neuronal network, experiments were performed. Cells were loaded with 3 μ M Fluo-4/AM for 45 min at 37 °C in Krebs-HEPES. Cells were then washed with Krebs-Hepes solution twice and kept at room temperature for 10 min before the beginning of the experiment. Compounds were incubated 5 min before application of NMDA 100 μ M to allow NMDA-sensitive glutamate receptors opening and [Ca²⁺] increase. At the end of the experiment, Triton X-100 (5%) and 1 mM MnCl₂ were applied to record maximal and basal fluorescence, respectively. Fluorescence was measured in a fluorescence microplate reader (FLUOstar Optima, BMG, Germany). Wavelengths of excitation and emission were 485 and 520 nm, respectively. Data were represented as percentage of fluorescence increase with respect to control, according to the formula $(\Delta F/\Delta F_{\text{control}}) \times 100$, where ΔF is the percent increase of fluorescence with respect to the $F_{\text{max}}-F_{\text{min}}$ interval.

